



저작자표시-비영리-변경금지 2.0 대한민국

이용자는 아래의 조건을 따르는 경우에 한하여 자유롭게

- 이 저작물을 복제, 배포, 전송, 전시, 공연 및 방송할 수 있습니다.

다음과 같은 조건을 따라야 합니다:



저작자표시. 귀하는 원저작자를 표시하여야 합니다.



비영리. 귀하는 이 저작물을 영리 목적으로 이용할 수 없습니다.



변경금지. 귀하는 이 저작물을 개작, 변형 또는 가공할 수 없습니다.

- 귀하는, 이 저작물의 재이용이나 배포의 경우, 이 저작물에 적용된 이용허락조건을 명확하게 나타내어야 합니다.
- 저작권자로부터 별도의 허가를 받으면 이러한 조건들은 적용되지 않습니다.

저작권법에 따른 이용자의 권리는 위의 내용에 의하여 영향을 받지 않습니다.

이것은 [이용허락규약\(Legal Code\)](#)을 이해하기 쉽게 요약한 것입니다.

[Disclaimer](#)

Thesis for the degree of Doctor of Philosophy

**Application of Bio-based Material for the
Removal of Heavy Metal and Bisphenol A
from Water Environment**

June 2020

The Graduate School

University of Ulsan

Department of Chemical Engineering and Bioengineering

XU YUE

Application of Bio-based Material for the Removal of Heavy Metal and Bisphenol A from Water Environment

Supervisor: Prof. Ik-keun Yoo

June 2020

The Graduate School

University of Ulsan

Department of Chemical Engineering and Bioengineering

XU YUE

Application of Bio-based Material for the Removal of Heavy Metal and Bisphenol A from Water Environment

Dissertation for the degree of Doctor of Philosophy by

XU YUE

has been approved



Committee Chair Prof. Ryu, Keun-Garp



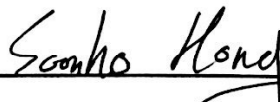
Committee Vice-Chair Prof. Yoo, Ik-Keun



Committee Member Prof. Kim, Yong-Hwan



Committee Member Prof. Hur, Seung-Hyun



Committee Member Prof. Hong, Soon-Ho

Department of Chemical Engineering and Bioengineering

University of Ulsan

June 2020

ACKNOWLEDGEMENT

*I would like to express my deep gratitude to my tutor, **Prof. Ikkeun Yoo**, for his excellent guidance, deep concern, and constant encouragement throughout this study, for supporting me to finish my PhD study. It has been my honor to work under his guidance, and the five-year in Korea would be my greatest life experience.*

*I would especially thank **Prof. Keungarp Ryu**, who has offered essential supports and supervision for my work.*

*I am grateful to the **University of Ulsan**, and **Shanghai University of Engineering Science**, for supporting my projects during this study.*

*I am thankful to all the **committee members** for their suggestions, review, and comments on the thesis.*

*I do really appreciate all the Professors of **Department of Chemical Engineering and Bioengineering** for their lectures and support during the course.*

*I appreciate the Office Manager **Lim KyoungJo** and other staffs for providing me all the facilities and helping me in all the official works whenever I am in need.*

*I want to give my thanks to my dear senior, **Jiyeon Hong**, who provided valuable assistance when I was a freshman. I am also thankful to my lab-mate, **Wu Yujie**, with whom we spent three years together, for giving me indispensable help and creating a wonderful working environment.*

*Most importantly, I would like to thank **my parents, my families, and my friends** for their support on whatever I do. I owe **my grandparents** who raised me up and be waiting for me during the five-year. They are and will be always the source of the motivity for my achievement.*

Table of Contents

Table of Contents.....	i
List of Figures.....	iv
List of Table.....	vi
Abstract	1
Chapter 1	3
Introduction.....	3
1.1 Various pollutants in water environment.....	4
1.2 Characteristics of metal pollutants and removal methods.....	5
1.3 Characteristics of bisphenol A and removal methods.....	10
1.4 Selective removal methods of pollutants from water environment.....	14
1.5 Application of peptide for environmental purpose.....	15
1.6 Research objectives.....	18
1.7 Reference.....	19
Chapter 2	25
Adsorptive removal of heavy metal ions in water using poly(<i>m</i>-phenylenediamine) synthesized by laccase	25
2.1 Introduction.....	26
2.2 Material and methods.....	28
2.2.1 Materials.....	28
2.2.2 Enzymatic synthesis of poly(<i>m</i> -PDA).....	28
2.2.3 Adsorption of metal ions by poly(<i>m</i> -PDA).....	29
2.2.4 Fourier transform infrared (FTIR) spectroscopy.....	30
2.3 Results and Discussion.....	30
2.3.1 Structural characterization of poly(<i>m</i> -PDA).....	30
2.3.2 Adsorption characteristics of poly(<i>m</i> -PDA) for Pb ²⁺ ion.....	33
2.3.3 Adsorption isotherms of poly(<i>m</i> -PDA) for heavy metal ions.....	34
2.4 Conclusions.....	40
2.5 References.....	41
Chapter 3	44
Selective Removal of Lead Ion from Water by Magnetic Bead fused with Lead- recognizing Peptide	44
3.1 Introduction.....	45
3.2 Materials and Methods.....	47

3.2.1	Materials	47
3.2.2	Adsorption onto bare magnetic bead.....	48
3.2.3	Construction of Peptide-binded magnetic bead	48
3.2.4	Lead adsorption.....	49
3.2.5	Analysis	50
3.3	Results and discussion.....	51
3.3.1	Selection of bead (Pb ²⁺ adsorption onto bare bead)	51
3.3.2	Pb ²⁺ adsorption using peptide-binded magnetic bead	52
3.3.3	Parallel experiment.....	53
3.3.4	Lead Adsorption isotherm study	56
3.3.5	Repeated use of peptide-coated bead	59
3.3.6	Selective lead adsorption.....	61
3.4	Conclusion	63
3.5	References	63
	Chapter 4	66
	Selective Removal of Bisphenol A from Water by Magnetic Bead fused with	
	Bisphenol A-binding Peptide.....	66
4.1	Introduction	67
4.2	Material and methods.....	69
4.2.1	Materials and apparatus.....	69
4.2.2	Preparation of peptide-binded / protein-coated magnetic bead.....	70
4.2.3	BPA adsorption experiments.....	71
4.2.4	Selective adsorption experiments.....	71
4.2.5	Desorption and regeneration studies	72
4.3	Results and discussion.....	72
4.3.1	Preparation and characterization of peptide-binded magnetic bead.....	72
4.3.2	Adsorption	74
4.3.2.1	Effect of pH on adsorption	74
4.3.2.2	BPA adsorption under mild solution	76
4.3.2.3	Effect of peptide concentration.....	78
4.3.2.4	BPA Adsorption isotherm study.....	79
4.3.3	Desorption and regeneration studies	81
4.3.4	Selectivity study.....	82
4.3.5	BPA adsorption by different length of peptide.....	83
4.4	Conclusions	85
4.5	Reference.....	85
	Chapter 5	89

Photocatalytic degradation of bisphenol A using TiO₂ synthesized via peptide-mineralization process	89
5.1 Introduction	90
5.2 Material and methods	92
5.2.1 Materials	92
5.2.2 Peptide binding and biomineralization	92
5.2.3 Characterization	93
5.2.4 Photocatalytic activity	93
5.3 Results and discussion.....	94
5.3.1 Influence of peptide concentration	94
5.3.2 Characterization	96
5.3.3 Photocatalytic activity	99
5.4 Conclusions	101
5.5 Reference.....	102
Chapter 6	105
Conclusion	105

List of Figures

Figure 2-1 FTIR spectra of poly(m-PDA) synthesized by laccase and the poly(m-PDA) with adsorbed heavy metal ions.	31
Figure 2-2 Pore size distribution of the poly(m-PDA) synthesized by laccase.....	32
Figure 2-3 Effect of different solutions on the Pb ²⁺ adsorption by enzymatically synthesized poly(m-PDA).....	34
Figure 2-4 Adsorption isotherms for various heavy metal ions on enzymatically synthesized poly(m-PDA).....	37
Figure 3-1 Pb ²⁺ adsorption onto bare bead (mg Pb ²⁺ /g bead)	51
Figure 3-2 Kinetics of Pb ²⁺ adsorption onto peptide-coated bead.....	53
Figure 3-3 Effect of different modification on Pb ²⁺ adsorption capacity.....	55
Figure 3-4 Adsorption isotherms for the adsorption of lead ions onto peptide-binded bead.	56
Figure 3-5 The adsorption and desorption of Pb ²⁺ with EDTA for 6 times.....	59
Figure 3-6 Comparison of the metal adsorption capacity in three different solution system.	61
Figure 4-1 FTIR spectra of bare bead, carboxyl activated bead and PBB.....	74
Figure 4-2 BPA adsorption under neutral, acid and base solution.....	76
Figure 4-3 BPA adsorption under mild solution.....	77
Figure 4-4 Chemical structure and the species distribution diagram of BPA.	78
Figure 4-5 Effect of peptide concentration on the adsorption of BPA by cyclic peptide.....	78
Figure 4-6 Adsorption isotherms for the adsorption of BPA onto bead.....	79
Figure 4-7 Adsorption and desorption study of BPA on PBB.	81
Figure 4-8 Comparison of the BPA selective adsorption capacity in three different solution system	82
Figure 4-9 Comparison of the BPA selective adsorption capacity	84
Figure 5-1 TGA curves of PS bead (b) and TiO ₂ synthesized from different concentration of pep-tide-binded PS bead.	95
Figure 5-2 SEM images of (a) bare PS bead, (b) PS bead binded with peptide, (c) the peptide-binded bead reacted with precursor before calcination, and (d) peptide-binded bead reacted with precursor after calcination.....	97
Figure 5-3 XRD spectra of commercial P25 TiO ₂ , and bare, STB1-, and PS-STB1-TiO ₂ after calcination at 800 °C.....	98
Figure 5-4 Adsorption in the dark and photocatalytic degradation of BPA under the solar light stimulator over the P25, bare-, STB1-, and PS-STB1-TiO ₂ photocatalysts at 20 minutes intervals.....	100

Figure 5-5 kinetic curves for BPA by P25, bare-, STB1-, and PS-STB1-TiO₂ photocatalysts 100

Figure 5-6 Degradation rate of BPA over PS-STB1-TiO₂ for 5 cycles..... 101

List of Table

Table 1-1 Permissible concentration limits of some heavy elements in potable water according to WHO and US EPA, their major sources, and impacts on human health. (Eskandari et al., 2020) Copy Right Elsevier	6
Table 1-2 The chemical and physical properties of BPA	11
Table 2-1 Langmuir isotherm parameters estimated by linear regression analysis and the calculated adsorbed fractions of BET surface area of poly(m-PDA) for the adsorption of the heavy metal ions	38
Table 3-1 Different peptide sequence on Pb ²⁺ adsorption capacity	54
Table 3-2 Parameters fitted with both nonlinear and linearized adsorption isotherm	58
Table 3-3 Chemical composition of the synthetic wastewater	61
Table 4-1 Bead-binding efficiency with different peptide/protein	72
Table 4-2 Parameters fitted with nonlinear adsorption isotherm.....	80
Table 5-1 Peptide binding amount on PS bead and TiO ₂ synthesized amount from different initial concentration of peptide.....	94
Table 5-2 Degradation rate and <i>k</i> _{app} values for BPA by P25, bare-, STB1-, and PS-STB1-TiO ₂	101

Abstract

Various kinds of toxic pollutants are being discharged into water environment with rapid development of society. The heavy metals and endocrine disrupters among them are representative pollutants causing severe concerns to human health. Biological methods to handle those issues have widely been investigated due to its low capital and operation cost, non-toxicity of materials, availability to materials, relatively simple equipment and operation required, and so on. Various biological materials and processes have been developed until now but, are still challenged for its weaknesses such as operational variability, non-selective removal to specific target component, and low efficiency under harsh condition. In this study, two kinds of bio-based materials are applied for the removal of target pollutants (heavy metals and bisphenol A (BPA)). The first material is the enzymatically-synthesized polymeric one for the removal of heavy metals in non-selective adsorptive way. The other material is the peptide fused with magnetic core and is applied for the removal of lead and BPA in selective adsorptive way.

Unlike chemical reactions, enzymatic reactions require no toxic oxidants for the polymerizations and do not produce harmful by-products. The enzymatic reaction replacing corresponding chemical reaction was applied to synthesize the polymer via environmentally friendly synthetic route. The polymer of m-phenylenediamine (poly(m-PDA)), synthesized by mild laccase-catalysis in an aqueous buffer, was investigated for the adsorption of several heavy metal ions including Pb^{2+} , Cu^{2+} , Co^{2+} , and Cr^{3+} . The adsorption isotherms of the four heavy metal ions on poly(m-PDA) were well described by Langmuir equation. Poly(m-PDA) shows high maximum adsorption capacities (q_{max}) for Cu^{2+} , Pb^{2+} , and Cr^{3+} , with the values of 556, 526, and 476 $\mu\text{mol} \cdot \text{g}^{-1}$, respectively. Thus, the synthesis of polymeric absorbents to remove heavy metals can be accomplished through simple and environmentally friendly enzymatic methods.

A 7-mer lead-binding peptide (TNTLSNN) was covalently bonded onto the surface of magnetic bead which is a reusable adsorbent to remove Pb^{2+} from water. Compared to the bare bead without the linked peptides (29.82 $\mu\text{mol} \cdot \text{g}^{-1}$), the peptide-linked adsorbent showed 9 times higher removal capacity of lead (246.05 $\mu\text{mol} \cdot \text{g}^{-1}$). The

sequence (TNTLSNN or NNSLTNT) of 7-mer peptide linked to the surface of bead did not significantly influence on whole adsorption capacity of lead. To examine the reusability of bead, the adsorbed lead was desorbed from the bead by using EDTA and then the recovered bead could be repeatedly used several times (6 cycles tested) without significant loss of adsorption capacity. A selective adsorption of lead in the presence of interfering other metals is verified with individual or combinatory use of four metal ions such as Pb^{2+} , Ni^{2+} , Co^{2+} and Cu^{2+} , where the amount of bound Pb^{2+} was remarkably higher than the other metal ions. The adsorption isotherm followed Langmuir fitting well with the maximum adsorption loading (q_{max}) of $308.86 \mu\text{mol}\cdot\text{g}^{-1}$ adsorbent.

A heptapeptide with specific affinity to BPA, LysSerLeuGluAsnSerTyr (KSLENSY) was covalently bonded onto the surface of magnetic bead. Compared to the bare bead without the linked peptides ($8.6 \mu\text{mol}\cdot\text{g}^{-1}$), the peptide-linked adsorbent showed 9 times higher removal capacity of BPA ($37.6 \mu\text{mol}\cdot\text{g}^{-1}$). BPA-binding peptide had higher selectivity toward BPA compared with structural analogs of BPA such as bisphenol F and bisphenol S. Around neutral pH, the adsorption capacity was maximum since the neutral form of BPA was favourable for the adsorption onto peptide. The magnetic-core bead was used in this study to separate the bead after use and reuse for the next round of adsorption. Various chemicals was tested to regenerate the bead used and almost 100% of regeneration efficiency was achieved by using methanol/acetic acid mixture. The adsorption capacities of BPA after sixth cycle maintained more than 87% of initial capacity

Finally, the degradation of BPA was investigated by using peptide-mineralized photocatalytic TiO_2 particle. Environmentally benign mineralization of TiO_2 particle was induced by using the polystyrene (PS) bead fused with mineralization-inducing peptide. The peptide (CHKKPSKSC) with specific affinity to TiO_2 was used in this studied. The synthesized TiO_2 showed a BPA degradation rate of 86.3%.

Chapter 1

Introduction

1.1 Various pollutants in water environment

Water is necessary as a primary material for the life on planet earth (Al-Amshawee et al., 2020). Adequate quantities of good quality freshwater are essential for achieving the Sustainable Development Goals for human health, food security and the aquatic environment itself (Achim Steiner, 2016). However, water pollution has worsened since the 1990s in the majority of rivers in most part of the world because of technological and industrial expansion of different sectors in modern society which brought increasing complexity and toxicity of wastes (Giovanella et al., 2020). Today, the water environment is suffering from severe contamination, leading to severe destruction in the natural water courses. Therefore, a massive decreasing occurs in the growth of the environment, human sustenance, and economic status (Carolin, Kumar, Saravanan, Joshiba, & Naushad, 2017; Elgallal, Fletcher, & Evans, 2016). Though domestic water and wastewater regulations for urbanisation usage have been enforced to protect natural water sources from contamination, deficient mediation of domestic wastewater still causes environmental problems because of the poor removal of organic compounds, toxic and nontoxic matters, viruses, et al. (Ahmed et al., 2017; Tee et al., 2016). Severe organic pollution already affects around one-seventh of all river stretches in Latin America, Africa and Asia according to A report of the World's Water Quality (Achim Steiner, 2016).

Industrial wastewater contains heavy metals, oil, aromatic hydrocarbons, dyes, pesticides, and high organic and inorganic matters which comprises the most significant role in water pollution (Carstea, Bridgeman, Baker, & Reynolds, 2016). As far back as the 1970s it was concerned that the discharge of waste products containing metals and chemical compounds was impacting the aquatic environment. Many metals

(e.g. mercury, lead, arsenic) and most synthetic organic compounds (e.g. phenols, pesticides) are toxic to living organisms (Visa, Bogatu, & Duta, 2010), including people, at high enough concentrations. Accordingly, wastewater industries aim to sustain water resources by using high organic loading rate, low cost, simple, feasible and safe mediation process.

1.2 Characteristics of metal pollutants and removal methods

Heavy metals are the chemical elements with atomic weights in the range of 63.5 and 200.6 a.m.u. and specific gravities larger than 5.0 (Srivastava & Majumder, 2008). Presence of low concentration of some of the metal ions such as Cu, Fe, and Zn is necessary for enzymatic processes in organisms as cofactors, living organisms and human diet (Kozlowski et al., 2009). But, with the growth of some of the specific industries such as fertilizer production, batteries manufacturing, metal plating facilities and mining operation, a large amount of heavy metal sewage has been produced. If these sewages are discharged into ecological waters without treatment, they will be extremely harmful to the natural environment and the human body (SIMON KAPAJ et al., 2011). Unlike organic pollutants, which can be decomposed and transformed by natural degradation or photocatalytic degradation (Sharma, Mishra, & Kumar, 2015), heavy metals are highly stable and not degradable. The components of heavy metal sewage can only be controlled by chemical or physical means to change its location and present form. Non-biodegradability, accumulation in living organisms and carcinogenic characteristics of heavy metals describe them as hazardous material for human and environment. Mercury, cadmium, lead, copper, zinc nickel, and chromium as toxic heavy metals are the major concern in industrial wastewaters treatments (Fu & Wang, 2011). In Japan, 2252 peoples have been affected and 1043 have died due to

Minamata disease, which is caused by elevated mercury pollution from a chemical plant(Kudo, Mahara, Santry, Miyahara, & Garrec, 1991).

The acceptable concentration of heavy metals in potable water according to World Health Organization (WHO) and United States Environmental Protection Agency (US EPA), their major sources and their impact on human are tabulated in Table 1.

Heavy metals	Permissible Concentration (mg L ⁻¹)		Major Sources	Impact on human health
	WHO	US EPA		
As(III)/As(V)	0.05	0.01	Pesticides, Metal smelter	Bronchitis, Dermatitis, poisoning
Ni(II)	0.1	–	Batteries manufacturing, mining, metal finishing, forging, electroplating	Dermatitis, allergic sensitization, lung and kidney problems and are a known human carcinogen
Pb(II)	0.05	0.015	Paint, burning of coal, mining, pesticide, smoking	dizziness, irritability, weakness of muscles, mental retardation in children, renal damage anemia, hallucination, insomnia, headache
Hg(II)	0.001	0.002	Pesticides, batteries, paper industry, fossil fuel combustion	Spontaneous abortion, damage to nervous system, tremors, protoplasm poisoning, gingivitis, lung irritation, skin rashes, vomiting, and diarrhea
Cr(VI)/Cr(III)	0.05	0.05	electroplating, textile industries, photography industries, nuclear power plant, leather tanning, metal finishing	Fatigue, damage to nervous system, irritability
Cd(II)	0.005	0.005	welding, fertilizers, electroplating, paints and plastics, Cd and Ni batteries, nuclear fission plants	Lung disease, bronchitis, kidney damage, bone marrow, blood pressure, bone defects, renal dysfunction
Cu(II)	1.5	1.3	Chemical industry, metal piping, mining, pesticide production	Stomach and intestinal irritation, vomiting, diarrhea, anemia
Co(II)	0.05	–	industrial processes such as mining, electronic, batteries, pigments, metallurgical, and nuclear power plants	Pralysis, low blood pressure, and lung irritation

Table 1-1 Permissible concentration limits of some heavy elements in potable water according to WHO and US EPA, their major sources, and impacts on human health. (Eskandari et al.,

2020) Copy Right Elsevier

Up to now, various treatment processes have been developed to remove the heavy metal ions from water and wastewater resources with some showing excellent ability towards heavy metal uptake from wastewater. Physical and chemical precipitation, ion exchange, reverse osmosis, membrane filtration, electrochemical treatment, coagulation and flocculation, solvent extraction, cathodic electrodeposition, and cementation processes are the most well-known process for removal of heavy metal ions from water and wastewater.

Among the many removal means, adsorption method has been widely used and studied for its advantages of easy operation, efficient removal of trace heavy metals, low cost, good selectivity and no secondary pollution to the environment. The adsorption method is one of the most effective methods to remove trace heavy metals from water. Adsorption is the process of transferring heavy metal ions from the solution phase to the surface of the adsorbent, and the heavy metal ions are binded through physical and chemical action. Generally, the process includes the transfer of pollutants from the solution to the surface of the adsorbent, adsorption on the adsorbent surface, and the diffusion of pollutants in the adsorbent. Economy and technical suitability are necessary and critical factors in selecting the best adsorbent for the removal of heavy metal ions in water.

There are many different types of adsorbents available until now, which can be roughly divided into the following categories according to their source and type of material.

a) Natural mineral materials. Including bentonite, olivine, zeolite, clay, kaolin, zircon, sea foam and diatom. These mineral materials have the advantages of wide distribution, easy access, low cost and so on. Their simple processed products show strong adsorption capacity. For example, He et al. prepared Fe(III) modified clay ash,

and studied its competitive adsorption of Cd (II), Pb(II) and Ni (II); Choi et al. prepared Mg modified zeolite, the material showed 1.5 times higher adsorption capacity to Pb (II), Cd (II) and Cu (II) than Na and K-modified zeolite, while the adsorption capacity increased by 1.5-2.0 times than unmodified zeolite;

b) Carbon materials. Including activated carbon, biochar, carbon nanotubes, graphene materials and other forms of carbon materials. Research on Carbon materials is one of the hot spots today, because of their high surface area, high stability, high biocompatibility, and high activity. Kotodyl ska et al. studied adsorption towards Cu (II), Zn (II), Cd (II) and Pb (II) in water solution by the biological carbon material. In addition, the highly active functional group on the surface of the carbon material can be modified with coordinating functional group (e.g. carboxyl, carbonyl, quinone, lactone, hydroxyl and carboxylic anhydride, etc.) to further improve its adsorption and selectivity to heavy metals. For example, Ihsanullah and others have introduced the removal of Cd (II) in aqueous solution with acid modified carbon materials in detail.

c) Natural organic materials. Such as starch, cellulose, and chitosan et al. These kinds of materials are with merits like large stock, easy to obtain, low cost and being sustainable. Besides, there are a certain number of functional groups within organic materials which make it possible to interact with metal ions, as well as offering the potential for the follow-up modification. Coconut shells, straw, grain shells, palm fruit, sugar cane slag, eggshells, wood chips, citrus peels, etc. from agriculture and forestry waste were all studied for heavy metal treatment. In Hydari's report, the maximum adsorption capacity of natural chitosan flakes in a water solution at pH 6 is 10 mg/g, which is similar with industrial active carbon with 10.3 mg/g, while the adsorption capacity of the nanomaterial obtained by the combination of chitosan / active carbon is as high as 52.63 mg/g.

d) Biology. In recent years, researchers have used bacteria, fungi, endophytes, aquatic plants and other organisms to remove heavy metal ions from the water. For example, Babu et al. used endophytes *Ginbacillus* (GDB-1) to promote the growth of ultra-rich plant mountain slugs and heavy metal accumulation speed, GDB-1 removal efficiency is affected by the initial metal ion concentration and solution pH, The removal rate of the heavy metals in the ore tailings leachate liquid was Pb(II) >Zn(II) >As(II) >Cd(II) >Cu(II)=Ni(II) within the growth cycle; The maximum amount of cadmium removal by *Hypnea valentiae* from Red algae was observed at 60 °C with 28.7 mg/g by Rathinam et al.

e) Synthetic materials. Synthetic materials include porous materials such as mesoporous silica, mesoporous calcium silicate and metal organic frame materials, as well as numerous polymer materials such as phenolic resins, polystyrene, synthetic hydrogels, polypropylene, polypyrrole, etc. P et al. prepared polyphenyl/polypyrrole /hexagonal mesoporous silica composite material and studied its adsorption towards Cd (II). P et al. studied the hydrogel prepared by acrylic acid and poly N-isopropylacrylamide for Cu(II) adsorption. The most important feature of this kind of material is that there are many active functional groups for adsorption and modification. These materials and the functional groups can also be designed according to specific needs, so generally synthetic materials have a higher adsorption capacity and selectivity compared to other adsorption materials, being one of the most attractive research directions of heavy metal adsorption materials.

To sum up, adsorption is one of the most used sewage treatment methods, as well as the most important water treatment method. The adsorption method has the advantages of fast reaction rate, high adsorption efficiency, no need to add adsorption catalyst, strong adaptability and so on. Generally, the adsorbent is not soluble in water, and the

adsorption process only reacts on the surface of the adsorbent, so it does not produce impurities and do not cause second pollution. Therefore, the adsorption method is more and more widely used in the field of water treatment. There is necessity to develop new adsorbents and improve the performance of adsorbents. For a sustainable solution to this problem, there is a need to shift from the conventional ways to new approaches requiring biological resources, which are eco-friendly

1.3 Characteristics of bisphenol A and removal methods

Since the 1990s, a large amount of studies have been conducted on environmental endocrine disruptors (EDs) to explore the causes of lesions such as reproductive disorders, dysplasia, and cancer. The structure of endocrine disruptors in the environment is with wide varieties. Bisphenol A (BPA) is known as a typical environmental endocrine disruptor, which is widely used as a primary intermediate product of polycarbonate plastics and epoxy resins (Fenichel et al., 2013). It is one of the highest production and consumption volume chemicals in the world. The global annual production of BPA has grown from 3.9 million tons in 2006 to 5 million tons in 2012 and has maintained an annual growth rate of more than 2%. Studies from different countries and areas have demonstrated the presence of urinary BPA in more than 90% of their study populations, suggesting a common exposure to BPA worldwide (Wang et al., 2015a). It has been confirmed that BPA will be released from some consumer goods, flowing into food, drinking water, wastewater, air and dust with natural and social circulation. BPA can interfere with the body through genomic and non-genomic estrogen-corresponding mechanisms and can cause damage to cells at low doses (below 0.23 ng/L), so the threat of BPA to humans and organisms cannot be ignored. Towards the toxic effects of BPA, the Canadian government, the European

Union, the U.S. and other Food and Drug Administration (FDA) have banned the use of BPA-containing infant bottles from 2010~2012.

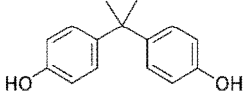
Properties	Value
Sturcture	
Molecular formula	C ₁₅ H ₁₆ O ₂
Molecular weight	228.29 g/mol
Melting point	156~158 °C
Boiling point	220 °C, 4 mmHg
Aqueous solubility	Non-soluble
Appearance	White solid
Application	Epoxy resin, Polycarbonate, Phenolic resin
Dissolvability	Soluble in organic solvents such as ethanol, acetone, ether, benzene, etc.

Table 1-2 The chemical and physical properties of BPA

In recent years, the methods for the treatment of Bisphenol A are paid attention on biodegradation, advanced oxidation, membrane separation technology and adsorption, which can be divided into physical method, advanced oxidation method and biological method.

a) Biodegradation

Environmental hormones can be biodegraded in a variety of environmental media, such as many bacteria in various types of surface water that can degrade the environmental hormone. Some relevant research results confirm that in the activated sludge method, only a small number of EDCs can be purified from primary precipitation, secondary precipitation and sludge adsorption, and biodegradation is the main way to remove EDCs. Marie Laure et al. studied the removal of EDCs from

different sewage plants in 30 countries, showed average removal rate of 90%. Svenson et al. studied the decontamination effects of environmental hormones in 20 sewage plants in Sweden. Data confirmed that the activated sludge method to purify estrogen owns the best effect, with decontamination rate of up to 81%. Zhang et al. screened out the degradation bacteria in the Municipal domestic waste compost, which showed the highest biodegradation activity on BPA. However, due to the complex molecular structure of microorganisms, there are many problems such as slow decomposition and incomplete decomposition of pollutants.

b) Membrane treatment technology.

Membrane separation technology is a very effective method to remove micro-polluting organic matter in water. However, few research currently studied this method to remove the environmental hormone. Agenson et al. used four nanofiltration reverse osmosis membranes to remove micro-contaminated organic matter from the water and found that the removal rate of high desalting membranes was above. Comerton et al. found that contaminated nanofiltration membranes have a higher decontamination capacity on BPA than clean membranes.

c) Adsorption

adsorption has been found to be a superior and rapid removal method as it is low cost, easy to operate, and no secondary pollutants. Regarding the adsorption technique, an effective adsorbent is crucial to guaranteeing the efficiency of water treatment. Nitrogen modified reduced graphene oxide (NRGO) was prepared by a hydrothermal method by Wang et al. (2015). The nitrogen modification was found to enhance its adsorption and catalysis ability. For an initial bisphenol concentration of 0.385 mmol/L, the adsorption capacity of N-RGO was observed as 1.56 mmol/g for

BPA. Iron nanoparticle-doped magnetic ordered mesoporous carbon (Fe/OMC) was prepared by co-impregnation and carbothermal reduction methods, and applied for highly effective adsorption and degradation of BPA (Tang et al., 2016).

d) Advanced oxidation

Advanced oxidation technology is an effective and safe water treatment technology, which has been used to remove a variety of organic matter in the water. With the frequent detection of environmental hormones in water environment, some advanced oxidation treatment technology has been widely used. The amount of catalyst, the initial concentration of environmental hormones, temperature, pH and light intensity all affect oxidation degradation. Sharma et al. (2015) carried out a study in which the UV/H₂O₂ was able to remove BPA by 85% in the duration of 240 min. Advanced oxidation can efficiently degrade EDCs, but some products are still toxic after oxidation, even more than before oxidation. Therefore, it is necessary to strengthen the research in this field based on chemical testing and bioanalytical evaluation.

e) Photocatalysts

Considering the potential draw backs of the conventional treatment methods, the alternative option such as photocatalysis was widely explored. Amongst all the available photocatalysts, titania has been investigated most extensively. TiO₂ possess three crystalline polymorphs in nature: anatase, rutile, and brookite (Tran et al., 2017). TiO₂ photocatalysts have been explored in detail for the degradation of BPA. For instance, in a study carried out by Jia et al. (2012), 97% of the BPA (at an initial concentration of 10 mg/L) was degraded by TiO₂ in the presence of UV irradiation after 80 min. Traditional synthesis of inorganic materials involves high temperature reaction environments such as thermal decomposition which is labor and cost

intensive, in addition to the surplus hazardous chemical waste generation. Thus, there is necessity to develop new method to synthesize TiO_2 for photocatalysts

1.4 Selective removal methods of pollutants from water environment

Although much research has been conducted on the separation of single species of pollutants, the selective adsorption of specific pollutant from complex mixture of real water is relatively little known. Such like activated carbon adsorption is very efficient for estrogens, but it is easily impacted by the interfering substances such as humic acids in the environmental water (Fukuhara et al., 2006). The search for cost-effective and selective binding methods is still warranted (Krupadam et al., 2010). Selective adsorbents, which would otherwise adsorb predominant pollutants of higher concentration, need to be developed to remove trace pollutants of low concentrations. There are now several kinds of methods researched to show selective removal towards micropollutants, including ion-exchange, molecular imprinting technology, ligand-functionalization as well as biosorption. Surface molecular imprinting technology (SMIT) has attracted much attention in the field of sensor, catalysis, drug delivery and adsorption (Ji et al., 2009). It is a powerful technique which produces cross-linked polymers with specific cavities that are complementary to a template molecule in terms of size, shape, and functionality (Pichon and Chapuis-Hugon, 2008). The generated recognition sites by reversible immobilization of template molecules have high affinity toward target molecule. It makes the selective and fast removal of target pollutants from water environment possible. A molecular imprinted particle for Bisphenol A (BPA-MIP) was successfully used for selective recognition of BPA in the water. The contaminants such as 3, 3', 5, 5'-

Tetrabromobisphenol A (TBBPA), phenol and phenol red (PSP) were selected as the latent interferon to investigate the selectivity.(Ren et al., 2014). Novel magnetic molecularly imprinted polymers based on multiwalled carbon nanotubes (MWNTs@MMIPs) with specific selectivity toward BPA were synthesized by Zhang et al. using bisphenol A as the template molecule, methacrylic acid, and β -cyclodextrin as binary functional monomers and ethylene glycol dimethacrylate as the cross-linker (Zhang et al., 2014). The MWNTs@MMIPs exhibited good affinity with a maximum adsorption capacity of 49.26 $\mu\text{mol/g}$ and excellent selectivity toward bisphenol A. Badruddoza et al. synthesized carboxymethyl- β -cyclodextrin (CM- β -CD) polymer modified Fe_3O_4 nanoparticles (CDpoly-MNPs) for selective removal of Pb^{2+} , Cd^{2+} , Ni^{2+} ions from water. The maximum uptakes for Pb^{2+} , Cd^{2+} and Ni^{2+} in non-competitive adsorption mode were 64.5, 27.7 and 13.2 mg g^{-1} , respectively at 25 °C. They assumed that the polymer grafted on MNPs enhanced the adsorption capacity because of the complexing abilities of the multiple hydroxyl and carboxyl groups in polymer backbone with metal ions. In competitive adsorption experiments, CDpoly-MNPs could preferentially adsorb Pb^{2+} ions with an affinity order of $\text{Pb}^{2+} \gg \text{Cd}^{2+} > \text{Ni}^{2+}$ which can be explained by hard and soft acids and bases (HASB) theory. (Badruddoza, Shawon, Tay, Hidajat, & Uddin, 2013)

1.5 Application of peptide for environmental purpose

Different types of microorganisms, such as algae, bacteria, filamentous fungi and yeast cells have the ability to remove, concentrate and immobilise different metals, providing a basis for the development of new methodologies to remove micropollutants (Gavrilescu 2004 ; Volesky 2003 ; Wang and Chen 2009)

Microorganisms are small in size and have a high surface area-to-volume ratio; as a consequence, they display a large contact area that can interact with metal ions present in solution. Due to their removal efficiency, environmental suitability, simplicity, and mode of operation analogous to well-established ion-exchange technology, waste microbial biomass has been identified as a promissory biotechnological approach in the fight against metal pollution.

Many polysaccharides and several functional groups, such as carboxyl, hydroxyl and amino are found in the cell wall of microorganisms, which are largely responsible for metal biosorption. However, the functional groups in the microorganisms do not show specific selectivity toward individual heavy metal species. There is practical interest to develop methods that can effectively remove the heavy metals from the water containing high concentration of co-ions. A possible solution to achieve this target is to use adsorbents that have selectivity toward the heavy metal ions. Therefore, modifications have been performed to improve the efficiency or selectivity of metal removal. Kuroda et al. used yeast cells with an increased capacity for intracellular metal accumulation due to over-production of metal-binding proteins in the cytoplasm, such as glutathione and cysteine-rich proteins (Kuroda and Ueda 2010). *S. cerevisiae* cells expressing *Arabidopsis thaliana* phytochelatin synthase showed enhanced intracellular arsenic (III) accumulation, which resulted in a sixfold increase in As removal (Singh et al. 2008). Another method involved the cell surface design of microorganisms using recombinant DNA techniques. In “cell-surface engineering”, also called “molecular display (arming) technology”, it is possible to anchor various functional metal-binding proteins/peptides on the cell surface (Shibasaki et al. 2009). The foreign peptide to be expressed is generally fused to a mannoprotein that is anchored covalently onto the yeast cell surface (Kondo and

Ueda 2004; Salem et al. 2008; Shibasaki et al. 2009). These yeast cells, which display the heterologous proteins on the cell surface, have exhibited an enhanced selective metal removal by a metabolism-independent process; in this case, metal recovery from yeasts does not require cell disruption, which allows for subsequent reuse (Kuroda and Ueda 2010; Salem et al. 2008). Cell-surface-engineered yeasts, which display a histidine oligopeptide (hexa-His), have the capability to chelate divalent heavy metals and have shown the ability to remove three to eight times more copper than parent yeast cells; additionally, the genetically engineered microorganisms (GEM) was more resistant to copper than was the parental strain (Kuroda et al. 2001).

Since peptide or protein is the core factor interacting with target metals, the direct use of a metal-binding peptide as a biosorbent is more effective for improving the selectivity of target-metal species. Peptides are polymeric biomolecules composed of amino acids. There are 20 naturally occurring amino acids, each with its own unique size and functionality. Since many peptides have coordination donor atoms (for example, N, O, and S atoms) which endow it abundant adsorption sites. And peptides undergo distinctive sequence-specific self-assembly and have recognition properties thus making them important structural and signaling molecules in biological systems. MT is well known for its cysteine-rich character and its high binding capacity for heavy metals, especially soft metals. Genetically engineered bacterial MT SmtA was immobilized on the microcarrier beads for selective preconcentration of trace cadmium. The immobilized SmtA showed outstanding selectivity towards cadmium, with up to 800,000-fold improvement in the tolerance level of coexisting metal species compared with bare microcarrier. It is of great potential to research selective removal property of peptides towards micropollutants.

1.6 Research objectives

Considering the increasing amount of toxic materials which would bring harmful effects towards both environment safety and human health, an efficient and cost effective system is under necessity. Bio-based material has attracted much attention because of its low cost, non-toxicity, simple equipment and operation required and so on. In this study, we constructed several materials for use of environmental micro-pollutants removal, including:

Enzymatic synthesis of *m*-phenylenediamine (poly(*m*-PDA)) which require no toxic oxidants for the polymerizations and do not produce harmful byproducts. The polymer of poly(*m*-PDA) which was synthesized by mild laccase-catalysis in an aqueous buffer was investigated for the adsorption of several heavy metal ions.

A 7-mer lead-binding peptide (TNTLSNN) which showed selectivity toward lead ion was covalently bonded onto the surface of magnetic bead to construct a reusable biosorbent to remove Pb^{2+} from water. Compared to the bare bead without the linked peptides ($29.82 \mu\text{mol}\cdot\text{g}^{-1}$), the peptide-linked adsorbent showed 9 times higher removal capacity of lead ($246.05 \mu\text{mol}\cdot\text{g}^{-1}$). A selective adsorption of lead in the presence of interfering other metals is verified.

A heptapeptide with specific affinity to BPA, LysSerLeuGluAsnSerTyr (KSLENSY), was binded to magnetic bead to construct a new bio-based adsorbent for selective adsorption of BPA from aqueous solution. The BPA-binding peptide had higher selectivity toward BPA compared with structural analogs of BPA such as bisphenol F and bisphenol S. Moreover, the degradation of BPA was investigated by using peptide-mineralized photocatalytic TiO_2 particle by using the polystyrene (PS) bead fused with mineralization-inducing peptide (CHKKPSKSC).

1.7 Reference

Achim Steiner. (2016). *A snapshot of the world's water quality: towards a global assessment. United Nations Environment Programme.*

Ahmed, M. B., Zhou, J. L., Ngo, H. H., Guo, W., Thomaidis, N. S., & Xu, J. (2017). Progress in the biological and chemical treatment technologies for emerging contaminant removal from wastewater: A critical review. *Journal of Hazardous Materials, 323*, 274–298.

Al-Amshawee, S., Yunus, M. Y. B. M., Azoddein, A. A. M., Hassell, D. G., Dakhil, I. H., & Hasan, H. A. (2020). Electrodialysis desalination for water and wastewater: A review. *Chemical Engineering Journal, 380*(July 2019).

Alhogbi, B. G., Salam, M. A., & Ibrahim, O. (2019). Environmental remediation of toxic lead ions from aqueous solution using palm tree waste fibers biosorbent. *Desalination and Water Treatment, 145*(January), 179–188.

Almasi, A., Navazeshkha, F., & Mousavi, S. A. (2017). Biosorption of lead from aqueous solution onto *Nasturtium officinale*: Performance and modeling. *Desalination and Water Treatment, 65*(January), 443–450.

Alrumman, S. A., El-kott, A. F., & Keshk, S. M. A. S. (2016). Water Pollution : Source and Treatment Water Pollution : Source & Treatment, *6*(June), 88–98.

Amarasinghe, B. M. W. P. K., & Williams, R. A. (2007). Tea waste as a low cost adsorbent for the removal of Cu and Pb from wastewater. *Chemical Engineering Journal, 132*(1–3), 299–309.

- Badruddoza, A. Z. M., Shawon, Z. B. Z., Tay, W. J. D., Hidajat, K., & Uddin, M. S. (2013). Fe 3O 4/cyclodextrin polymer nanocomposites for selective heavy metals removal from industrial wastewater. *Carbohydrate Polymers*, *91*(1), 322–332.
- Blank-Shim, S. A., Schwaminger, S. P., Borkowska-Panek, M., Anand, P., Yamin, P., Fraga-García, P., ... Berensmeier, S. (2017). Binding patterns of homo-peptides on bare magnetic nanoparticles: Insights into environmental dependence. *Scientific Reports*, *7*(1), 1–11.
- Budinova, T. K., Petrov, N. V., Minkova, V. N., & Gergova, K. M. (1994). Removal of metal ions from aqueous solution by activated carbons obtained from different raw materials. *Journal of Chemical Technology & Biotechnology*, *60*(2), 177–182.
- Carolin, C. F., Kumar, P. S., Saravanan, A., Joshiba, G. J., & Naushad, M. (2017). Efficient techniques for the removal of toxic heavy metals from aquatic environment: A review. *Journal of Environmental Chemical Engineering*, *5*(3), 2782–2799.
- Carstea, E. M., Bridgeman, J., Baker, A., & Reynolds, D. M. (2016). Fluorescence spectroscopy for wastewater monitoring: A review. *Water Research*, *95*, 205–219.
- Dehghani, M. H., Ghadermazi, M., Bhatnagar, A., Sadighara, P., Jahed-Khaniki, G., Heibati, B., & McKay, G. (2016). Adsorptive removal of endocrine disrupting bisphenol A from aqueous solution using chitosan. *Journal of Environmental Chemical Engineering*, *4*(3), 2647–2655.
- Duffus, J. H. (1980). Environmental toxicology. *Environmental Toxicology*, 19–26.
- Elgallal, M., Fletcher, L., & Evans, B. (2016). Assessment of potential risks associated with chemicals in wastewater used for irrigation in arid and semiarid zones: A review. *Agricultural Water Management*, *177*, 419–431.

Fu, F., & Wang, Q. (2011). Removal of heavy metal ions from wastewaters: A review. *Journal of Environmental Management*, 92(3), 407–418.

Giovanella, P., Vieira, G. A. L., Ramos Otero, I. V., Pais Pellizzer, E., de Jesus Fontes, B., & Sette, L. D. (2020). Metal and organic pollutants bioremediation by extremophile microorganisms. *Journal of Hazardous Materials*, 382(July 2019), 121024.

Ji, Y., Yin, J., Xu, Z., Zhao, C., Huang, H., Zhang, H., & Wang, C. (2009). Preparation of magnetic molecularly imprinted polymer for rapid determination of bisphenol A in environmental water and milk samples. *Analytical and Bioanalytical Chemistry*, 395(4), 1125–1133.

Kositzki, M., Poullos, I., Malato, S., Caceres, J., & Campos, A. (2004). Solar photocatalytic treatment of synthetic municipal wastewater. *Water Research*, 38(5), 1147–1154.

Kozłowski, H., Janicka-Kłos, A., Brasun, J., Gaggelli, E., Valensin, D., & Valensin, G. (2009). Copper, iron, and zinc ions homeostasis and their role in neurodegenerative disorders (metal uptake, transport, distribution and regulation). *Coordination Chemistry Reviews*, 253(21–22), 2665–2685.

Kudo, A., Mahara, Y., Santry, D. C., Miyahara, S., & Garrec, J. P. (1991). Geographical distribution of fractioned local fallout from the Nagasaki A-bomb. *Journal of Environmental Radioactivity*, 14(4), 305–316.

Kusvuran, E., & Yildirim, D. (2013). Degradation of bisphenol A by ozonation and determination of degradation intermediates by gas chromatography-mass spectrometry and liquid chromatography-mass spectrometry. *Chemical Engineering Journal*, 220, 6–14.

- Ma, Y. R., Zhang, X. Le, Zeng, T., Cao, D., Zhou, Z., Li, W. H., ... Cai, Y. Q. (2013). Polydopamine-coated magnetic nanoparticles for enrichment and direct detection of small molecule pollutants coupled with MALDI-TOF-MS. *ACS Applied Materials and Interfaces*, 5(3), 1024–1030.
- Ma, Y., Shen, B., Sun, R., Zhou, W., & Zhang, Y. (2012). Lead(II) biosorption of an Antarctic sea-ice bacterial exopolysaccharide. *Desalination and Water Treatment*, 42(1–3), 202–209.
- Maruthamuthu, M. kannan, Hong, J., Arulsamy, K., Somasundaram, S., Hong, S. H., Choe, W. S., & Yoo, I. K. (2018). Development of bisphenol A-removing recombinant *Escherichia coli* by monomeric and dimeric surface display of bisphenol A-binding peptide. *Bioprocess and Biosystems Engineering*, 41(4), 479–487.
- Meeker, J. D. (2010). Exposure to environmental endocrine disrupting compounds and men's health. *Maturitas*, 66(3), 236–241.
- Nian, R., Kim, D. S., Nguyen, T., Tan, L., Kim, C. W., Yoo, I. K., & Choe, W. S. (2010). Chromatographic biopanning for the selection of peptides with high specificity to Pb²⁺ from phage displayed peptide library. *Journal of Chromatography A*, 1217(38), 5940–5949.
- Ren, Y. M., Yang, J., Ma, W. Q., Ma, J., Feng, J., & Liu, X. L. (2014). The selective binding character of a molecular imprinted particle for Bisphenol A from water. *Water Research*, 50, 90–100.
- Sharma, J., Mishra, I. M., & Kumar, V. (2015). Degradation and mineralization of Bisphenol A (BPA) in aqueous solution using advanced oxidation processes: UV/H₂O₂ and UV/S₂O₈²⁻ oxidation systems. *Journal of Environmental Management*, 156, 266–275.

- SIMON KAPAJ , HANS PETERSON, K. L. & P., & BHATTACHARYA. (2011). Human Health Effects From Chronic Arsenic Poisoning—A Review. *Journal of Environmental Science and Health - Part A Toxic/Hazardous Substances and Environmental Engineering*, 46(7), 677–679.
- Srivastava, N. K., & Majumder, C. B. (2008). Novel biofiltration methods for the treatment of heavy metals from industrial wastewater. *Journal of Hazardous Materials*, 151(1), 1–8.
- Tee, P. F., Abdullah, M. O., Tan, I. A. W., Rashid, N. K. A., Amin, M. A. M., Nolasco-Hipolito, C., & Bujang, K. (2016). Review on hybrid energy systems for wastewater treatment and bio-energy production. *Renewable and Sustainable Energy Reviews*, 54, 235–246.
- Visa, M., Bogatu, C., & Duta, A. (2010). Simultaneous adsorption of dyes and heavy metals from multicomponent solutions using fly ash. *Applied Surface Science*, 256(17), 5486–5491.
- Xiao, G., Fu, L., & Li, A. (2012). Enhanced adsorption of bisphenol A from water by acetylaniline modified hyper-cross-linked polymeric adsorbent: Effect of the cross-linked bridge. *Chemical Engineering Journal*, 191, 171–176.
- Xu, Z., Bae, W., Mulchandani, A., Mehra, R. K., & Chen, W. (2002). Heavy metal removal by novel CBD-EC20 sorbents immobilized on cellulose. *Biomacromolecules*, 3(3), 462–465.
- Yang, T., Liu, L. H., Liu, J. W., Chen, M. L., & Wang, J. H. (2012). Cyanobacterium metallothionein decorated graphene oxide nanosheets for highly selective adsorption of ultra-trace cadmium. *Journal of Materials Chemistry*, 22(41), 21909–21916.

Yu, Q., Deng, S., & Yu, G. (2008). Selective removal of perfluorooctane sulfonate from aqueous solution using chitosan-based molecularly imprinted polymer adsorbents.

Water Research, 42(12), 3089–3097.

Chapter 2

**Adsorptive removal of heavy metal ions in water using
poly(m-phenylenediamine) synthesized by laccase**

2.1 Introduction

Industrial waste effluents are known to contain various harmful pollutants including heavy metal ions and other toxic materials (Fu & Wang 2011). Water pollution due to heavy metal ions has, especially, become a serious problem because heavy metal ions are found to be highly toxic to human health. Until now, a variety of technologies have been developed for the removal of the toxic pollutants from the waste effluents such as ion exchange, membrane filtration, coagulation-flocculation, adsorption, precipitation, and electrochemical treatments (Ho 2006; Zularisam *et al.* 2006; Alyuz & Veli 2009; Martinez-Huitle & Brillas 2009; Verma *et al.* 2012). Among these methods, adsorption methods are considered simple and flexible in design and operation of the processes (Ho 2006). For these reasons, adsorptive removal of heavy metal ions has been actively explored employing various adsorbent materials such as activated carbons, biosorbents (Bin Yua, 2000), and polymers (Xiao & Thomas 2005; Huang *et al.* 2006; Pan *et al.* 2009; Rangel-Mendez *et al.* 2009; Bai *et al.* 2015).

Recently, polymers synthesized from aromatic amines and diamines have attracted growing interest for the adsorptive removal of pollutants because the polymers possess multiple amine functional groups and high thermal stability (Li *et al.* 2002). Particularly, phenylenediamine polymers have been actively studied to use as adsorbents for heavy metal ions such as Cr^{6+} , Ag^+ , Hg^{2+} or Pb^{2+} (Huang *et al.* 2006; Zhang *et al.* 2011). Conventionally, phenylenediamine polymers have been synthesized through chemical oxidation reactions using strong oxidants such as ammonium persulfate in strong acidic solutions (Huang *et al.* 2006). Unlike the chemical reactions, enzymatic reactions require no toxic oxidants for the polymerizations and do not produce harmful byproducts. Therefore, enzymatic

reactions have been applied as alternatives to chemical methods to develop environmentally friendly synthetic processes of polymers. Until now, syntheses of diverse polymers such as polyesters, polylactones, polyphenols, and conducting polymers have been attempted by using various enzymes including peroxidases, laccases, and lipases (Gross et al. 2001). Among these enzymes, laccases (benzenediol: oxygen oxidoreductase, EC 1.10.3.2) are versatile enzymes to catalyze oxidation of various organic and inorganic compounds using molecular oxygen contained in air as an oxidant (Madhavi & Lele 2009). Laccases have multicopper ions at their active sites which play essential roles in the oxidation mechanism; one oxygen molecule is reduced to water while four monomeric substrates are concomitantly oxidized to the corresponding cationic radicals. These enzymatically produced cationic radicals then undergo subsequent radical reactions to form corresponding oligomers or polymers (Madhavi & Lele 2009).

In our previous study, we successfully synthesized poly(m-PDA) using a laccase purified from *Trametes versicolor* as a catalyst in a benign 100% aqueous buffer without using any toxic oxidants, strong acids, or organic solvents (Raseda et al. 2016). In this paper, we report and compare the adsorptive properties of the enzymatically synthesized poly(m-PDA) for the adsorption of several heavy metal ions (Pb^{2+} , Cu^{2+} , Cr^{2+} , and Co^{2+}). We believe that this is the first work to characterize the adsorption properties of enzymatically synthesized poly(m-PDA) for the removal of diverse heavy metal ions from aqueous solutions.

2.2 Material and methods

2.2.1 Materials

Laccase (Sigma 53739) purified from *Trametes versicolor* was purchased from Sigma-Aldrich. Previous studies using both native-PAGE and sodium dodecyl sulfate (SDS)-PAGE methods revealed that this laccase is a pure enzyme of a molecular weight of about 66 kDa (Birhanli and Yesilada 2010; Raseda et al. 2014). Other chemicals including *m*-phenylenediamine (*m*-PDA), $\text{Pb}(\text{NO}_3)_2$, CoCl_2 , $\text{CuSO}_4 \cdot 5\text{H}_2\text{O}$, and $\text{Cr}(\text{NO}_3)_3 \cdot 9\text{H}_2\text{O}$ were also purchased from Sigma-Aldrich and used without further purification.

2.2.2 Enzymatic synthesis of poly(*m*-PDA)

Laccase-catalyzed synthesis of poly(*m*-PDA) was carried out in aqueous solutions as previously reported (Raseda *et al.* 2016). Typically, to a 10 mL buffer (10 mM citrate-phosphate buffer at pH 3) which was bubbled with air, *m*-phenylenediamine monomer was added to make a 50 mM *m*-phenylenediamine solution. Subsequently, 10 mg of laccase was added as a catalyst to initiate the polymerization reaction. After the addition of laccase, the reaction solution slowly turned dark green. The reaction solution was shaken at 25 °C for 48 h then filtered on a nylon membrane (0.2 μm, Whatman) to separate produced polymer precipitates from the solution. The polymer precipitates were repeatedly washed with copious amount of distilled water and methanol to remove enzymes and remaining monomers. Finally, poly(*m*-PDA) precipitates on a nylon membrane were dried under vacuum then stored at room temperature.

Previously, we reported that the poly(*m*-PDA) synthesized by laccase was found to be insoluble in water as well as in most organic solvents (Raseda *et al.* 2016). Poor solubility of poly(*m*-PDA) in water and most common organic solvents enables the easy separation of the polymer from aqueous solutions after the adsorption experiments using simple methods such as centrifugation or filtration. The enzymatically synthesized poly(*m*-PDA) has the morphology of aggregated globular particles of approximately 1 μm as detected by scanning electron microscopy (SEM) (Raseda *et al.* 2016).

2.2.3 Adsorption of metal ions by poly(*m*-PDA)

To characterize the adsorption behaviour of the enzymatically synthesized poly(*m*-PDA) for various metal ions, batch-type adsorption experiments were performed in distilled water. The initial concentrations of the metal ion salts were varied from 100 mg L^{-1} to 1,000 mg L^{-1} . The adsorption experiments were carried out in centrifuge tubes containing 10 mL adsorption solution where typically 10 mg of poly(*m*-PDA) was added as the adsorbent. Poly(*m*-PDA) was sonicated for 30 min to improve dispersion before adding to the adsorption solution. The adsorption reaction was performed with gentle shaking for 12 h at 25 °C. After the adsorption, the solutions were centrifuged to separate poly(*m*-PDA) adsorbent. The concentrations of dissolved metal ions were measured using an atomic absorption spectrophotometer (Shimadzu AA-7000). For each adsorption solution containing both a metal ion and poly(*m*-PDA), a separate control solution containing only the metal ion of the same concentration as in the corresponding adsorption solution was prepared and shaken for 12 h at 25 °C. No formation of precipitates in the control solutions was assured to exclude the errors in the calculation of adsorption capacity caused by the presence of the precipitates.

The adsorbed quantities of metal ions were calculated from the differences in the dissolved metal ion concentrations between the initial and the final adsorption solutions according to Eq. (2.1):

$$Q=(C_i-C)V/M, \quad (2.1)$$

where q ($\mu\text{mol g}^{-1}$) is the adsorbed quantity of a metal ion, C_i and C are the concentrations ($\mu\text{mol L}^{-1}$) of the metal ion in the initial solution before adding the adsorbent and the final solution after the adsorption, respectively, V (L) is the volume of the metal ion solution, and M (g) is the mass of the used adsorbent.

2.2.4 Fourier transform infrared (FTIR) spectroscopy

Chemical structures of poly(*m*-PDA) and the polymers containing adsorbed metal ions were analyzed using FTIR spectroscopy (Nicolet 380 FTIR spectrometer, Thermo Electron Co.). The wave number range was from 500 to 4000 cm^{-1} . Samples of poly(*m*-PDA) mixed with KBr were compressed to form pellets for the analysis by FTIR spectroscopy.

2.3 Results and Discussion

2.3.1 Structural characterization of poly(*m*-PDA)

Changes in the chemical structures of the poly(*m*-PDA) due to the adsorption of heavy metal ions were investigated by FTIR spectroscopy. Fig. 2-1 shows that FTIR spectra of poly(*m*-PDA) after the adsorption of the heavy metal ions are almost identical to that of initial intact poly(*m*-PDA) without adsorbed metal ions indicating that no chemical bonds are formed between the metal ions and the functional groups of the polymer. In all the FTIR spectra, the characteristic absorption bands at 3200~3400 cm^{-1} for N-H stretching of the primary amine ($-\text{NH}_2$) groups of *m*-PDA monomer are

broadened for poly(*m*-PDA) samples due to the formation of the secondary amines (-NH-) for poly(*m*-PDA) during the polymerization process through the formations of N-N or N-C bonds (Ichinohe *et al.* 1998).

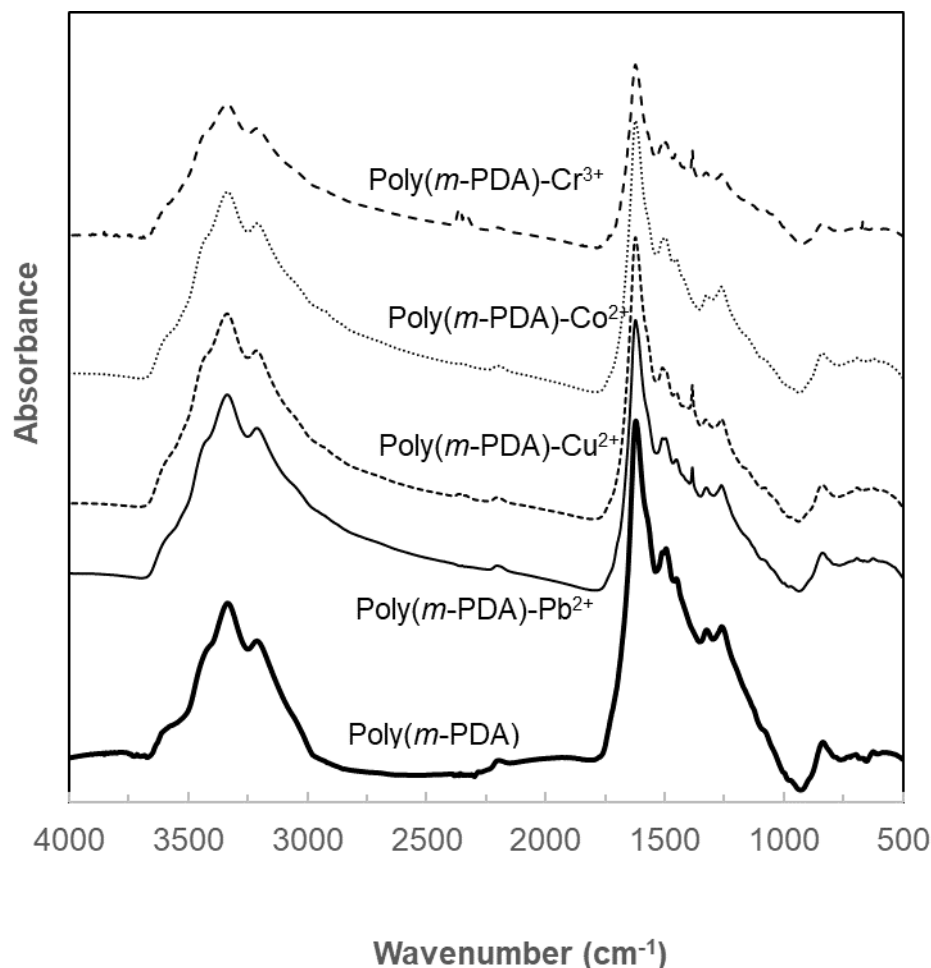


Figure 2-1 FTIR spectra of poly(*m*-PDA) synthesized by laccase and the poly(*m*-PDA) with adsorbed heavy metal ions.

The structural properties related to the adsorption capacity of the enzymatically synthesized poly(*m*-PDA) were assessed by measuring the Brunauer–Emmett–Teller (BET) specific surface area and pore size distribution of the polymer. The measured BET surface area is 32.2 m²/g with an average pore diameter of 14.6 nm. The Barrett-Joyner-Halenda (BJH) pore volume is 0.111 cm³/g. As shown in Fig. 2-2, the pores of poly(*m*-PDA) are found to be mostly in the mesoporous range (Pan *et al.* 2009). The

specific surface area and pore volume of the enzymatically synthesized poly(m-PDA) in this study are almost same as those of poly(m-PDA) synthesized by chemical oxidation method (Su et al. 2014) and about two times larger than another type of chemically synthesized poly(m-PDA) (Yu et al. 2013).

The specific surface area of poly(m-PDA) is, however, lower than various organic-inorganic hybrid adsorbents (Samiey et al. 2014). This entails the necessity for future work on the enzymatic synthesis of poly(m-PDA) hybrid materials which possess higher surface area and larger adsorption capability for heavy metal ions.

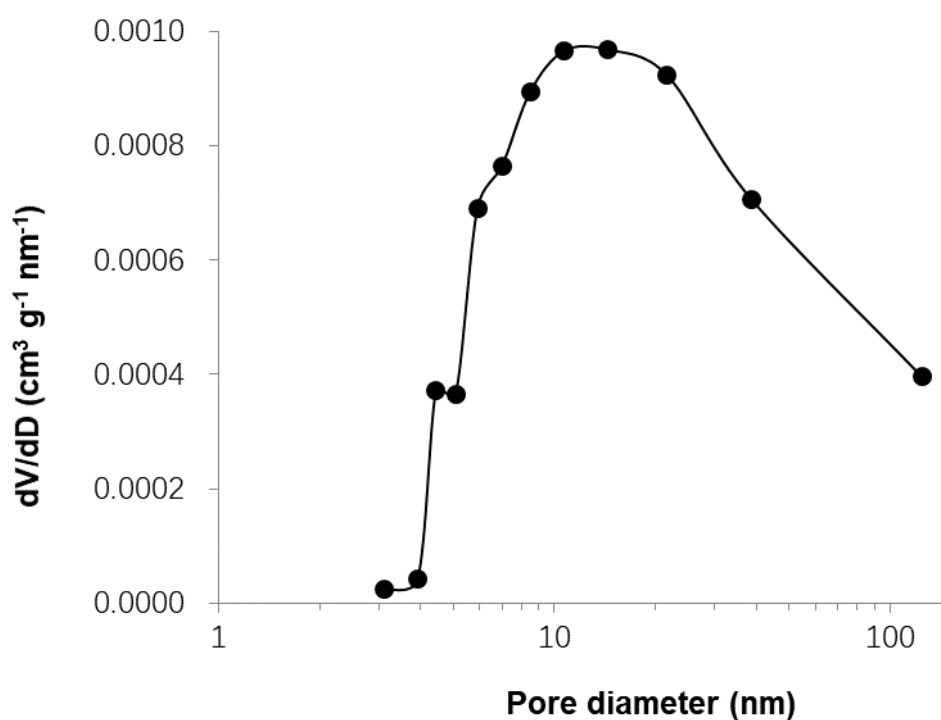


Figure 2-2 Pore size distribution of the poly(m-PDA) synthesized by laccase.

BET experiments were performed on an ASAP2020 analyzer (Micromeritics) using the adsorption of N₂ at 77K. Prior to measurement, the polymer samples were degassed at 423 K for 12 h then outgassed to 10⁻³ Torr.

2.3.2 Adsorption characteristics of poly(*m*-PDA) for Pb²⁺ ion

To evaluate the potential of poly(*m*-PDA) for the adsorptive removal of heavy metal ions, we selected Pb²⁺ as the representative heavy metal ion to perform preliminary studies. Pb²⁺ has particularly been of great environmental concerns among many heavy metal ions due to its widespread presence in various industrial effluents and strong toxicity to human health even at low concentrations (Fu & Wang 2011). At first, the influence of solutions on the adsorption of Pb²⁺ was measured using buffers of different pHs as well as distilled water to dissolve Pb(NO₃)₂. When pH of the solution was higher than or equal to 7, addition of Pb(NO₃)₂ in the solutions resulted in the formation of precipitates presumably due to the production of Pb(OH)₂ as also previously observed by Huang et al. (2006). Therefore, adsorption studies were not possible to perform in those basic solutions of higher pHs. Initial solution pH was, accordingly, adjusted between 2 to 5 by adding concentrated HCl to distilled water. As shown in Fig. 2-3, the adsorption capacity of poly(*m*-PDA) for Pb²⁺ was the highest in distilled water then decreased drastically as the solution pH was lowered to 2. Huang et al. (2006) proposed that Pb²⁺ cations bind to poly(*m*-PDA) by complexing with the nitrogen atoms contained in the polymer which donate electron pairs to the metal cations. The decreased adsorption capacity at lower pH was assumed to be caused by the competitive binding of H⁺ ions against lead ions on the same nitrogen adsorption sites of the polymer (Xiao & Thomas 2005). From these results, distilled water was selected as the solution for further adsorption experiments.

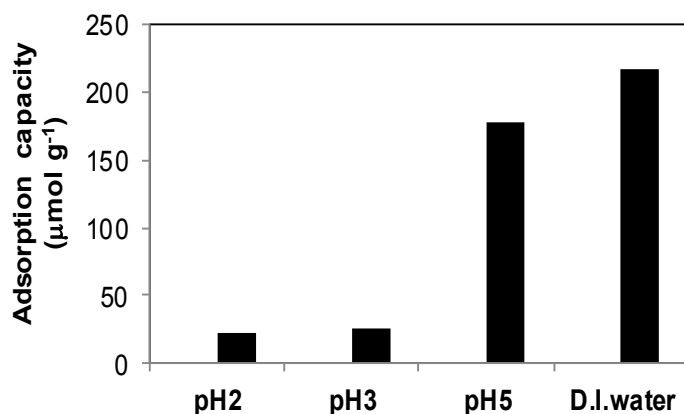


Figure 2-3 Effect of different solutions on the Pb²⁺ adsorption by enzymatically synthesized poly(*m*-PDA).

Adsorption of Pb²⁺ was performed in 10 mL of each solution initially containing 500 mg L⁻¹ of Pb(NO₃)₂ and 10 mg of poly(*m*-PDA) at 25 °C for 12 h.

2.3.3 Adsorption isotherms of poly(*m*-PDA) for heavy metal ions

To characterize the adsorption properties of poly(*m*-PDA) for various heavy metal ions, adsorption isotherm experiments were performed in distilled water containing varying concentrations of four different heavy metal ions (Pb²⁺, Cu²⁺, Co²⁺, Cr³⁺). Nonlinear adsorption isotherms presented in Fig. 2-4 indicate that adsorptions of the heavy metal ions onto poly(*m*-PDA) follow saturation isotherms at high concentrations of metal ions. Such adsorption data are, typically, described by the Langmuir isotherm equation (1) between q_e and C_e :

$$q_e = q_{max} K_L C_e / (1 + K_L C_e) \quad (2.2)$$

Where, q_e (μmol g⁻¹) is the adsorption capacity of an adsorbent at equilibrium and C_e (μmol L⁻¹) is the equilibrium concentration of a metal ion dissolved in solution. The two empirical parameters in the Langmuir isotherm equation, q_{max} (μmol g⁻¹) and K_L (L μmol⁻¹), represent the maximum adsorption capacity of the adsorbent and the

Langmuir equilibrium constant, respectively. The nonlinear equation (2.2) is linearized into equation (2.3) which can be used to verify that the adsorption takes place according to the Langmuir isotherm mechanism: The monolayer adsorption of adsorbate molecules is assumed on adsorbent's surface containing a finite number of adsorption sites. Once all adsorption sites are occupied due to the adsorption of the adsorbate molecules, no further adsorption takes place leading to the saturation point where the maximum adsorption capacity of the adsorbent is achieved (Chong & Volesky 1995).

$$C_e/q_e = C_e/q_{max} + 1/(q_{max} K_L) \quad (2.3)$$

Another frequently used adsorption isotherm model is Freundlich model which is used to describe multilayer adsorption and expressed by nonlinear equation (2.4) and the corresponding linearized equation (2.5):

$$q_e = K_F C_e^{1/n} \quad (2.4)$$

$$\ln q_e = \ln K_F + (\ln C_e)/n \quad (2.5)$$

Where the two parameters, K_F and n , are associated with adsorption capacity and adsorption affinity, respectively (Huang *et al.* 2006). We also tested the Freundlich equation to fit adsorption isotherm data and results are shown in Fig. 2.4. The results revealed that Freundlich equation cannot adequately describe the adsorption isotherms for the heavy metal ions on poly(*m*-PDA) with lower correlation coefficients R^2 (data not showed) than those for the Langmuir equation (Table 2.1). Therefore, it can be concluded that the heavy metals ions adsorb on poly(*m*-PDA) according to the Langmuir-type monolayer adsorption mechanism.

Figure 2.4 shows that the adsorption of the metal ions onto poly(m-PDA) satisfactorily follows Langmuir isotherm mechanism with high values of coefficients of determination, R^2 . The values of q_{max} and K_L listed in Table 1 were estimated by best fitting of the experimental data to Eq. (2.3) using a linear regression method.

The maximum adsorption capacity, q_{max} , of poly(m-PDA) is in the increasing order of Co^{2+} , Cr^{3+} , Pb^{2+} , and Cu^{2+} with the highest value of $556 \mu\text{mol g}^{-1}$ for Cu^{2+} and the lowest value of $172 \mu\text{mol g}^{-1}$ for Co^{2+} . The Langmuir equilibrium constant, K_L , is in the increasing order of Pb^{2+} , Cr^{3+} , Cu^{2+} , and Co^{2+} with the highest value of $14.8 \text{ L } \mu\text{mol}^{-1}$ for Co^{2+} and the lowest value of $1.15 \text{ L } \mu\text{mol}^{-1}$ for Pb^{2+} . The maximum adsorption capacities of the enzymatically synthesized poly(m-PDA) for heavy metal ions are found to be higher or comparable to existing adsorbents. For examples, carbon nanotubes were reported to have adsorption capacity of $492 \mu\text{mol g}^{-1}$ for Pb^{2+} (Kabbashi et al. 2009). Kongsuwan et al. (2009) used a biomass-derived activated carbon for the adsorption of Cu^{2+} and Pb^{2+} with the maximum adsorption capacity of 450 and $530 \mu\text{mol g}^{-1}$, respectively.

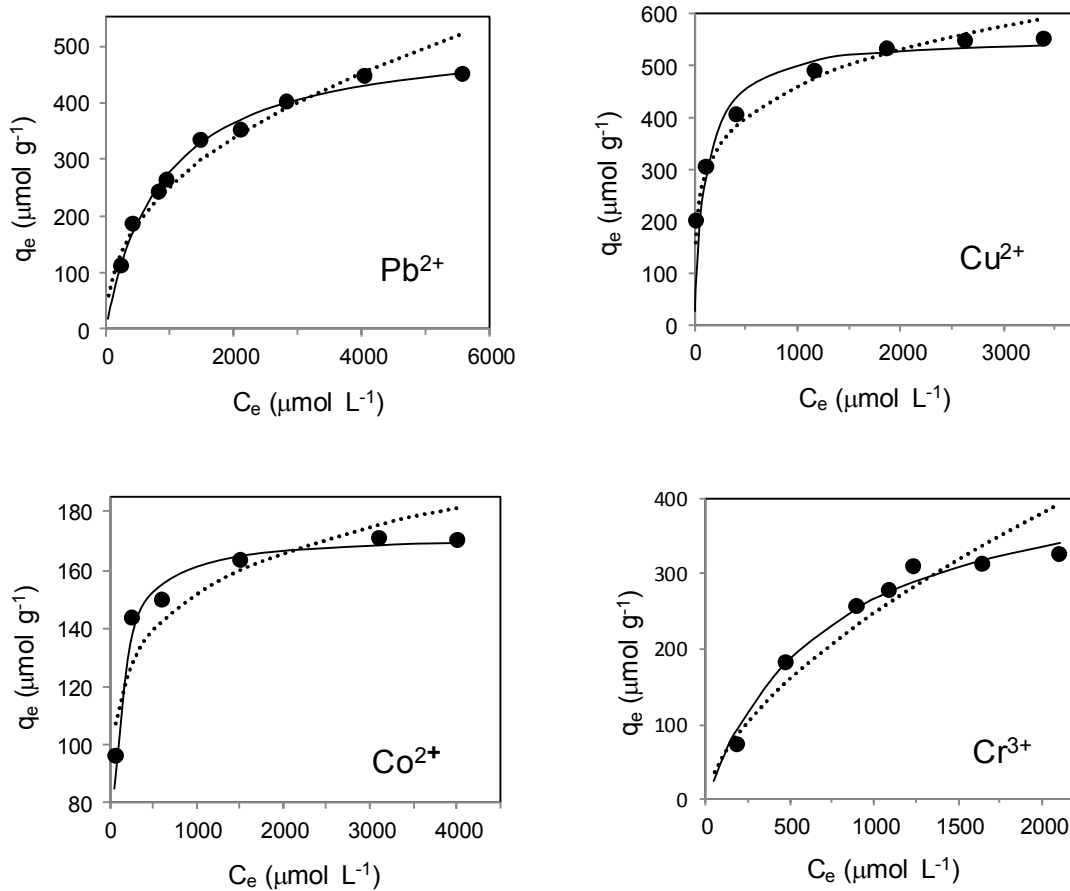


Figure 2-4 Adsorption isotherms for various heavy metal ions on enzymatically synthesized poly(*m*-PDA).

with optimum parameters estimated by linear regression analysis of the experimental data. Adsorption experiments were performed in 10 mL distilled water containing 10 mg poly(*m*-PDA) and varying concentrations of the metal ions at 25°C for 12 h.

Table 2-1 Langmuir isotherm parameters estimated by linear regression analysis and the calculated adsorbed fractions of BET surface area of poly(m-PDA) for the adsorption of the heavy metal ions

Metal ions	Langmuir model			Theoretical calculation		
	q max ($\mu\text{mol g}^{-1}$)	K_L (L $\mu\text{mol}^{-1}) \times 10^3$	R^2	Ionic radi- us(10^{-12} m) ^a	q_{mono} ($\mu\text{mol g}^{-1}$) ^b	q_{max}/q_{mono}
Pb ²⁺	526	1.15	0.9965	119	1202	0.44
Cu ²⁺	556	9.29	0.9986	73	3203	0.17
Cr ²⁺	476	1.23	0.9665	61.5	4495	0.11
Co ²⁺	172	14.8	0.9996	74.5	3074	0.056

^a Ionic radii of the metal ions were obtained from the report by Persson (2010)

^b The calculated amounts of metal ions required for the complete monolayer coverage of BET surface area ($32.2 \text{ m}^2 \text{ g}^{-1}$) of the enzymatically synthesized poly(m-PDA)

We defined q_{mono} as the theoretical amounts of metal ions necessary for complete monolayer coverage of BET surface area of poly(m-PDA), and calculated the q_{mono} values from Eq. (4) for Pb²⁺, Cr³⁺, Cu²⁺, and Co²⁺ using the reported ionic radii (r_i) of the metal ions (Persson 2010):

$$q_{mono} (\mu\text{mol g}^{-1}) = \text{surface area} (\text{m}^2 \text{g}^{-1}) \times 10^6 / (\pi (r_i(\text{m}))^2 \times 6.02 \times 10^{23}) \quad (2.4)$$

In addition, the ratio of the experimentally determined q_{max} to the calculated q_{mono} , q_{max}/q_{mono} , enables the theoretical determination of the maximum adsorbed fraction of BET surface area of the poly(m-PDA) with the metal ions. As listed in Table 1, Pb²⁺, which has the largest ionic radius of 119 pm, shows the highest maximum adsorbed fraction of 0.44. This means that 44% of the total BET surface area of poly(m-PDA) is theoretically occupied by the adsorbed Pb²⁺ molecules at saturation. For the metal ions

of smaller sizes, q_{max}/q_{mono} values decreased implying that less fractions of the surface area were occupied by the adsorbed smaller metal ions at saturation. Bohli et al. (2013) proposed that the hydration of the metal ions with water molecules in aqueous solutions can inhibit the adsorption of the metal ions on the adsorbent materials. Since smaller and higher valent metal ions have greater charge densities, it can be presumed that they are more strongly hydrated in aqueous solutions, and thereby experience decreased ability to adsorb on the adsorbent materials. This rationale can explain the lower calculated adsorbed fractions of the surface area of poly(m-PDA) for smaller metal ions, Cr^{3+} , Cu^{2+} , and Co^{2+} . However, the lowest q_{max}/q_{mono} value of 0.056 for Co^{2+} which has a slightly larger ionic radius than Cu^{2+} cannot be explained solely by the hydration effects and is to be investigated furthermore.

A few previous studies reported that chemically synthesized poly(m-PDA)s showed very high q_{max} values for the adsorption of metal ions (Huang et al. 2006; Su et al. 2014; Yu et al. 2013). For an example, Su et al. (2014) reported extremely high q_{max} value of 2359.3 mg g⁻¹ (21.9 mmol g⁻¹) for the adsorption of Ag^+ (ionic radius = 100 pm, molar mass = 107.9) on a chemically synthesized poly(m-PDA) which has a BET surface area of 60.2 m² g⁻¹. The q_{mono} and q_{max}/q_{mono} values calculated using our methods for this result are 3183 μ mol g⁻¹ and 6.9, respectively. These calculated values indicate that Ag^+ ions could be adsorbed about seven times of the complete monolayer coverage of the surface area of the poly(m-PDA) at saturation. Another study reported that Cr^{6+} was adsorbed with a q_{max} value of 500 mg g⁻¹ (9615 μ mol g⁻¹) on a chemically synthesized poly(m-PDA) having BET surface area of about 14 m² g⁻¹ (Yu et al. 2013). As found by the authors, upon adsorption, most Cr^{6+} are reduced to Cr^{3+} . Hence, we calculated q_{mono} and q_{max}/q_{mono} values for Cr^{3+} to be 1957 μ mol g⁻¹ and 4.9, respectively. These results suggest the possibility that q_{max} value in this report

is large enough to completely cover the surface area of the polymer adsorbent about five times. Huang et al. (2006) also reported a large q_{max} value of 242.7 mg g^{-1} ($1171 \text{ } \mu\text{mol g}^{-1}$) for the adsorption of Pb^{2+} on a chemically synthesized poly(*m*-PDA). Since BET surface area of this polymer was not reported, we cannot calculate the q_{max}/q_{mono} value for this case. Considering the fact that the principle assumption of the Langmuir isotherm model is the monolayer adsorption of molecules on the adsorbents, the use of the Langmuir model in these previous studies seems inappropriate. Furthermore, the possibility cannot be ruled out that some phenomena other than adsorption such as precipitation or aggregation of metal ions or their hydroxide complexes were involved interfering with the correct analyses of those experimental results.

2.4 Conclusions

Application of polymeric adsorbents which contain functional groups for the removal of metal ions dissolved in aqueous waste effluents is a promising environmental technology since the polymers can be prepared by simple synthetic methods utilizing cheap monomeric feedstocks. In this study, poly(*m*-PDA) which was enzymatically synthesized by laccase in aqueous buffer (10 mM citrate-phosphate, pH 3) was found to be useful in adsorbing diverse heavy metal ions. The adsorption isotherms of poly(*m*-PDA) for four different heavy metal ions including Pb^{2+} , Cu^{2+} , Co^{2+} , and Cr^{3+} were successfully described by Langmuir isotherm model. The poly(*m*-PDA) has high maximum adsorption capacity (q_{max}) especially for Cu^{2+} and Pb^{2+} demonstrating that the adsorption capacities of the enzymatically synthesized poly(*m*-PDA) for heavy metal ions are comparable to the common adsorbents such as activated carbons, carbon nanotubes, biomasses, and etc. According to our results on the effect of

solution pH on the Pb^{2+} adsorption, the enzymatically synthesized poly(*m*-PDA) was found to retain the similar adsorption mechanisms for heavy metal ions as that of the chemically synthesized poly(*m*-PDA) (Huang *et al.* 2006; Zhang *et al.* 2011). Most importantly, our study suggests that the synthesis of polymeric absorbents to remove heavy metal ions from waste water can be accomplished through simple and benign enzymatic methods.

2.5 References

Alyuz B. & Veli S. 2009 Kinetics and equilibrium studies for the removal of nickel and zinc from aqueous solutions by ion exchange resins. *Journal of Hazardous Materials*, 167(1-3), 482-488.

Chong K. H. & Volesky B. 1995 Description of two metal biosorption equilibria by Langmuir-type models. *Biotechnology and Bioengineering*, 47(4), 451-460.

Djebbar M. & Djafri F. 2016 Adsorption of Cu(II) on natural and treated clays. *Water Quality Research Journal*, 51 (1), 26-32.

Fu F. & Wang Q. 2011 Removal of heavy metal ions from wastewaters: a review. *Journal of Environmental Management*, 92(3), 407-418.

Gross R. A., Kumar A. & Kalra B. 2001 Polymer Synthesis by In Vitro Enzyme Catalysis. *Chemistry Reviews*, 101(7), 2097-2124.

Ho Y. S. 2006 Review of second-order models for adsorption systems *Journal of Hazardous Materials*, 136(3), 681-689.

Huang M., Peng Q. & Li X. 2006 Rapid and effective adsorption of lead ions on fine poly(phenylenediamine) microparticles. *Chemistry A European Journal*, 12(16), 4341-4350.

- Ichinohe D., Muranaka T. & Kise H. 1998 Oxidative polymerization of phenylenediamines by enzyme and magnetic properties of the products. *Journal of Applied Polymer Science*, 70(4), 717-721.
- Kabbashi N. A., Atieh M. A., Al-Mamun A., Mirghami M. E. S., Alam M. D. Z. & Yahya N. 2009 Kinetic adsorption of application of carbon nanotubes for Pb(II) removal from aqueous solution. *Journal of Environmental Science*, 21(4), 539-544.
- Kongsuwan A., Patnukao P. & Pavasant P. 2009 Binary component sorption of Cu(II) and Pb(II) with activated carbon from *Eucalyptus camaldulensis* Dehn bark. *Journal of Industrial and Engineering Chemistry*, 15(4), 465-470.
- Li X. G., Huang M. R., Duan W. & Yang Y. L. 2002 Novel multifunctional polymers from aromatic diamines by oxidative polymerizations. *Chemistry Reviews*, 102(9), 2925-3030.
- Madhavi V. & Lele S. S. 2009 Laccase: Properties and applications. *BioResources*, 4(4), 1694-1717.
- Martínez-Huitle C. A. & Brillas E. 2009 Decontamination of wastewaters containing synthetic organic dyes by electrochemical methods: A general review. *Applied Catalysis B:Environmental*, 87(3-4), 105-145.
- Pan B., Pan B., Zhang W., Lv L., Zhang Q. & Zheng S. 2009 Development of polymeric and polymer-based hybrid adsorbents for pollutants removal from waters. *Chemical Engineering Journal*, 151(1-3), 19-29.
- Raseda N., Hong S., Kwon O. Y. & Ryu K. 2014 Kinetic evidence for the interactive inhibition of laccase from *Trametes versicolor* by pH and chloride. *Journal of Microbiology and Biotechnology*, 24(12), 1673-1678.

- Raseda N., Park J. & Ryu K. 2016 Laccase-catalyzed polymerization of m-phenylenediamine in aqueous buffers. *Korean Journal of Chemical Engineering*, 33(10), 3011-3015.
- Samiey B., Cheng C. H. & Wu J. 2014 Organic-inorganic hybrid polymers as adsorbents for removal of heavy metal ions from solutions: A review. *Materials*, 7(2), 673-726.
- Su Z., Zhang L., Chai L., Wang H., Yu W., Wanga T. & Yang J. 2014 High-yield synthesis of poly(m-phenylenediamine) hollow nanostructures by a diethanolamine assisted method and their enhanced ability for Ag⁺ adsorption. *New Journal of Chemistry*, 38(8), 3984-3991.
- Tolian G., Jafari S. A. & Zarei S. 2015 Optimization of biosorption of nickel(II) and cadmium(II) by indigenous seaweed *Enteromorpha* using response surface methodology *Water Quality Research Journal*, 50(2), 109-122.
- Verma A. K., Dash R. R. & Bhunia P. 2012 A review on chemical coagulation/flocculation technologies for removal of colour from textile wastewaters. *Journal of Environmental Management*, 93(1), 154-168.
- Xiao B. & Thomas K. M. 2005 Adsorption of aqueous metal ions on oxygen and nitrogen functionalized nanoporous activated carbons. *Langmuir*, 21(9), 3892-3902.
- Zhang Y., Wang L., Tian J., Li H., Luo Y. & Sun X. 2011 Ag@Poly(m-phenylenediamine) Core-shell nanoparticles for highly selective, multiplex nucleic acid detection. *Langmuir*, 27(6), 2170-2175.
- Zularisam A. W., Ismail A. F. & Salim R. 2006 Behaviours of natural organic matter in membrane filtration for surface water treatment-a review. *Desalination*, 194(1-3), 211-231.

Chapter 3

Selective Removal of Lead Ion from Water by Magnetic Bead fused with Lead-recognizing Peptide

3.1 Introduction

Water pollution caused from heavy metals has become a serious problem since they are found to be highly toxic to human health. Among heavy metals, Pb(II) certified to be one of the highly toxic metals (Grau Benitez & Saul, 1983). Lead and its compounds are widely used in mining, printing, storage batteries, fuel, automobile batteries, plumbing and various other industries which resultantly released into water, producing an undesirable change in

the chemical and physical properties of water (Alrumman, El-kott, & Keshk, 2016). The awareness of increasing lead releasing implies studies concerning water and wastewater treatment to achieve the level of standards for drinking water and discharge into receiving water (Almasi, Navazeshkha, & Mousavi, 2017; Budinova, Petrov, Minkova, & Gergova, 1994).

Among various methods to handle lead issue (i.e. precipitation, ion exchange, membrane technologies), adsorption is regarded as efficient technique for the removal of lead from polluted water (Visa, Bogatu, & Duta, 2010). In the past decade, the search for low-cost adsorbents has got attention of the researcher worldwide. Biosorption has been confirmed a very promising process by using biological materials as biosorbents with different surface functional groups in the removal of heavy metals from wastewater (Alhogbi, Salam, & Ibrahim, 2019). Biomasses such as bacteria, fungi, algae, agricultural and industrial byproducts, and other biomaterials have been widely investigated. Yuhong Ma et al. studied the biosorption behavior and mechanism of an exopolysaccharide (EPS) secreted by a psychrotolerant bacterium *Pseudoalteromonas sp.* Bsi20310 for Pb(II) and assumed the functional groups such as -OH, C=O and C-O-C on Bsi20310 EPS may play important roles as biosorption

sites(Ma, Shen, Sun, Zhou, & Zhang, 2012). Amarasinghe et al. studied adsorption of copper and lead ions onto tea waste. Highest metal uptake of 48 and 65 mg/g were observed for Cu and Pb, respectively(Amarasinghe & Williams, 2007). Nevertheless, most of adsorbent reported has a weakness in terms of selectivity toward target component in complex environmental matrices, resulting in the excessive amount of adsorbent required for complete removal of target component. Considering of the practical value of lead in industry, an effective way to deal with lead contaminant water is to construct a selective removal adsorbent which means after the process, the adsorbed lead ion can be released and used again.

Specific peptide, the simplest biological recognition elements, are known to have high affinity toward corresponding targets which has received great attention. Compared with other biomolecules, peptides are small and easy to synthesize in a cost-efficient manner, as well as the target recognition by a peptide is rarely compromised despite the complex composition in the environment.

So various length of peptide sequences have been screened to be used as metal binders from aqueous solutions. Mejare, M et al. selected the peptide His-Ser-Gln-Lys-Val-Phe from a hexapeptide library with affinity for cadmium(Mejare, Ljung, & Bülow, 1997). Hnilova M et al. selected two novel gold-binding peptide (AuBP) sequences using a FLITrx random peptide display library(Shen, Cetinel, Sharma, Borujeny, & Montemagno, 2017). A highly specific lead-binding peptide TNTLSNN was screened in our former report by a chromatographic biopanning technique(Nian et al., 2010). The selected peptide sequence has high affinity to Pb^{2+} while displaying low binding affinities to different divalent metal ions such as Ni^{2+} , Cu^{2+} and Co^{2+} .

Recombinant Escherichia coli displaying this peptide has been researched for lead adsorption capacity(Nguyen et al., 2013). However, the centrifugation step for

isolating the bacteria is time-consuming and would complicate the experimental procedure. Furthermore, it is impossible to thoroughly retrieve the analyte-adsorbed material from solution even by centrifugation at high speed, which would cause sample loss during separation step and limit the determination of trace analytes. Magnetic bead, with unique magnetic separation ability, can simplify the isolation procedure and speed up the assay process.

As a follow-up study herein, we constructed a reusable peptide-based adsorbent based on magnetic bead, which could be easily recovered by magnetic force from water after a single use. The adsorbent mass, contact time, pH, kinetics, and isotherm for constructed adsorbent were determined. While the selectivity is the most important property, the competitive adsorption of Pb^{2+} within the existence of Ni^{2+} , Cu^{2+} and Co^{2+} was also tested. Our results demonstrate that the adsorption process was fitted well with Langmuir isotherm and the constructed adsorbent still shows high selectivity towards lead ion. As it can be recycled easily from waste water, it also shows a potential for lead recycle.

3.2 Materials and Methods

3.2.1 Materials

4-morpholineethanesulfonic acid (MES), N-(3-dimethyl aminopropyl)-N'-ethylcarbodiimide hydrochloride (EDC), N-hydroxy-succinimide (NHS), ethylene diamine tetraacetic acid (EDTA), bovine serum albumin (BSA, A7906), anhydrous acetonitrile (ACN) and the nitrate salts of all the cations (Pb^{2+} , Cu^{2+} , Co^{2+} , Ni^{2+}) were purchased from Sigma-Aldrich (St. Louis, MO, USA) and used without further purification. EDC, NHS and EDTA were dissolved in 25mM MES buffer (pH 5). The

lead-binding peptide (TNTLSNN, M=1189.25), previously screened (Nian et al. 2010), and the reverse sequence peptide (NNSLTNT) were custom synthesized by Bio-FD&C (Incheon, Republic of Korea). Both sequence of the peptides was dissolved in 100 mM MES buffer (pH 6.8) to give 0.1 g·L⁻¹, respectively and stored at 4 °C before use.

3.2.2 Adsorption onto bare magnetic bead

Depending on the surface characteristics of magnetic bead, lead may be adsorbed onto bare bead itself. Thus, several types of commercially available magnetic beads were compared to select the bead adsorbing the least amount of lead on its bare surface. Four kinds of beads with functional carboxyl group such as DynabeadsTM M-270 Carboxylic Acid (Thermo Fisher Scientific, Oslo, Norway), AccuBeadTM COOH magnetic beads (Bioneer Inc, Daejeon, Korea), Cytodiagnostic ZeptoTM Mag Carboxyl Microspheres (CytoDiagnostics Inc., Ontario, Canada) and BcMagTM long-arm carboxy-terminated magnetic beads (Bioclone Inc., San Diego, US) were purchased and compared. 3 mg of each bead was washed with 25 mM MES buffer twice and then incubated in 5 mL of 60 mg·L⁻¹ Pb(NO₃)₂ for 1 h, respectively. The supernatant were collected and analyzed using atomic absorption spectrophotometer (AAS, Shimadzu AA-7000).

3.2.3 Construction of Peptide-binded magnetic bead

The AccuBeadTM COOH magnetic bead, selected as the bead adsorbing the least amount of lead on its bare surface, was washed twice with 25 mM MES buffer (pH 5). Then, the peptide was fused onto the bead surface by carbodiimide-mediated amide bond formation between N-terminus of peptide and the carboxylic acid groups on the

bead surface, according to the slightly modified protocol of Thermo Fisher Scientific (Fischer, 2010). 3 mg of bead was mixed with 50 μL of EDC (50 g/L in cold 25 mM MES) and NHS (50 g/L in 25 mM MES) with slow tilt rotation at room temperature for 30 minutes. Then, the activated bead was collected by magnet and washed again with 25 mM MES. 100 μL of peptide (100 $\text{mg}\cdot\text{L}^{-1}$) was incubated with the EDC/NHS-activated bead at room temperature in 25 mM MES buffer for 1 hour. After collection of peptide-coated bead, the peptide concentration remained in the supernatant was measured to determine the amount of peptide coated onto bead. For the comparison purpose, the activated bead coated by BSA protein was prepared via similar protocol.

3.2.4 Lead adsorption

1000 $\text{mg}\cdot\text{L}^{-1}$ of Pb^{2+} solution was prepared with analytical grade lead nitrate as stock solution and was further diluted to corresponding concentrations before use.

Before adsorption, the peptide-coated bead is additionally incubated with BSA in order to block the adsorption of lead ion on the surface of bare bead where were not coated by peptide successfully. All the adsorption experiments were carried out at a temperature of 25 $^{\circ}\text{C}$. All the adsorption data were averaged from three independent experiments.

Adsorption were conducted by adding prepared peptide-coated bead into 5 mL $\text{Pb}(\text{NO}_3)_2$ under corresponding concentration, and record the initial concentration as C_i . After shaking for 1 hour, use magnet to separate the adsorbent and the solution. Then take the supernatant for measurement by AAS and record the concentration as C_e . The removal rate of lead by the magnetic adsorbent is recorded as $(C_i - C_e) / C_i$.

For clear comparison for showing the adsorption capacity of peptide, activated bead by EDC/NHS and bead which were modified with BSA, forward sequence or reverse sequence separately were used to adsorb Pb^{2+} of $60 \text{ mg}\cdot\text{L}^{-1}$.

In order to investigate kinetics of Pb^{2+} adsorption, concentration of supernatant were measured under different time interval (10, 30, 60, 90 min).

Adsorption isotherm were studied by adding previously prepared peptide-binded bead into 5 ml Pb^{2+} solutions with initial concentrations from $20 \text{ mg}\cdot\text{L}^{-1}$ to $600 \text{ mg}\cdot\text{L}^{-1}$.

The reusable property is conducted with 5 mL 1 mM EDTA for 5 minutes after adsorption. After being separated and washed with MES, the regenerated bead was put in 5 mL $60 \text{ mg}\cdot\text{L}^{-1}$ Pb^{2+} solutions again and the regenerability was tested 6 times.

As for selectivity, adsorption experiments were practiced in Pb^{2+} , Cu^{2+} , Co^{2+} and Ni^{2+} respective single metal species as well in quaternary metal species. Finally, we also tested the selectivity in synthetic municipal wastewater. The concentration of initial metal ion keeps $60 \text{ mg}\cdot\text{L}^{-1}$.

3.2.5 Analysis

The amount of peptide or protein fused to the bead was determined by measuring the concentrations of peptide in MES supernatant via HPLC (Agilent 1200, UV 220 nm, USA) at 25°C . A C18 column (250*4.6 mm 5micron, Kromasil 100-5-C18, Kromasil.) was used. Acetonitrile and water with 0.1%(v/v) TFA were used for gradient elution from 0 to 70% (v/v) of acetonitrile at a flow rate of 1 mL/min.

3.3 Results and discussion

3.3.1 Selection of bead (Pb^{2+} adsorption onto bare bead)

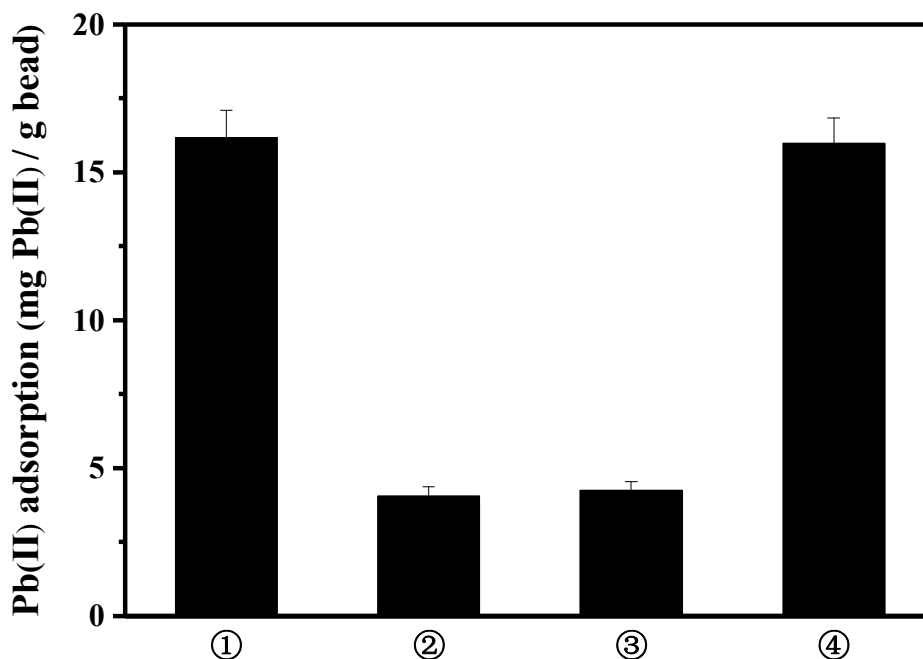


Figure 3-1 Pb^{2+} adsorption onto bare bead (mg Pb^{2+} /g bead)

① Dynabeads[®] M-270 Carboxylic Acid ② AccuBead[™] COOH magnetic beads ③ Cytodiagnostic Zepto[™] Mag Carboxyl Microspheres and ④ BcMag[™] Long-arm Carboxy-terminated magnetic beads

3mg bead + 60 mg/L $\text{Pb}(\text{NO}_3)_2$, 1 hour, 25°C

To construct reusable adsorbing system, the magnetic-core bead enabling magnetic separation from water, was used as a basic frame to bind the peptide on the bead surface. Since the peptide has amine and carboxylic group in both ends, the lead-binding peptide can be linked, via EDC/NHS chemistry, to the bead functionalized with NH_2/COOH on its surface. Depending on the surface characteristic of bead, meanwhile, the lead ion can be adsorbed to the bare surface of bead, not occupied with peptide. To examine the lead removal performance mainly caused by lead-binding peptide, not by the raw bead, various kinds of commercially available magnetic bead was tested to select the bead with low affinity to lead. Among four type of beads,

shown in Fig. 1, AccuBead™ COOH magnetic beads and Cytodiagnostic Zepto™ Mag bead adsorbed less amount of lead compared to the two other types of bead. Since AccBead™ COOH magnetic beads was cheaper and separated better by magnet, it was selected as a frame to bind peptide.

3.3.2 Pb²⁺ adsorption using peptide-binded magnetic bead

After choosing AccuBead™ COOH magnetic beads as the experiment material, we conduct EDC/NHS experiment to combine the peptide to bead. 1 hour is investigated to be the best reaction period for combining the peptide to bead.

In order to determine the optimal adsorption time towards lead ion, the Pb²⁺ adsorption period was investigated from 10 to 90 minutes. Then peptide-binded bead reacted with 5 mL 60 mg/L Pb(NO₃)₂. As shown in Figure 2, adsorption capacity towards Pb²⁺ almost get the maximum while the peptide incubation time is 30 minutes. It can be seen that within 30 minutes, the adsorption process is rapid and the speed is relatively high. After 60 minutes, the adsorption rate decreases and tend to balance, which means the adsorption site had been occupied sufficiently. While previous work used our peptide inducted to E.coli system(Nguyen et al., 2013) need 2 hours to get the maximum adsorption, using magnetic bead seems to be faster and more convenient. Although the adsorption capacity almost got the maximum at 30 minutes, it still got growing till 90 minutes, so we choose 60 minutes as the following experiment condition.

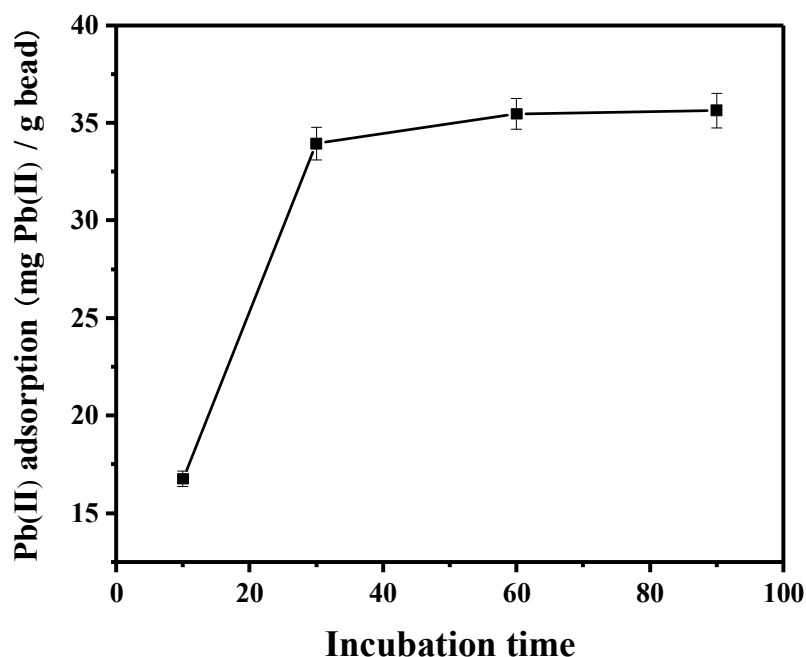


Figure 3-2 Kinetics of Pb²⁺ adsorption onto peptide-coated bead

100 μL 100 mg·L⁻¹ peptide incubated with 3 mg bead for 1 hour

peptide-binded bead reacted with 5 mL 60 mg·L⁻¹ Pb²⁺ from 10 to 90 minutes

3.3.3 Parallel experiment

In order to show that lead ion is adsorbed by peptide but not the bead, we calculate the amount of peptide adsorbed by bead and compare the difference among each independent experiment.

Pb²⁺ adsorption capacity (mg/g bead) was calculated using the mass balance

$$q = \frac{V (C_i - C_e)}{m}$$

where V is the solution volume, m is the amount of bead, and C_i and C_e are the initial and equilibrium metal concentrations, respectively.

As we can see in the table 1, the lead ion adsorption capacity is changed with the amount of peptide which means the lead ion adsorption is decided by peptide.

Furthermore, adsorption capacity of activated bead which is just reacted with EDC/NHS, bead which were further modified with BSA, forward sequence peptide, respectively, were compared in figure 3. We can see that beads without lead selective peptide almost show no adsorption towards lead ion. Compared with peptide-binded bead that show 34.1 mg/g towards lead ion, BSA-coated bead only shows 3.5 mg/g which is almost 10 times difference. We presume that since BSA is a large protein, it would compete the binding site on bead with metal ion. And after peptide folding, there isn't much function group on the protein surface such as $-NH_2$ which can complex metal ion. So, even there may be some blank sites on magnetic bead that didn't combine peptide successfully, BSA can block the blank site. We can conclude that the adsorption of lead ion in our experiment is due to peptide.

Peptide sequence	peptide bonded onto bead (mg/g)	Pb ²⁺ adsorbed onto peptide-binded bead (mg/g)
TNTLSNN (Forward sequence)	0.89 ± 0.049	34.1 ± 1.3
NNSLTNT (Reverse sequence)	0.79 ± 0.052	30.9 ± 1.6

Table 3-1 Different peptide sequence on Pb²⁺ adsorption capacity

100 μL 100 mg·L⁻¹ peptide incubated with 3 mg bead for 1 hour

5 mL 60 mg·L⁻¹ Pb²⁺

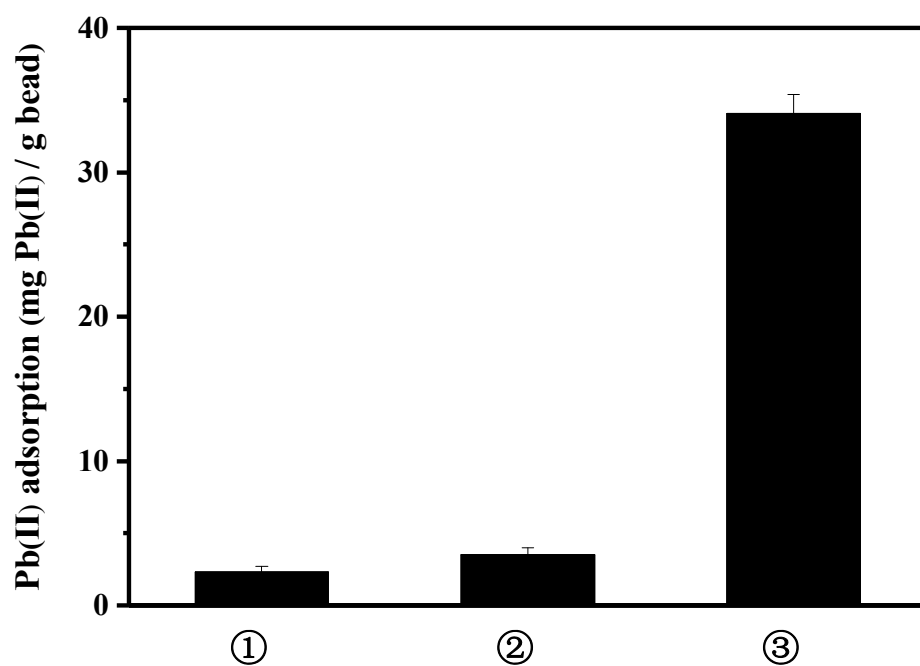


Figure 3-3 Effect of different modification on Pb^{2+} adsorption capacity

① NHS/EDC Activeted bead ② BSA-coated bead

③ peptide-binded bead

5 mL $60 \text{ mg} \cdot \text{L}^{-1} \text{ Pb}^{2+}$

3.3.4 Lead Adsorption isotherm study

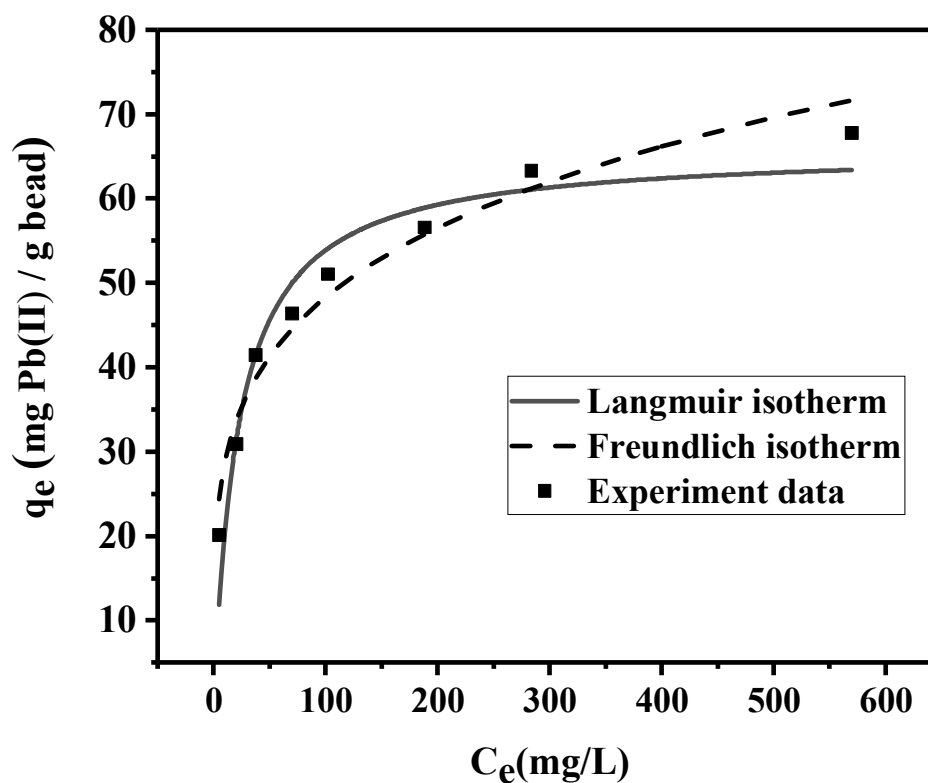
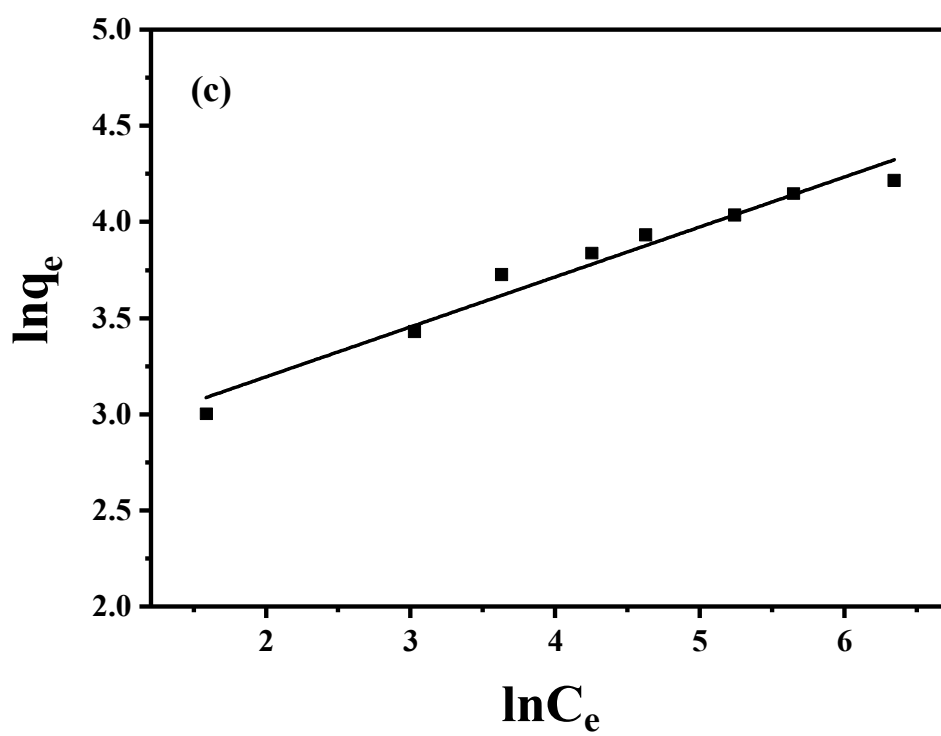
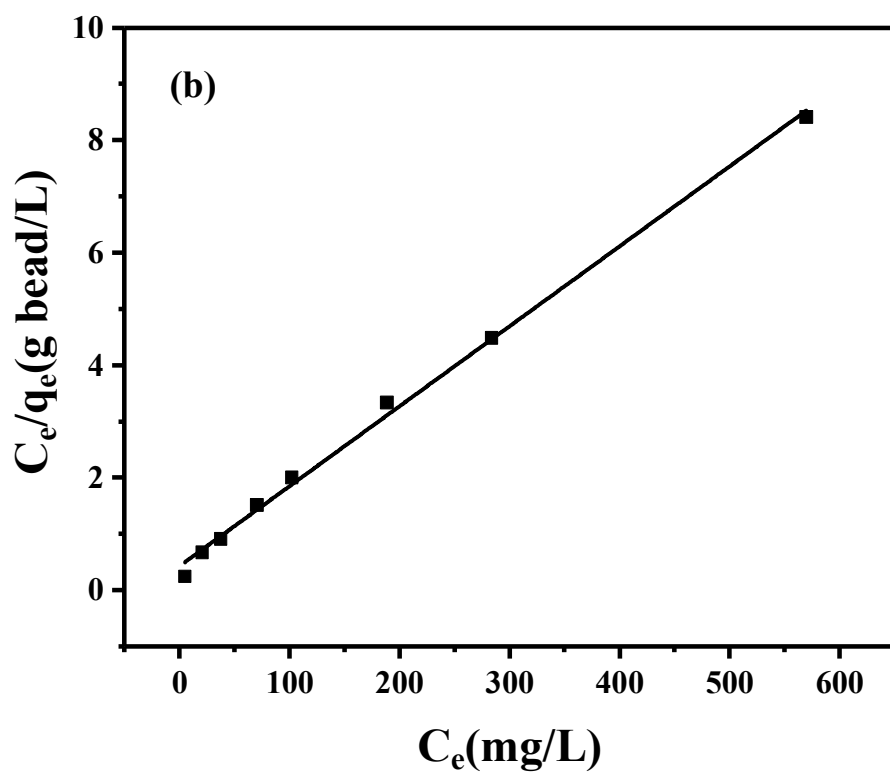


Figure 3-4 Adsorption isotherms for the adsorption of lead ions onto peptide-binded bead.

(a Experimental data and non-linear modeling by Langmuir and Freundlich isotherms; b linear Langmuir isotherm and c linear Freundlich)

100 μ L peptide incubated with 3mg bead for 1 hour. Then incubated with 5mL lead nitrate for 1 hour, from 20~600mg L⁻¹



	Langmuir isotherm			Freundlich isotherms		
	q_{max} (mg g ⁻¹)	K_L (L mg ⁻¹)	r^2	k_f	n	r^2
Nonlinear- ized	65.852 ± 3.25	0.045 ± 0.010	0.9222	16.97 ± 1.77	4.41	0.9590
Linearized	70.42	0.033	0.9969	14.51	3.85	0.9671

Table 3-2 Parameters fitted with both nonlinear and linearized adsorption isotherm

To characterize the adsorption properties of peptide-binded bead for lead ion, adsorption isotherm experiments were performed under varying initial concentrations of lead ion. Both Langmuir and Freundlich isotherm were used to fit the data. Langmuir model is used to describe the homogeneous adsorption, with the equation expressed by following equation:

$$q_e = \frac{q_{max}K_L C_e}{1 + K_L C_e} \quad (1)$$

Its linearized equation is present as below:

$$\frac{C_e}{q_e} = \frac{1}{q_{max}} C_e + \frac{1}{q_{max}K_L} \quad (2)$$

Freundlich model is applicable to heterogeneous adsorption, which is described by

$$q_e = k_f C_e^{1/n} \quad (3)$$

Its linearized equation is shown as follows:

$$\ln q_e = \ln k_f + \frac{1}{n} \ln C_e \quad (4)$$

Where, q_e (mg·g⁻¹) is the adsorption capacity of peptide-binded bead at equilibrium and C_e (mg·L⁻¹) is the equilibrium concentration of lead ion dissolved in solution. The

two empirical parameters in the Langmuir isotherm equation, q_{max} ($\text{mg}\cdot\text{g}^{-1}$) and K_L ($\text{L}\cdot\text{mg}^{-1}$), represent the maximum adsorption capacity of the adsorbent and the Langmuir equilibrium constant, respectively. Nonlinear adsorption isotherms in Figure 3-4 indicate that adsorptions of the lead ions onto our adsorbent follow saturation isotherms at high concentrations.

3.3.5 Repeated use of peptide-coated bead

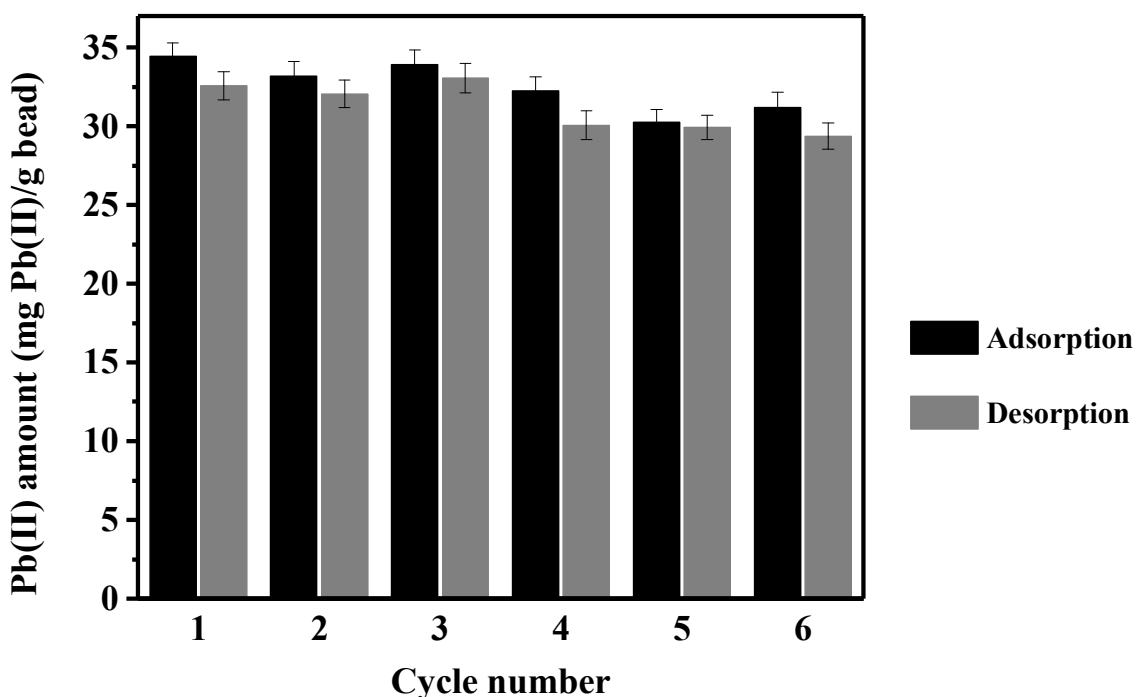


Figure 3-5 The adsorption and desorption of Pb^{2+} with EDTA for 6 times

Regenerability experiment is performed to prove that the combined adsorbent can be reused. Desorption studies were conducted by mixing the used adsorbent with 5 mL 1 mM EDTA for 5 minutes at room temperature. The mixture was magnetically separated and the final concentration of Pb^{2+} were determined. The initial concentration of Pb^{2+} in adsorption-desorption experiment was $60 \text{ mg}\cdot\text{L}^{-1}$. The result

obtained shows that the spent adsorbent can be regenerated and reused with a high desorption efficiency. Fig.3-5 shows the adsorption and desorption amount of Pb^{2+} , we can see there is no large loss after 6 cycles. Compared with the first adsorption capacity which was $33.4 \text{ mg}\cdot\text{g}^{-1}$, the last cycle showed $31.8 \text{ mg}\cdot\text{g}^{-1}$ adsorption capacity, which is only around 4.8% lost. Since the most important problem with biosorbent is that most of them have low mechanical strength and are hard to be recycled, our novel adsorbent showed good regenerability thereby preventing the discharge of secondary pollutants into the environment, as well as reducing cost and enhancing the availability of adsorbent.

3.3.6 Selective lead adsorption

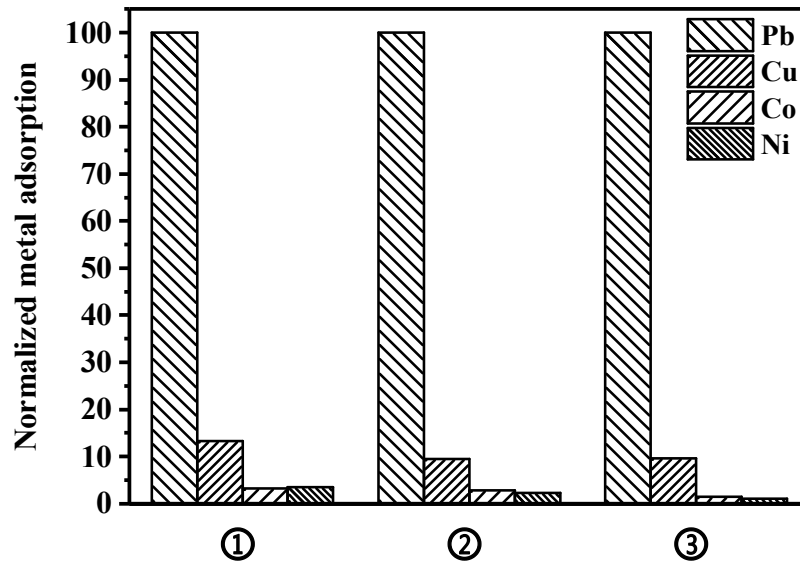


Figure 3-6 Comparison of the metal adsorption capacity in three different solution system

100 μ L peptide incubated with 3mg bead for 1 hour.

Then incubated with 5mL corresponding solution for 1 hour

① Single metal solution: 60mg \cdot L⁻¹ Pb²⁺, Cu²⁺, Co²⁺ and Ni²⁺ respectively; ② Mixed metal solution: 60mg \cdot L⁻¹ Pb²⁺, Cu²⁺, Co²⁺ and Ni²⁺ mixed together; ③ Artificial wastewater: solution ② mixed with solution made with method in table 3.

Chemicals	Concentration (mg L ⁻¹)
Peptone	160
Yeast extract	110
Urea	30
K ₂ HPO ₄	28
NaCl	7
CaCl ₂ ·2H ₂ O	4
Mg ₂ SO ₄ ·7 H ₂ O	2

Table 3-3 Chemical composition of the synthetic wastewater

(Kositzi, Poullos, Malato, Caceres, & Campos, 2004)

Since all of them are divalent cation ion as well the most common pollution ion in water, we choose Pb^{2+} , Cu^{2+} , Co^{2+} and Ni^{2+} for selective adsorption experiments. We practiced experiment in single metal species as well as in quaternary metal species in order to highlight the selectivity of the biosorbent. In addition, to certificate its application in industry, we also tested the selectivity in synthetic municipal wastewater. The concentration of initiate metal ion keeps $60 \text{ mg}\cdot\text{L}^{-1}$.

As we can see in the figure 3-6, no matter in which system, the constructed biosorbent always shows the highest removal capacity toward Pb^{2+} while the adsorption capacity towards Ni^{2+} and Co^{2+} is always negligible, and the Cu^{2+} remains partly removed. We suspect it may be caused by the similar property of lead and copper ion. Bare bead shows adsorption capacity of 7.12 and 8.06 mg/g towards Pb^{2+} and Cu^{2+} relatively, we can say that the binding affinity of bare bead seems higher toward Cu^{2+} . In contrast, the peptide-binding bead showed significantly improved binding to Pb^{2+} rather than other ions. This indicates that the adsorption of lead ion on constructed biosorbent is conducted by the lead-binding peptide on the surface of bead. Although there is a bit decrease of lead adsorption capacity in mixture metal ion system, the corresponding selectivity $K_{\text{Pb/Cu}}$ is improved from 4.08 to 4.36, which ensures that the constructed biosorbent shows an increase binding specificity to Pb^{2+} over Cu^{2+} even in the competitive adsorption environment. More importantly, the adsorption capacity in artificial wastewater still shows 6 times higher toward Cu^{2+} and 13 times higher toward Ni^{2+} and Co^{2+} which certificate the possibility to use the constructed biosorbent in real industry. The selectivity experiments showed that the peptide-binded bead showed high specificity and affinity to Pb^{2+} while displaying low binding affinities to other divalent metal ions, which means not only the absorbent can be reused but also exists the possibility for application in lead ion recovery.

3.4 Conclusion

We succeeded in combining the previously discovered peptide sequence, TNTLSNN which exhibit a specific affinity to lead ion with the magnetic bead and successfully implement the selective removal of lead with the constructed biosorbent. The adsorption capacity was investigate and adsorption equilibrium data are very well fitted to the Langmuir isotherm, the maximum adsorption rate (q_{\max}) came out to be $70.42 \text{ mg}\cdot\text{g}^{-1}$; And with the strong mechanical strength of the magnetic bead, the constructed biosorbent can be reused for several times; The selectivity toward lead ions over other metal ions in M13 phage while the peptide sequence was discovered was also maintained here in the constructed magnetic bead based biosorbent. While the newly constructed biosorbent owns a high magnet response property and can be separated easily from water, this biosorbent can also be used as a material to selectively separate lead ions from other metals for possible recovery in water treatment.

3.5 References

- Alhogbi, B. G., Salam, M. A., & Ibrahim, O. (2019). Environmental remediation of toxic lead ions from aqueous solution using palm tree waste fibers biosorbent. *Desalination and Water Treatment*, 145(January), 179–188.
- Almasi, A., Navazeshkha, F., & Mousavi, S. A. (2017). Biosorption of lead from aqueous solution onto *Nasturtium officinale*: Performance and modeling. *Desalination and Water Treatment*, 65(January), 443–450.
- Alrumman, S. A., El-kott, A. F., & Keshk, S. M. A. S. (2016). Water Pollution : Source and Treatment Water Pollution : Source & Treatment, 6(June), 88–98.

- Amarasinghe, B. M. W. P. K., & Williams, R. A. (2007). Tea waste as a low cost adsorbent for the removal of Cu and Pb from wastewater. *Chemical Engineering Journal*, 132(1–3), 299–309.
- Budinova, T. K., Petrov, N. V., Minkova, V. N., & Gergova, K. M. (1994). Removal of metal ions from aqueous solution by activated carbons obtained from different raw materials. *Journal of Chemical Technology & Biotechnology*, 60(2), 177–182.
- Fischer, M. J. E. (2010). Amine Coupling Through EDC/NHS: A Practical Approach. *Surface Plasmon Resonance*, 627, 55–73.
- Grau Benitez, N. F., & Saul, G. M. (1983). The effect of β -dicalcium silicate, α -monocalcium silicate and calcium hydroxide upon the removal of lead (pb²⁺) ions from aqueous solution. *Journal of Chemical Technology and Biotechnology. Chemical Technology*, 33(6), 309–321.
- Kositzki, M., Poulis, I., Malato, S., Caceres, J., & Campos, A. (2004). Solar photocatalytic treatment of synthetic municipal wastewater. *Water Research*, 38(5), 1147–1154.
- Ma, Y., Shen, B., Sun, R., Zhou, W., & Zhang, Y. (2012). Lead(II) biosorption of an Antarctic sea-ice bacterial exopolysaccharide. *Desalination and Water Treatment*, 42(1–3), 202–209.
- Mejåre, M., Ljung, S., & Bülow, L. (1997). Selection of cadmium specific hexapeptides and their expression as ompa fusion proteins in e.coli. *FASEB Journal*, 11(9), 489–494.
- Nguyen, T. T. L., Lee, H. R., Hong, S. H., Jang, J. R., Choe, W. S., & Yoo, I. K. (2013). Selective lead adsorption by recombinant Escherichia coli Displaying a Lead-Binding Peptide. *Applied Biochemistry and Biotechnology*, 169(4), 1188–1196.

Nian, R., Kim, D. S., Nguyen, T., Tan, L., Kim, C. W., Yoo, I. K., & Choe, W. S. (2010). Chromatographic biopanning for the selection of peptides with high specificity to Pb²⁺ from phage displayed peptide library. *Journal of Chromatography A*, 1217(38), 5940–5949.

Shen, W. Z., Cetinel, S., Sharma, K., Borujeny, E. R., & Montemagno, C. (2017). Peptide-functionalized iron oxide magnetic nanoparticle for gold mining. *Journal of Nanoparticle Research*, 19(2).

Visa, M., Bogatu, C., & Duta, A. (2010). Simultaneous adsorption of dyes and heavy metals from multicomponent solutions using fly ash. *Applied Surface Science*, 256(17), 5486–5491.

Chapter 4

Selective Removal of Bisphenol A from Water by Magnetic Bead fused with Bisphenol A-binding Peptide

4.1 Introduction

The research of endocrine disrupters in the environment has received increasing attention in recent years (Meeker, 2010). Bisphenol A (BPA) is a representative endocrine disrupter, which has been shown to interact with estrogen receptors due to its phenolic structure (Fenichel, Chevalier, & Brucker-Davis, 2013). BPA is produced in large quantities worldwide. It is not only used in the production of plastics intended to a direct contact with food, including plastic packaging and kitchenware, but also in inner coatings of cans and jar caps (Konieczna, Rutkowska, & Rachoń, 2015). Because of daily exposure and its tendency of bio-accumulation, BPA seems to require special attention and the development of methods to remove BPA is under necessity (Zhang, Causserand, Aimar, Cravedi, & Gao, 2011).

It was studied that BPA has an acute toxicity in the range of about $1\text{--}10\text{mg}\cdot\text{l}^{-1}$ for a number of freshwater and marine species (Zhang et al., 2011). Thus, the development of methods to remove BPA under trace concentration is needed urgently. Among many methods to remove BPA from wastewater such as nanofiltration (Yüksel, Kabay, & Yüksel, 2013), reverse osmosis (Khazaali, Kargari, & Rokhsaran, 2014), advanced oxidation processes (Sharma, Mishra, & Kumar, 2015), ozone (Kusvuran & Yildirim, 2013) and membrane bioreactors (Wintgens, Gallenkemper, & Melin, 2002). biological processes have been considered as a viable alternative compared to these conventional ones because of its low operating cost, simple design, ease of operation and less production of secondary harmful by-products (Bhatnagar & Anastopoulos, 2017). However, most of the biological processes investigated up to now are about biodegradation. Such as Lassouane et al. tested the BPA degradation performance of crude laccase from *Trametes pubescens* from aqueous solutions and achieved 99% BPA

removal in 2h (Lassouane, Aït-Amar, Amrani, & Rodriguez-Couto, 2019). As is known to all that BPA is heavily used in industry, it would be a waste to degrade it directly. So selective adsorbent which can adsorb micropollutant selectively and then release it for reuse is under development.

In recent years, the use of peptides has received great attention in environmental remediation field. Instead of microorganisms, the use of peptide formed from their cells presents several advantages such as no toxicity, sequence specific self-assembly, target recognition, shorter reaction time and mild reaction conditions. Although various peptide sequences exhibiting affinity to particular substrates have been found (Sarıkaya et al., 2003), peptide molecules capable of recognizing low molecular weight organic compounds, such as BPA, have rarely been reported. In a previous study, a heptapeptide with specific affinity to BPA, LysSerLeuGluAsnSerTyr (KSLENSY), was screened via with biopanning using a combinatorial constrained peptide library displayed on an M13 phage surface. The BPA-binding peptide had higher selectivity toward BPA compared with structural analogs of BPA such as bisphenol F and bisphenol S.

Magnetic carrier technology (MCT), first reported by Robinson et al. in 1973 (P. J. Robinson P. Dunnill M. D. Lilly, 1973), has become an increasingly popular tool in bioseparations, environmental and material science (Farmany, Shirmohammadi, Kazemi, Hatami, & Mortazavi, 2016; Ma et al., 2013). Recently, the combination of magnetic particles with certain functional ligands have attracted more attention. While special functional ligands with affinities for target molecules are bound onto these magnetic nanoparticles, convenient and fast selective removal of toxic target compounds from complex environmental matrices can be obtained.

In this work, magnetic bead fused with selective BPA-binding peptide was investigated as a new BPA adsorbent. By incorporating magnetic bead, the resulting magnetic peptide-binded bead (PBB) can not only selectively recognize BPA from complex samples but can also be quickly collected and regenerated using an external magnetic field. The newly constructed adsorbent was evaluated under different pH, initial concentration of BPA, amount of peptide to determine whether PBB could be employed for selective removal of BPA, as previously demonstrated for the removal of lead ion. A mixture of bisphenol S and bisphenol F which are structural BPA analogs were used to verify the selective removal efficiency of BPA. Moreover, synthesized wastewater including BPA was tested to determine whether the developed adsorbent could be employed under complex conditions. To further increase the removal capacity by providing more adsorption sites, bead binded with dimeric and triple BPA-binding peptides were also investigated.

4.2 Material and methods

4.2.1 Materials and apparatus

BPA-binding peptide, both cyclic and linear form (CKSLENSYC), capable of selectively recognizing BPA were custom synthesized by Lugen Sci Co., Ltd. (Bucheon, Korea). Magnetic beads AccuBead™ COOH were obtained from Bioneer Inc (Daejeon, Korea). 4-morpholineethanesulfonic acid (MES), N-(3-dimethyl aminopropyl)-N'-ethylcarbodiimide hydrochloride (EDC), N-hydroxy-succinimide (NHS), bovine serum albumin (BSA, A7906) , anhydrous acetonitrile (ACN) , BPA and its analogue BPF and BPS were purchased from Sigma-Aldrich(St. Louis, MO, USA). In view of its high value of log Kow (3.32), the stock solution of 1000 ppm bisphenol A was prepared with methanol. Then the working solution of bisphenol A

was obtained by diluting the stock solution with pure water. Deionized water (DI) was used to prepare solutions and wash all samples.

Apparatuses applied in this study include Nicolet 380 Fourier transform infrared (FTIR) spectrophotometer (ThermoFisher Scientific Co., Waltham, MA, USA), field-emission scanning electron microscopy (FE-SEM, JEOL, JSM-600F, Tokyo, Japan), high performance liquid chromatography (HPLC, Agilent 1200, UV-vis detector, USA), Fluorescence microscope(Olympus, Japan). TA instrument (TGA Q50)

4.2.2 Preparation of peptide-binded / protein-coated magnetic bead

BPA-binding peptides were introduced to magnetic bare bead with carboxylate groups via the EDC/NHS mediated coupling reaction(Fischer, 2010). For the detail, 3 mg bare bead was dispersed in 500 μL of 25 mM MES buffer (pH 5) and washed twice. Then, the carboxylate groups were activated by addition of EDC/NHS (50 $\text{g}\cdot\text{L}^{-1}$ in cold 25 mM MES each) and were shaken for 30 min. The excess EDC/NHS was washed away by 25 mM MES and collected with magnetic separation. Of the carboxylate-activated bead, 100 μL of peptide (100 $\text{mg}\cdot\text{L}^{-1}$) in a pH 7.4 PBS buffer was added and incubated for 1 hour. After incubation, the supernatant was collected for quantifying the amount of peptide binded to bead by HPLC with a C18 column (250*4.6 mm 5micron, Kromasil 100-5-C18, Kromasil). Acetonitrile and water with 0.1%(v/v) TFA were used for gradient elution from 0 to 70% (v/v) of acetonitrile at a flow rate of 1 mL/min. The absorption of the supernatant at 220 nm was recorded in comparison with that of the peptide solution before the reaction. The non-reacted activated carboxylic acid groups were quenched by incubating the NPs in 50 mM ethanolamine in PBS for 1 h at room temperature. The resulting peptide-binded bead were washed in PBS buffer twice under magnetic separation and diluted 10x for further characterization and adsorption

experiment. The reaction was repeated three times for each peptide. For the comparison purpose, the activated bead coated by BSA protein was prepared via similar protocol.

4.2.3 BPA adsorption experiments

The influences such as pH value (2.0-10), peptide amount (10-1000 mg L⁻¹), initial BPA concentration (1-50 mg L⁻¹) on the adsorption of BPA were investigated. A total of 0.3 mg adsorbent was mixed in 500 μL of a certain concentration of BPA. The mixture was stirred for a 1 hour at room temperature. Then, the magnetic adsorbent was separated by an external magnet. The remained concentration of BPA in the solution was determined by using HPLC at a 280-nm wavelength with a C18 column (Phenomenex 250 × 4.60 mm, USA) and a mobile phase consisting of acetonitrile:water at a ratio of 57:43 (v/v) at a flow rate of 1 mL/min. The amounts of BPA adsorbed per unit mass of adsorbent were calculated from the differences between the initial and the final solute concentrations in solution before and after adsorption by a mass balance relationship: $Q_t = (C_0 - C_t)V/W$, where C_0 and C_t are the initial and final concentration of BPA in the solution, respectively, mg L⁻¹; V is the volume of BPA solution (L); and W is the adsorbent dosage (g). When concentration at equilibrium, C_e is used instead of C_t in Eq. (1), Q_e is calculated. Each experiment was repeated three times and the average value is reported.

4.2.4 Selective adsorption experiments

The selective recognition of the peptide-binded bead was evaluated using BPA and another two structurally related analogs, BPS and BPF. The specific adsorption was carried out in a single pollutant system first. 0.3 mg of constructed adsorbent was

reacted with 500 μl 15 mg L^{-1} of BPA, BPS and BPF solution separately for 1 hour. Then, a ternary mixed solution resolving BPA, BPS and BPF was prepared, with the same concentration 15 mg L^{-1} . In order to evaluate the feasibility of using the adsorbent for removing BPA from complex matrices, a system of synthesized simulated wastewater was also applied. After reaction, the supernatant was separated from the tubes and analyzed by HPLC.

4.2.5 Desorption and regeneration studies

After BPA in solution (500 μl , 20 mg L^{-1}) was adsorbed onto the peptide-binded bead (0.3 mg) at initial pH 6.0 for 1 h, the BPA-adsorbed bead were collected by magnetic separation and washed with NaCl for twice. After that the adsorbents were regenerated in 500 μl methanol/acetic acid mixture in a thermostatic shaker at 25°C for 30 minutes. And the recycled adsorbent was used for adsorption again, which repeated 6 cycles.

4.3 Results and discussion

4.3.1 Preparation and characterization of peptide-binded magnetic bead

	Bead-binding efficiency
BSA	2.506×10^7 BSA / bead
Linearized peptide	1.56×10^8 peptide/bead
Cyclic peptide	1.73×10^8 peptide/bead

Table 4-1 Bead-binding efficiency with different peptide/protein

Peptide-binded / protein-coated magnetic nanoparticles were prepared at room temperature. The BPA-binding peptide (linear and cyclic type) was loaded onto magnetic bead in two steps. First, the magnetic bead with carboxyl was activated by

EDC/NHS in a MES buffer (pH = 5.0) to form a stable Fe₃O₄@NHS salt formation. Second, the 100 μl of 100 mg • L⁻¹ peptide was binded to carboxyl-activated bead through an amide bond formation in PBS buffer (pH = 7.4). The concentration of peptide was measured with HPLC while the concentration of BSA was tested with BCA Protein Assay(Walker, 1994) with UV-vis spectrophotometer at 280nm. The reaction efficiency of each molecule was shown in table 4-1. The theoretical carboxyl group amount on the bead is 2.74*10⁸ -COOH/bead. So the binding efficiency is reasonable.

FT-IR spectra of bare bead, carboxyl activated and BBP were compared in Fig.4-1. The strong IR band at 580cm⁻¹ is characteristic of the Fe-O vibrations related to the magnetic core, and the bands at 1030 cm⁻¹ correspond to Si-O-Si or Si-O-Fe stretching vibrations of the silica shell. The strong IR bands at 1553 and 1633 cm⁻¹ are characteristic of the amide bond for peptide-binded bead. A clear distinction between bare bead and peptide-binded bead through the strong band at 1732 cm⁻¹, corresponding to the C=O stretch vibration of the carboxylic acid. There is an apparent shift after the peptide conjugation demonstrates covalent binding of the peptide to the carboxyl groups of bead. The coupling of the N-H in-plane bending and C-N stretching vibration of the peptide backbone, was evidenced by the peaks at 1658 and 1546 cm⁻¹, respectively, demonstrating good agreement with those reported elsewhere (Liu et al., 2009; Zeng et al., 2014). The peaks located at 3305.8 and 1458.6 cm⁻¹ were attributed to the stretching and in-plane bending vibration of O-H in the COOH groups; Also, there are the characteristic absorption bands of -OH (-NH),-C=O,-CH₂-/-CH₃, and C-O ester/ether at 3458, 1732,2974, and 1161-1259 cm⁻¹, respectively.

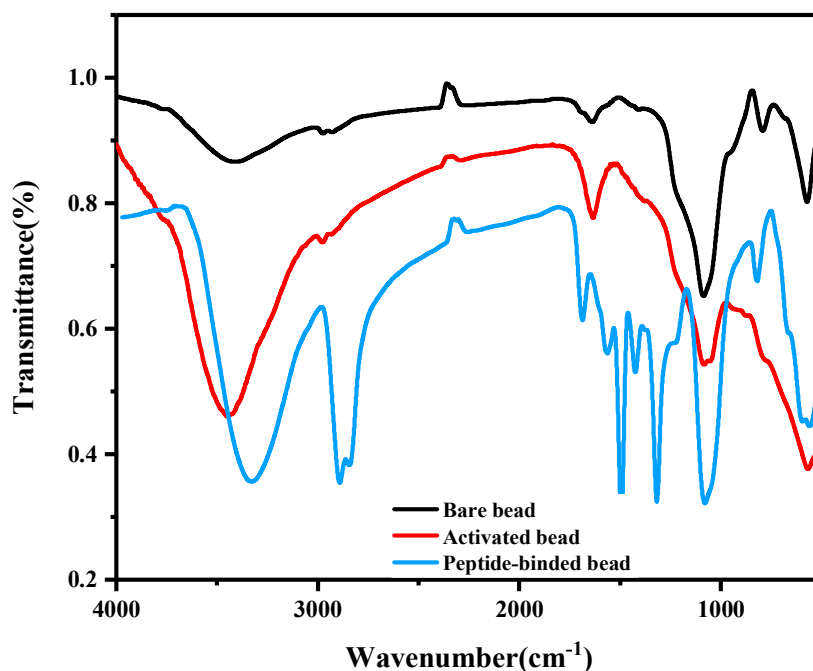


Figure 4-1 FTIR spectra of bare bead, carboxyl activated bead and PBB

4.3.2 Adsorption

4.3.2.1 Effect of pH on adsorption

The initial pH of the BPA solution is an important parameter toward adsorption especially effect the adsorption capacity (Guo et al., 2011). pH of the solution may change the degree of ionization of the adsorbate molecule, the surface charge of the adsorbent and extent of dissociation of functional groups on the active sites of the adsorbent (Yu, Deng, & Yu, 2008). In this study, the adsorbate was BPA which contains hydroxyl groups and the adsorbents peptide-binded bead contains amine and carboxyl group which means pH can affect the dissociation status of the BPA and the adsorbents. So it was necessary to study the effect of pH on adsorption. Fig.4-2 illustrated the adsorption of BPA onto bare bead, BSA-coated bead, linearized peptide-binded bead

and cyclic peptide-binded bead at various pH value including extreme condition of pH 2 and pH 10. As we can see in fig. 4-2, the adsorption capacity under acid and base solution were almost same among 4 types of adsorbent. While pH is 6, which is near the isoelectric point of our peptide, the linearized peptide-binded bead and cyclic peptide-binded bead showed much higher adsorption capacity than bare bead and BSA-coated bead which are 33.89, 39.12, 7.90 and 9.2430 $\mu\text{mol}\cdot\text{g}^{-1}$, respectively. Isoelectric point, also called the pI of the protein, is the pH at which the net charge of the protein is zero. A protein that is in a pH region below its isoelectric point (pI) will be positively charged(Blank-Shim et al., 2017), while be negatively charged in a pH region higher its pI. Since the pI of our peptide is 6.1, it would be positively charged in pH 2 solution and negatively charged in pH 10 solution. While the molecular state of BPA mainly exist in the pH range of 3.0 to 7.0, it would exist in the cationic form under pH 2 and anionic form above pH 7, which means both situation are electrostatic repulsive with peptide. Which certificated that the binding affinity between BPA and selective binding sites of peptide was the main driving force for adsorption in this work. The results of this study are in accordance with other studies (Hamdaoui & Naffrechoux, 2007; Xiao, Fu, & Li, 2012)

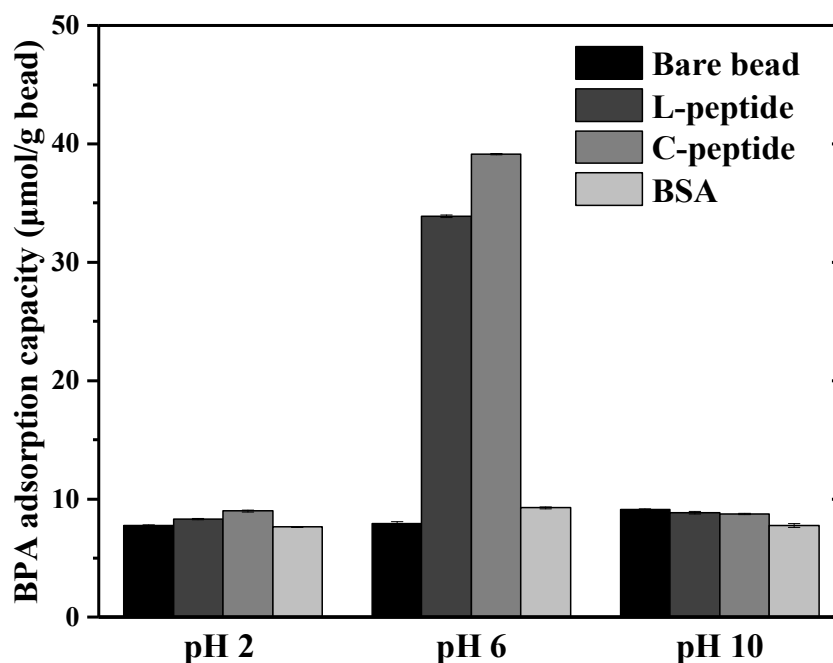


Figure 4-2 BPA adsorption under neutral, acid and base solution

(0.3 mg bead, [peptide] = 100 mg • L⁻¹ ; [BPA] = 20 mg • L⁻¹; contact time 1 hour)

4.3.2.2 BPA adsorption under mild solution

Furthermore, we investigated the solution pH around 6 with bare bead, linearized peptide-binded bead and cyclic peptide-binded bead. Although the adsorption capacity among different neutral pH are not very apparent, we can see in fig 4-3 that it showed the highest under solution of pH 6 near the peptide pI which is 37.64 µmol • g⁻¹ for cyclic peptide-binded bead and 31.98 µmol • g⁻¹ for linearized peptide-binded bead. While the solution pH is 6, BPA is in its molecular state (Bautista-Toledo et al. 2005) and the peptide-binded beads represent a surface charge density close to zero. Under these circumstances, π - π dispersion interaction and hydrogen bonding interaction could be strengthened. Although the main form of BPA is in the molecular state under all these solutions, the π - π dispersion interaction or hydrogen bonding interaction could also be weakened because of the existence of positive or negative charges on

the surface of peptide-bound bead. So that's may be why the adsorption capacity of the constructed bead is a bit weakened under pH 5 and pH 7. Hence, one is of hydrogen-bonding interaction between the hydroxyl groups of BPA and the hydrophilic groups (Dehghani et al., 2016) such as carboxyl groups and hydroxyl groups of the peptide. The other is of π - π dispersion interactions between the benzene rings of BPA and the phenyl groups in tyrosine of peptide. Furthermore, cyclic peptide-bound bead always showed higher capacity due to its higher binding efficiency on bead which may be caused by its lower steric hindrance. Therefore, cyclic peptide-bound bead was selected for further experiments.

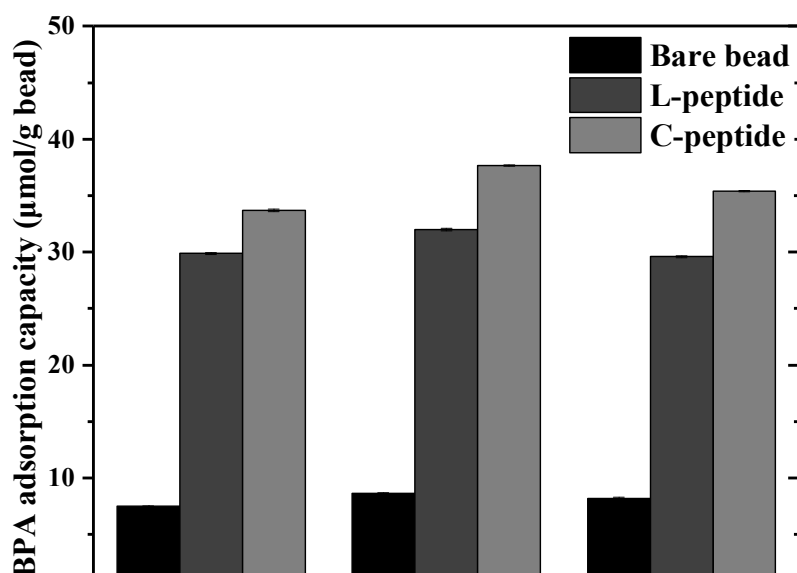


Figure 4-3 BPA adsorption under mild solution

(0.3 mg bead, [peptide] = 100 mg · L⁻¹ ; [BPA] = 20 mg · L⁻¹; contact time 1 hour)

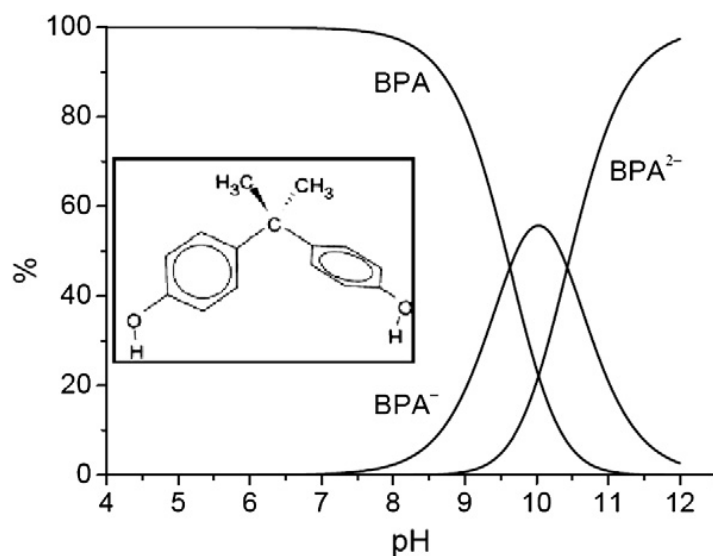


Figure 4-4 Chemical structure and the species distribution diagram of BPA.

(Bautista-Toledo et al. 2005)

4.3.2.3 Effect of peptide concentration

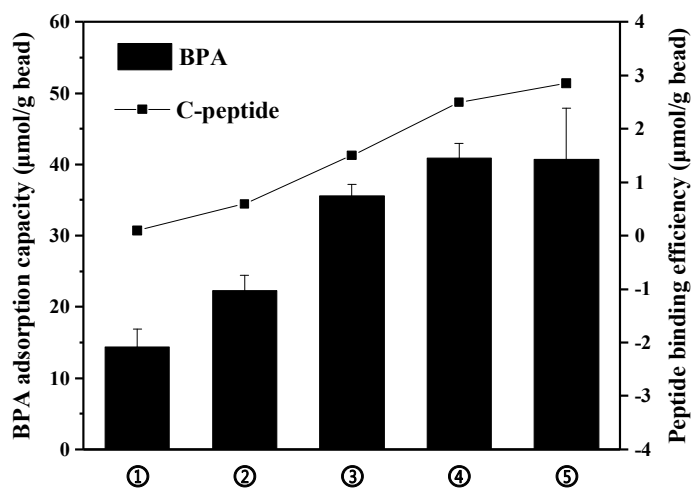


Figure 4-5 Effect of peptide concentration on the adsorption of BPA by cyclic peptide

([BPA] = 20 mg • L⁻¹; pH = 6 and contact time 1 hour)

The effect of initial concentration of peptide on the removal efficiency of BPA was examined at different initial concentrations of the peptide with 10,50,100,500,1000 mg/L at pH = 6, BPA concentration of 20 mg•L⁻¹, and contact time of 1 hour. As can

be observed from Fig. 4-5, as the amount of peptide increases, so does the removal efficiency of the BPA. The highest removal efficiency was obtained at the peptide concentration of $500 \text{ mg}\cdot\text{L}^{-1}$. Increased removal efficiency with higher dose of peptide is related to the increased number of adsorption sites. It was calculated that the carboxyl group of the bare bead is $2.74\cdot 10^8$ -COOH/bead, as the peptide molecular is $1044.19 \text{ g}\cdot\text{mol}^{-1}$, we can assume that the maximum peptide binding efficiency on bead is $2.75 \text{ }\mu\text{mol}\cdot\text{g}^{-1}$. So we can see that the while the initial peptide concentration is $500 \text{ mg}\cdot\text{L}^{-1}$, the peptide binding efficiency has almost arrived the maximum binding efficiency of $2.61 \text{ }\mu\text{mol}\cdot\text{g}^{-1}$. The results revealed that adsorption capacity of BPA increased with increased amount of peptide, while the peptide binding efficiency arrived the maximum, the increasing concentration of peptide do not benefit BPA adsorption anymore.

4.3.2.4 BPA Adsorption isotherm study

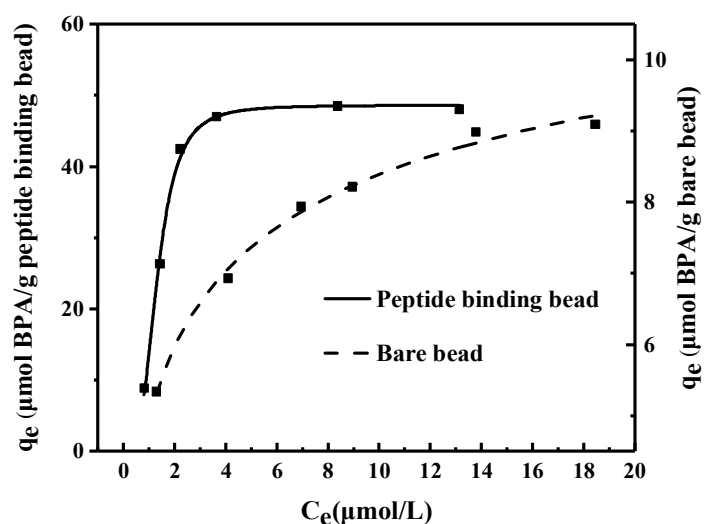


Figure 4-6 Adsorption isotherms for the adsorption of BPA onto bead.

(Solid and dotted lines are drawn using peptide-binded bead and bare bead, respectively)

Bead type	q_{max} ($\mu\text{mol}\cdot\text{g}^{-1}$)	K_L ($\text{L}\cdot\mu\text{mol}$)	R^2
PBB	48.61±0.74	0.3998±0.1581	0.9948
Bare bead	13.12±2.40	0.6030±0.1581	0.9861

Table 4-2 Parameters fitted with nonlinear adsorption isotherm

To characterize the adsorption properties of peptide-binded bead for BPA, adsorption isotherm experiments were performed under varying initial concentrations of BPA with 1,5, 10, 15, 20, 50 $\text{mg}\cdot\text{L}^{-1}$. Adsorption data are described by the Langmuir isotherm equation mentioned before. Adsorption isotherms of BPA from water on PBB and bare bead are shown in Fig.4.6. With the initial concentration of BPA increasing, the equilibrium adsorption capacity for BPA firstly increased significantly, then increased slightly, and in the end reached to equilibrium, as expected. The adsorption capacity of BPA by bare bead was negligible, but it was augmented greatly by binding peptide. The isotherm parameters obtained from the nonlinear analysis are presented in Table 4-2. It can be observed that the langmuir isotherm model yielded a better fit with PBB than bare bead, for the correlation coefficients (R^2) is above 0.99. Notably, the adsorption capacity of BPA by PBB reached to equilibrium quickly with initial concentration of 15 $\text{mg}\cdot\text{L}^{-1}$, which make it a potential adsorbent for trace BPA removal.

4.3.3 Desorption and regeneration studies

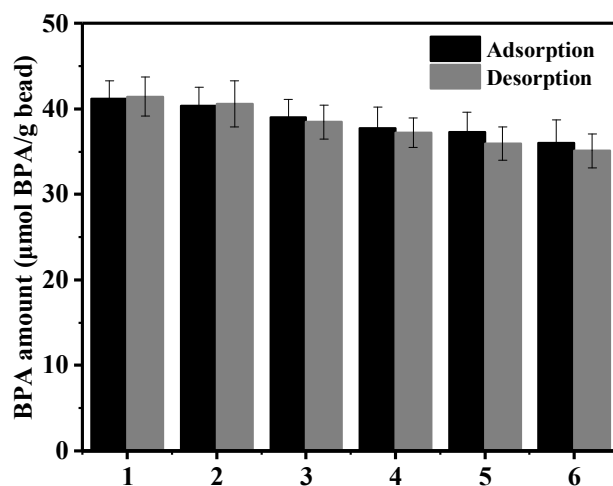


Figure 4-7 Adsorption and desorption study of BPA on PBB.

Reusability is one of the most important property of adsorbents in terms of decreasing cost. So, desorption and regeneration studies which express the capacity of reuse is practiced. While we tried the ethanol desorption technique, the result did not fulfil much regeneration cycles. We found that the polarity and acidity of elution solvent would play a vital role in complex extraction, and then the elution solvent with volume ratio of methanol:acetic acid at 8:2 was used.

The regenerated BPA-binded bead were tested for six times. The adsorption and desorption capacities in the adsorption-desorption-adsorption cycles were shown in Fig.4-7. The mass of desorbed BPA (g) was calculated from the supernatant concentration of solution after desorbing. As illustrated in the figure, the adsorption capacities of BPA for the sixth step is $36.02 \mu\text{mol}\cdot\text{g}^{-1}$ maintain more than 87% of that for the first adsorption step which is $41.21 \mu\text{mol}\cdot\text{g}^{-1}$, indicating that the PBB had the potentiality to be reused without great loss.

4.3.4 Selectivity study

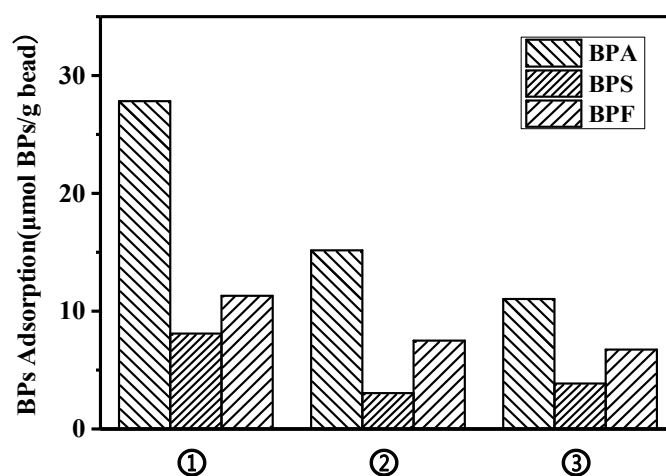


Figure 4-8 Comparison of the BPA selective adsorption capacity in three different solution system

① Specific adsorption in a single pollutant system. In order to examine the specificity of PBB, the adsorption capacity of PBB for BPA was compared to BPS and BPF which were used when the BPA-binding peptide was screened. They all had a certain degree of similar chemical structure, and the results are shown in Fig.4.8. The initial concentration of each of the pollutants was $15 \text{ mg}\cdot\text{L}^{-1}$. As illustrated in the figure, PBB possessed the highest adsorption capacity for BPA out of the 3 adsorbates. However, because of the similar structural homology ($-\text{OH}$) to the template (BPA), the same hydrogen bond may form between the structural analog and functional monomers, thereby resulting in their adsorption capacity in a single system.

② Competitive adsorption in binary pollutant system. To further evaluate the selectivity of PBB for BPA, the batch experiments were conducted by preparing a mixture of BPA, BPS and BPF, in which the initial concentration of each of the pollutants was $5 \text{ mg}\cdot\text{L}^{-1}$ to construct a total $15 \text{ mg}\cdot\text{L}^{-1}$ pollution environment. As shown in figure4-8, PBB also showed good selectivity for BPA in the mixture system.

The adsorption capacity was $15.14 \mu\text{mol}\cdot\text{g}^{-1}$, $3.03\mu\text{mol}\cdot\text{g}^{-1}$, $7.50 \mu\text{mol}\cdot\text{g}^{-1}$ for BPA, BPS and BPF, respectively, indicating that the BPA-binding peptide was effective and PBB could selectively rebind BPA from complex samples.

③ Removal of BPA from synthesized simulated wastewater samples. In order to evaluate the feasibility of using PBB for removing BPA from complex matrices, a same simulated wastewater system as mentioned in Chapter 3 was used. The initial concentration of each pollutant, BPA, BPS and BPF, was $5 \text{ mg}\cdot\text{L}^{-1}$. As can be seen from Fig. 4-8, though the adsorption capacity of PBB for BPA was still the highest, the capacity of PBB in removing BPA in simulated wastewater was reduced rather than in binary pollutant system. This phenomenon may be attributed to the presence of many different organic/ inorganic contaminants in wastewater solution, which can also bind to bead, thus reducing the adsorption capacity of PBB for BPA. Nevertheless, the results suggested that there was a potential application for the PBB to be used to selectively remove BPA from water and wastewater.

4.3.5 BPA adsorption by different length of peptide

In a previous study of BPA adsorption on recombinant cells, dimeric display of BPA-binding peptide on the cell surface was employed to improve the BPA adsorption capacity (Maruthamuthu, Selvamani, Eom, & Hong, 2017). In the dimeric strain, the amount of adsorbed BPA arrived $230.4 \mu\text{mol BPA/g DCW}$ at BPA concentration of 15 ppm which showed 3 times higher than in the monomeric strain. In order to certify the peptide-binded bead can show the same capacity, we constructed double and triple peptide sequence binded bead to improve the removal capacity further. As shown in figure 4-9, the adsorption capacity of bare bead, cyclic peptide-binded bead, linearized peptide-binded bead, double linearized sequence binded bead and triple sequence

linearized sequence binded bead were $10.18 \mu\text{mol}\cdot\text{g}^{-1}$, $40.37 \mu\text{mol}\cdot\text{g}^{-1}$, $38.74 \mu\text{mol}\cdot\text{g}^{-1}$, $62.39 \mu\text{mol}\cdot\text{g}^{-1}$, $72.99 \mu\text{mol}\cdot\text{g}^{-1}$, respectively. Which means that the longer sequence did not multiply the adsorption capacity. Then we calculated the adsorption relationship between BPA and peptide sequence, which resulted 4.34, 8.22, 12.42 BPA molecules per peptide molecule. The result certificate that the BPA adsorbed on peptide sequence is increased in linear, so we assumed that the low adsorption capacity of BPA on bead is due to low peptide binding efficiency. While the peptide sequence is lengthened, the space it need on bead surface is also increased, so the total amount of peptide binded on bead will be almost the same no matter the peptide is single sequence or triple sequence. To improve the removal capacity further, methods to increase the number of peptides binded on the bead surface will need to be investigated in a future study.

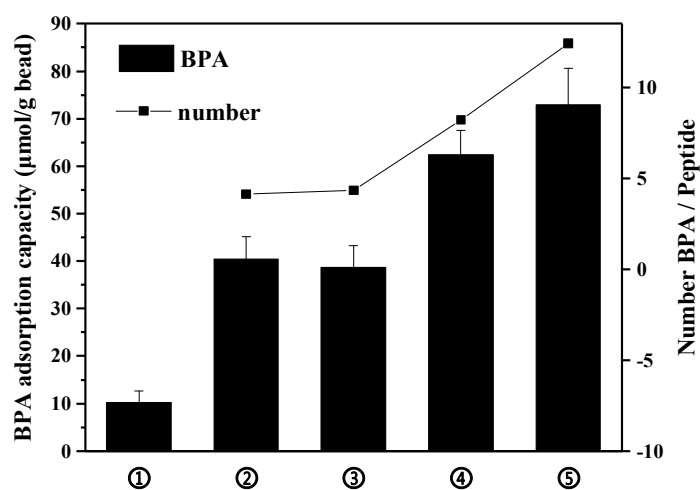


Figure 4-9 Comparison of the BPA selective adsorption capacity with different length of peptide

① bare bead, ② cyclic peptide-binded bead, ③ linearized peptide-binded bead, ④ double linearized sequence binded bead and ⑤ triple sequence linearized sequence binded bead

4.4 Conclusions

BPA-binding peptide was successfully binded to magnetic bead which construct a new biomolecule-based adsorbent for selective adsorption of BPA from aqueous solution. All adsorption experiments were carried out by batch method. The solution pH has effect on the adsorption capacity which certificated the molecular form of BPA is favorable for the adsorption on PPB. For BPA adsorbed onto PBB and Bare bead, the Langmuir isotherm model yielded a better fit with PBB with a maximum adsorption capacity of $48.61 \mu\text{mol}\cdot\text{g}^{-1}$. This study can be regarded as a combination of selective adsorption and magnetic separation, and the obtained PBB was assigned with higher specific recognition and selectivity to BPA even when it was in the mixed solution. More importantly, in desorption and regeneration studies, nearly 100% regeneration efficiency for the adsorbent was achieved by the methanol/acetic acid mixture, and the adsorption capacities of BPA after sixth cycle maintained more than 87% of that for the first adsorption, which illustrated that the constructed adsorbent have the potentiality to be reused.

4.5 Reference

- Bhatnagar, A., & Anastopoulos, I. (2017). Adsorptive removal of bisphenol A (BPA) from aqueous solution: A review. *Chemosphere*, *168*, 885–902.
- Blank-Shim, S. A., Schwaminger, S. P., Borkowska-Panek, M., Anand, P., Yamin, P., Fraga-García, P., ... Berensmeier, S. (2017). Binding patterns of homo-peptides on bare magnetic nanoparticles: Insights into environmental dependence. *Scientific Reports*, *7*(1), 1–11.

- Dehghani, M. H., Ghadermazi, M., Bhatnagar, A., Sadighara, P., Jahed-Khaniki, G., Heibati, B., & McKay, G. (2016). Adsorptive removal of endocrine disrupting bisphenol A from aqueous solution using chitosan. *Journal of Environmental Chemical Engineering*, 4(3), 2647–2655.
- Farmany, A., Shirmohammadi, M. M., Kazemi, S., Hatami, M., & Mortazavi, S. S. (2016). Aminopropyl functionalization of superparamagnetic iron oxide/SiO₂nanocrystals for adsorption of bisphenol A from water. *Desalination and Water Treatment*, 57(56), 27355–27362.
- Fenichel, P., Chevalier, N., & Brucker-Davis, F. (2013). Bisphenol A: An endocrine and metabolic disruptor. *Annales d'Endocrinologie*, 74(3), 211–220.
- Fischer, M. J. E. (2010). Amine Coupling Through EDC/NHS: A Practical Approach. *Surface Plasmon Resonance*, 627, 55–73.
- Guo, W., Hu, W., Pan, J., Zhou, H., Guan, W., Wang, X., ... Xu, L. (2011). Selective adsorption and separation of BPA from aqueous solution using novel molecularly imprinted polymers based on kaolinite/Fe₃O₄ composites. *Chemical Engineering Journal*, 171(2), 603–611.
- Hamdaoui, O., & Naffrechoux, E. (2007). Modeling of adsorption isotherms of phenol and chlorophenols onto granular activated carbon. Part II. Models with more than two parameters. *Journal of Hazardous Materials*, 147(1–2), 401–411.
- Khazaali, F., Kargari, A., & Rokhsaran, M. (2014). Application of low-pressure reverse osmosis for effective recovery of bisphenol A from aqueous wastes. *Desalination and Water Treatment*, 52(40–42), 7543–7551.
- Konieczna, A., Rutkowska, A., & Rachoń, D. (2015). Health risk of exposure to Bisphenol A (BPA). *Roczniki Państwowego Zakładu Higieny*, 66(1), 5–11.

- Kusvuran, E., & Yildirim, D. (2013). Degradation of bisphenol A by ozonation and determination of degradation intermediates by gas chromatography-mass spectrometry and liquid chromatography-mass spectrometry. *Chemical Engineering Journal*, 220, 6–14.
- Lassouane, F., Aït-Amar, H., Amrani, S., & Rodriguez-Couto, S. (2019). A promising laccase immobilization approach for Bisphenol A removal from aqueous solutions. *Bioresource Technology*, 271(September 2018), 360–367.
- Ma, Y. R., Zhang, X. Le, Zeng, T., Cao, D., Zhou, Z., Li, W. H., ... Cai, Y. Q. (2013). Polydopamine-coated magnetic nanoparticles for enrichment and direct detection of small molecule pollutants coupled with MALDI-TOF-MS. *ACS Applied Materials and Interfaces*, 5(3), 1024–1030.
- Maruthamuthu, M. kannan, Selvamani, V., Eom, G. T., & Hong, S. H. (2017). Development of recA promoter based bisphenol-A sensing and adsorption system by recombinant Escherichia coli. *Biochemical Engineering Journal*, 122(November), 31–37.
- Meeker, J. D. (2010). Exposure to environmental endocrine disrupting compounds and men's health. *Maturitas*, 66(3), 236–241.
- P. J. Robinson P. Dunnill M. D. Lilly. (1973). The properties of magnetic supports in relation to immobilized enzyme reactors. *Biotechnology and Bioengineering*, XV, 603–606.
- Sharma, J., Mishra, I. M., & Kumar, V. (2015). Degradation and mineralization of Bisphenol A (BPA) in aqueous solution using advanced oxidation processes: UV/H₂O₂ and UV/S₂O₈²⁻ oxidation systems. *Journal of Environmental Management*, 156, 266–275.

Walker, J. M. (1994). The bicinchoninic acid (BCA) assay for protein quantitation. *Methods in Molecular Biology (Clifton, N.J.)*, 32, 5–8. <https://doi.org/10.1385/1-59259-169-8:11>

Wintgens, T., Gallenkemper, M., & Melin, T. (2002). Endocrine disrupter removal from wastewater using membrane bioreactor and nanofiltration technology. *Desalination*, 146(1–3), 387–391.

Xiao, G., Fu, L., & Li, A. (2012). Enhanced adsorption of bisphenol A from water by acetylaniline modified hyper-cross-linked polymeric adsorbent: Effect of the cross-linked bridge. *Chemical Engineering Journal*, 191, 171–176.

Yu, Q., Deng, S., & Yu, G. (2008). Selective removal of perfluorooctane sulfonate from aqueous solution using chitosan-based molecularly imprinted polymer adsorbents. *Water Research*, 42(12), 3089–3097.

Yüksel, S., Kabay, N., & Yüksel, M. (2013). Removal of bisphenol A (BPA) from water by various nanofiltration (NF) and reverse osmosis (RO) membranes. *Journal of Hazardous Materials*, 263, 307–310.

Zhang, Y., Causserand, C., Aimar, P., Cravedi, J. P., & Gao, N. Y. (2011). Removal of Bisphenol A by a nanofiltration membrane. *Aquatech Amsterdam 2011*, 33(253), 3–4.

Chapter 5

Photocatalytic degradation of bisphenol A using TiO₂ synthesized via peptide-mineralization process

5.1 Introduction

Due to human activities, the widespread existence of EDCs in food, water and soil has become a worldwide problem because it can lead to a decline in the reproductive function, genital tumors, and immunity of various organisms, including humans, and cause various physiological abnormalities(Wang et al., 2018, Wee and Aris, 2017, Kim et al., 2019). Among the many EDCs, bisphenol A (BPA, bisphenol A) has attracted the attention of environmental departments and academia in various countries due to its large production volume, wide application, and obvious reproductive hormone effects(Antoniou and Dionysiou, 2007, Wu et al., 2017). The research on the degradation of BPA in the environment and the evaluation of its toxicity has become a research hotspot(Reddy et al., 2018).

Recently, the photocatalytic process in the presence of a semiconductor such as TiO_2 , ZnO etc., is known as a supplementary treatment method for its capability to remove a large number of organic compounds by the formation of strongly reactive radical species, mainly hydroxyl radical (Wang et al., 2016, Hodaifa et al., 2013). Among the diverse semiconductor oxides, the performance of nano TiO_2 because of its nontoxicity, cost-effectiveness, high chemical stability, high activity and ease of availability has been reported to be considerably better than others(Ahmed et al., 2010, Fatima et al., 2019). Nevertheless, TiO_2 as a photocatalyst is still insufficient in practical applications, and there are three major drawbacks. (1) The energy band structure of TiO_2 determines that it can only use ultraviolet light irradiated (Daneshvar et al., 2005; M'Bra et al., 2018) on the ground, and ultraviolet light only accounts for 5% of sunlight, which greatly limits the utilization rate of solar energy. Visible light absorption by TiO_2 can be effectively improved by ion doping; (2) The recombination probability of photogenerated electron-hole pairs is high, which causes the low quantum efficiency, resulting in a relatively low photocatalytic efficiency of TiO_2 ; (3) Powdered titanium dioxide particles are tend to agglomerate and deactivate in aqueous solution, and such suspension are difficult to recycle and reuse in practical applications, thus the industrial production and application are limited(Salaeh et al., 2017). Rational design of the external structure and adjustment of intrinsic electronic status by impurity doping are two main effective ways to improve these problems.

Biom mineralization is an environmentally friendly process can be facilitated by mimicking the synthesis routes of natural biomolecules or utilizing the functional groups in biomolecules as structure directing or stabilizing agents under mild conditions (Sewell and Wright, 2006, Chen et al., 2010, Kim et al., 2014). Peptides have rich and diverse functional groups (-COOH, -SH, -OH and -NH₂ groups), which play an important role in combining with metals, hydrophobic and hydrophilic amino acids, different secondary structures, and biological recognition of gene sequence. All these characteristics are encoded in the amino acid sequence and promote biom mineralization activity (Rutledge and Wright, 2009). A variety of peptide sequences have been used in the biomimetic synthesis of ceramics, metal sulfides, metal oxides and metal nanoparticles. Spoerke et al. produced cadmium sulfide particles of various sizes using peptides rich in cysteine and aspartic acid in the presence of Cd²⁺ and Na₂S (Spoerke and Voigt, 2007); Kriplani et al. used genetic technology to screen five peptides capable of binding ZnO, and the modified peptides can promote the generation of flower-like ZnO nanostructures at room temperature (Kriplani and Kay, 2005). They have low dispersion, good crystallinity, variable morphology, and have a wide range of biological functions in mild water environment (Fan et al., 2009). Moreover, biom mineralization enables the formation of metal oxides that are complexed with biomolecules enriched with carbon and nitrogen sources, which are capable of acting as dopants. the configuration, morphology, and crystallinity of metal oxide nanomaterials can be systematically tailored through various bioinspired synthesis techniques (Matsumura et al., 2016, Lee et al., 2012).

Previously, a TiO₂ specific STB1 peptide (CHKKPSKSC) was identified using phage display technique (Chen et al., 2006), and the roles of peptide sequence on TiO₂ mineralization were investigated (Choi et al., 2012). In this study, based on the fact that the template direction of peptide assembly is not strong in the process of TiO₂ mineralization (Kim et al., 2019), PS microspheres were introduced as templates and peptides were fixed to form PS-peptide-TiO₂ composite materials, and PS microspheres were removed by calcination to form titania hollow microspheres which provide a certain theoretical feasibility for reuse of TiO₂ photocatalyst. As-synthesized hollow TiO₂ was used for photocatalytic degradation of bisphenol A and compared with some other kinds of TiO₂.

5.2 Material and methods

5.2.1 Materials

The heptapeptide STB1 (CHKKPSKSC), including constrained type with a cyclic loop formed via a disulfide bridge between the flanking cysteine residues were provided by Lugen Sci Co., Ltd. (Bucheon, Korea). Carboxyl polystyrene particles were obtained from SpheroTech Inc (Illinois, USA). 4-morpholineethanesulfonic acid (MES), N-(3-dimethyl aminopropyl)-N'-ethylcarbodiimide hydrochloride (EDC), N-hydroxy-succinimide (NHS), anhydrous acetonitrile (ACN), TiO₂ precursor (Titanium (IV)-bis-ammonium-lactato-dihydroxide or TiBALDH) and bisphenol A were purchased from Sigma-Aldrich (St. Louis, MO, USA). In view of its high value of log K_{ow} (3.32), the stock solution of 100 ppm bisphenol A was prepared with methanol. Then the working solution of bisphenol A was obtained by diluting the stock solution with pure water. Deionized water (DI) was used to prepare solutions and wash all samples.

5.2.2 Peptide binding and biomineralization

The peptide (STB1) were introduced to PS bead with carboxylate groups via the EDC/NHS mediated coupling reaction (Fischer, 2010). For the detail, 5 mg bare PS bead was dispersed in 500 μ L of 25 mM MES buffer (pH 5) and washed twice. Then, the carboxylate groups were activated by addition of EDC/NHS (50 $g \cdot L^{-1}$ in cold 25 mM MES each) and were shaken for 1 hour. The excess EDC/NHS was washed away by 25 mM MES and collected by centrifugation (8000 rpm, 10min). Of the carboxylate-activated bead, 200 μ L of peptide (25~500 $mg \cdot L^{-1}$) in TAE Buffer (50X) (0.04 M, pH 8.5) was added and incubated for 1 hour. After incubation, the supernatant was collected for quantifying the amount of peptide binded to bead by ultraviolet-visible spectrometer (UV-Vis, Spectramax Plus 384, Molecular Devices Co., San Jose, CA, USA) with Pierce™ BCA Protein Assay Kit (Thermo Fisher, USA). The absorption of the supernatant at 220 nm was recorded in comparison with that of the peptide solution before the reaction. The reaction was repeated in three tubes for each peptide.

The peptide-binded bead was dispersed in 500 μ l TAE Buffer and for comparison, 25 $\mu g ml^{-1}$ pure STB1 in 500 μ l TAE Buffer was also taken to incubate with 50 μ l of 1 M TiBALDH for 1 h at room temperature. After biomineralization, 125 μ l of 6 N

trichloroacetic acid was added and TiO₂ precipitates were collected by centrifugation (8000 rpm, 5 min). As a control experiment, a bare TiO₂ sample was also synthesized by the same procedure in the absence of biotemplate. The precipitates resuspended in water were freeze-dried under -40 °C and 20 Pa by using a freeze dryer. All the TiO₂ samples were calcined at 800 °C for 2 h by using a digital muffle furnace.

5.2.3 Characterization

The surface morphology were analyzed by field-emission scanning electron microscopy (FE-SEM-EDX, JEOL, JSM-600F, Tokyo, Japan) with an energy dispersive spectrometer. Thermogravimetric analysis (TGA, Q50 TA Instrument) was carried out under a nitrogen atmosphere at a temperature range from room temperature to 800 °C at a heating rate of 10 °C min⁻¹. X-ray diffraction (XRD, Rigaku D/MAZX 2500V/PC model, Japan) was carried out to investigate crystalline structure using Cu K α radiation (40 kV, 30 mA, $\lambda = 1.5415 \text{ \AA}$) operated at a scan rate of 2° min⁻¹ over a 2 θ range of 10-100°.

5.2.4 Photocatalytic activity

The photocatalytic activity of biomineralized TiO₂ was investigated via the photodegradation of BPA solution with solar simulator (Sol1A™ ABB, Newport, USA). 1 mg of TiO₂ sample was added to 2 mL 50 mg L⁻¹ BPA and the solution was kept in the dark for 1 h to attain adsorption/desorption equilibrium. After that, it was irradiated under 1 sun AM 1.5 G for 120 min, 200 μ l of the solution was extracted at 20 min intervals and centrifuged to obtain the supernatant. The changes in the concentration of the supernatant were measured by HPLC at a 280 nm wavelength.

5.3 Results and discussion

5.3.1 Influence of peptide concentration

Peptide concentration (mg L^{-1})	Peptide binded to bead (μg)	TiO ₂ synthesized (mg)	TiO ₂ / peptide
25	2.70	0.0781	368.3
100	6.24	0.4013	817.4
200	10.38	1.3807	1690.6
400	13.87	2.0265	1856.8
500	15.36	2.2831	1889.4

Table 5-1 Peptide binding amount on PS bead and TiO₂ synthesized amount from different initial concentration of peptide

In the previous studies, three different biomolecules containing the STB1 (CHKKPSKSC) peptide moiety, which was shown to be efficient in catalyzing TiO₂ biomineralization, were used as biotemplates for TiO₂ biomineralization, and the peptide concentration were fixed on $25 \text{ mg}\cdot\text{l}^{-1}$. In order to compare the biotemplate function of peptide on PS bead, different initial peptide concentration (25, 100, 200, 400, 500 $\text{mg}\cdot\text{l}^{-1}$, respectively) was investigated and the final amount of peptide binded to PS bead was thus calculated in table 5-1. The peptide binding result shows that when the initial concentration is 200 mg L^{-1} , the peptide amount on bead is the most closely to previous study which was $12.5 \mu\text{g}$ (Kim et al., 2019).

Before taken to calcinate, the PS-STB1-TiBALDH reaction product was analyzed by TGA to quantitatively measure the amount of TiO₂ synthesized from different concentration of peptide (Figure 5-1). When bare TiO₂ was heated from room temperature to 800°C the remained weight was 38.5%, which are due to the degradation and decomposition of TiBALDH. The pure PS bead totally degrade in one step around $400\text{-}450^\circ\text{C}$. So we can assume that the remained weight in PS-STB1 compound is the TiO₂ synthesized. The total amount of titania was thus calculated in table 5-1. The TiO₂ molecules synthesized via per peptide molecule was calculated through equation:

$$\text{TiO}_2 / \text{peptide} = \frac{W_{\text{TiO}_2}}{M_{\text{TiO}_2}} * 6.23 * 10^{23} / \frac{W_{\text{peptide}}}{M_{\text{peptide}}} * 6.23 * 10^{23},$$

where W_{TiO_2} and W_{peptide} is the weight of TiO_2 synthesized and the weight of peptide binded to bead, respectively; M_{TiO_2} and M_{peptide} is the molecule weight of TiO_2 and peptide which is $79.866 \text{ g}\cdot\text{mol}^{-1}$ and $1015.22 \text{ g}\cdot\text{mol}^{-1}$, respectively. From the result we can see that the TiO_2 synthesis efficiency almost get the maximum when the peptide initial concentration is 200 mg L^{-1} , which is also consistent to the peptide amount used in previous study. So in the following study, the experiment was all done by peptide concentration of 200 mg L^{-1} .

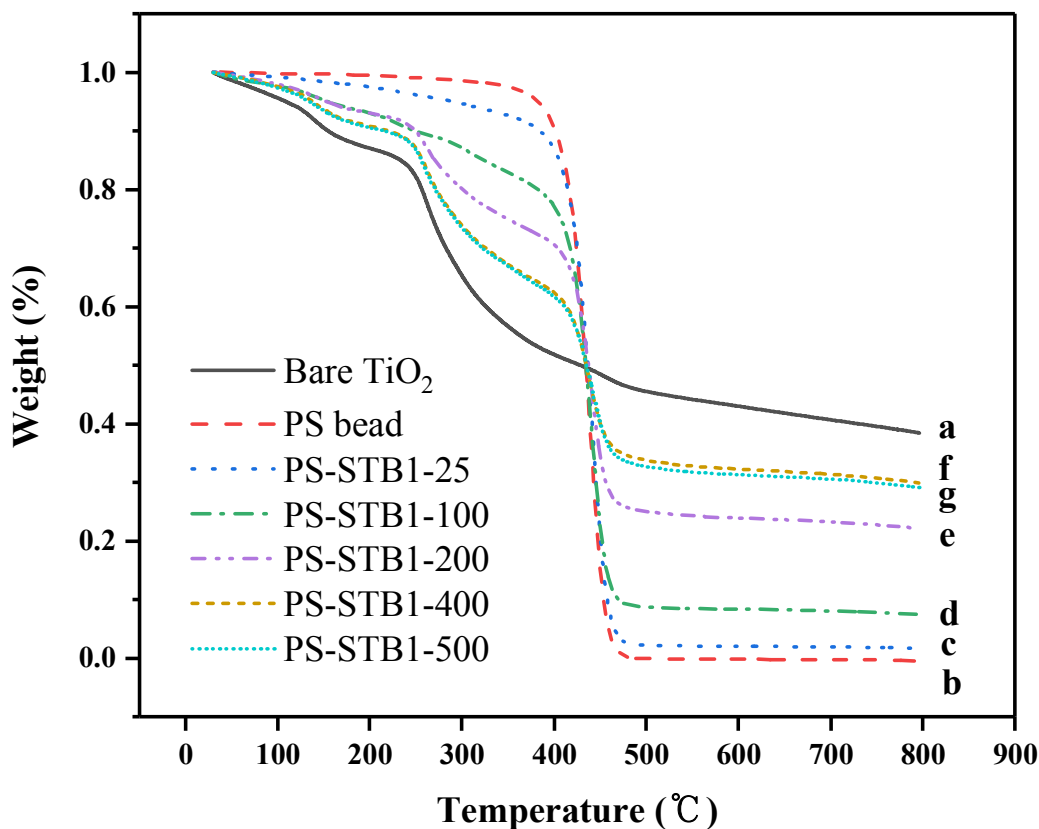


Figure 5-1 TGA curves of PS bead (b) and TiO_2 synthesized from different concentration of peptide-binded PS bead.

(a) $0 \text{ mg}\cdot\text{l}^{-1}$, (c) $25 \text{ mg}\cdot\text{l}^{-1}$, (d) $100 \text{ mg}\cdot\text{l}^{-1}$, (e) $200 \text{ mg}\cdot\text{l}^{-1}$, (f) $500 \text{ mg}\cdot\text{l}^{-1}$, (g) $400 \text{ mg}\cdot\text{l}^{-1}$.

5.3.2 Characterization

Figure 5-2 shows SEM images of (a) bare PS bead, (b) PS bead binded with peptide, (c) the peptide-binded bead reacted with precursor before calcination, and (d) peptide-binded bead reacted with precursor after calcination. Figure 5-2 (a) displays a very homogenous, smooth sphere and the average size is about 1 μm . After reacting with peptide through EDC/NHS protocol, there is peptide obviously seen on bead surface shown by figure (b). When TiO_2 precursor was introduced to the system, the bead surface looks different from PS-STB1 bead. We could observe in figure 5-2 (c) that there is a layer on the surface. The EDS analysis shows that the weight of Ti atom is 27.33% in the complex. After calcinated under 800°C , we can see in figure5-2 (d) that the surface of the bead was rough and the EDS analysis shows that the weight of Ti atom reach up to 71.33% which means that the bead is totally TiO_2 as the PS bead was burnt.

X-ray diffraction (XRD) was employed for further analyzing the crystalline phase of TiO_2 , STB1- TiO_2 and PS-STB1- TiO_2 after calcination at 800°C (Figure 5-3). And the commercial P25 TiO_2 was also tested. It can be seen in fig.3-3 that commercial P25 TiO_2 shows typical diffraction peaks of anatase peaks at 2θ of 25.3° (101) and 37.8° (004). And for bare TiO_2 , there showed rutile peaks at 27.4° (110), 36.1° (101), 39.2° (111), and 41.2° (210) but no anatase peak. The anatase/rutile mixed phase was observed for STB1- TiO_2 and PS-STB1- TiO_2 , while the rutile peaks are much sharper and stronger for STB1- TiO_2 , the intensity of typical anatase peak and rutile peak for PS-STB1- TiO_2 was almost the same. In general, the crystalline phase transition behavior (i.e. amorphous \rightarrow anatase \rightarrow mixed anatase/rutile \rightarrow rutile) is highly dependent on the calcination temperature, which in turn is closely affected by the amount of mineralizing biomolecules present during biomineralization. It has been studied that crystalline phase transition became slower with the increasing amount of organic content in the biomineralizing milieu. In particular, anatase/rutile mixed phase TiO_2 is also reported to be beneficial for photocatalytic activity. This is because the different band edge states between the anatase and rutile phases within a nanoparticle can efficiently dissociate and transport the photoinduced charges (Tsukamoto et al., 2012, Liu et al., 2007, Zhu and Wang, 2017).

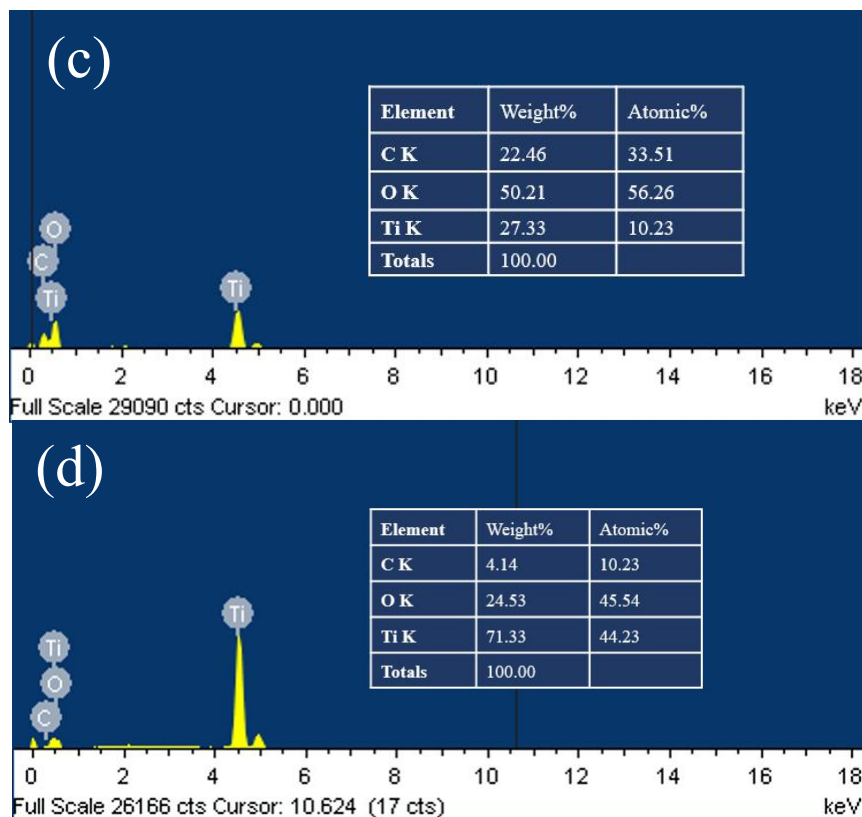
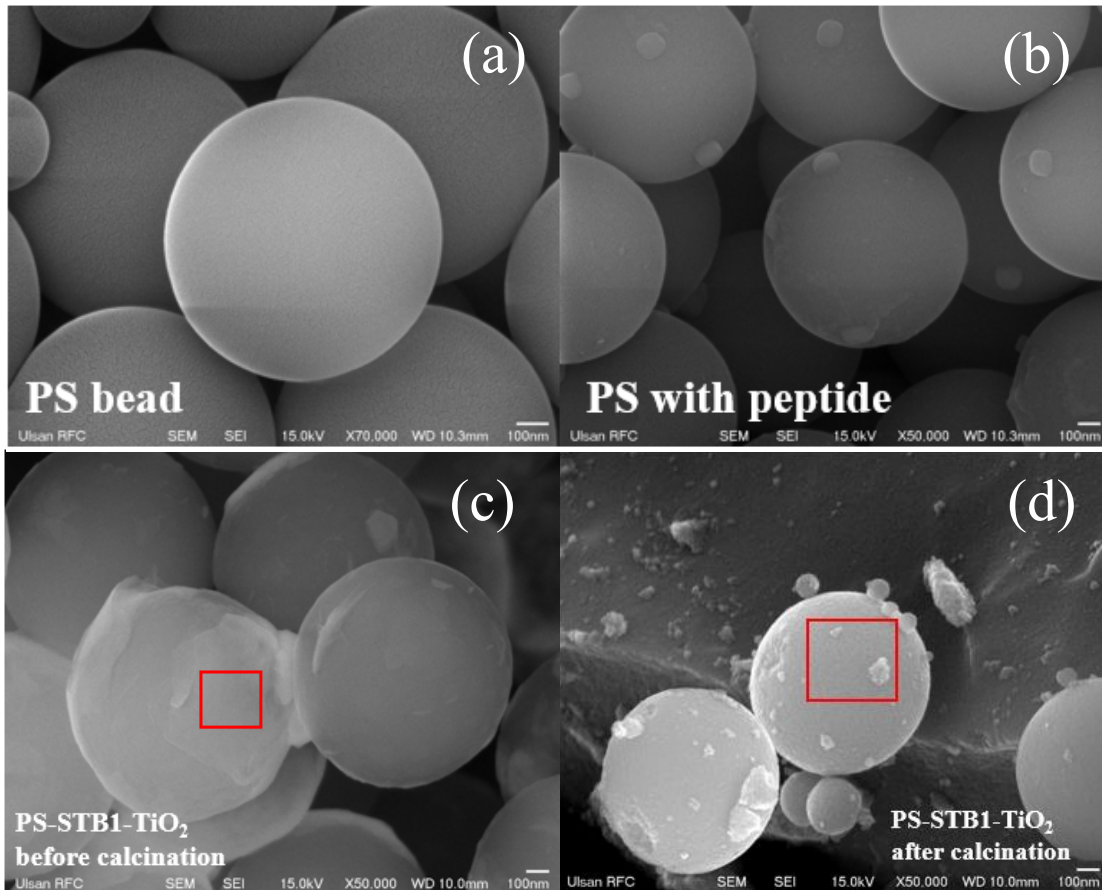


Figure 5-2 SEM images of (a) bare PS bead, (b) PS bead binded with peptide, (c) the peptide-binded bead reacted with precursor before calcination, and (d) peptide-binded bead reacted with precursor after calcination.

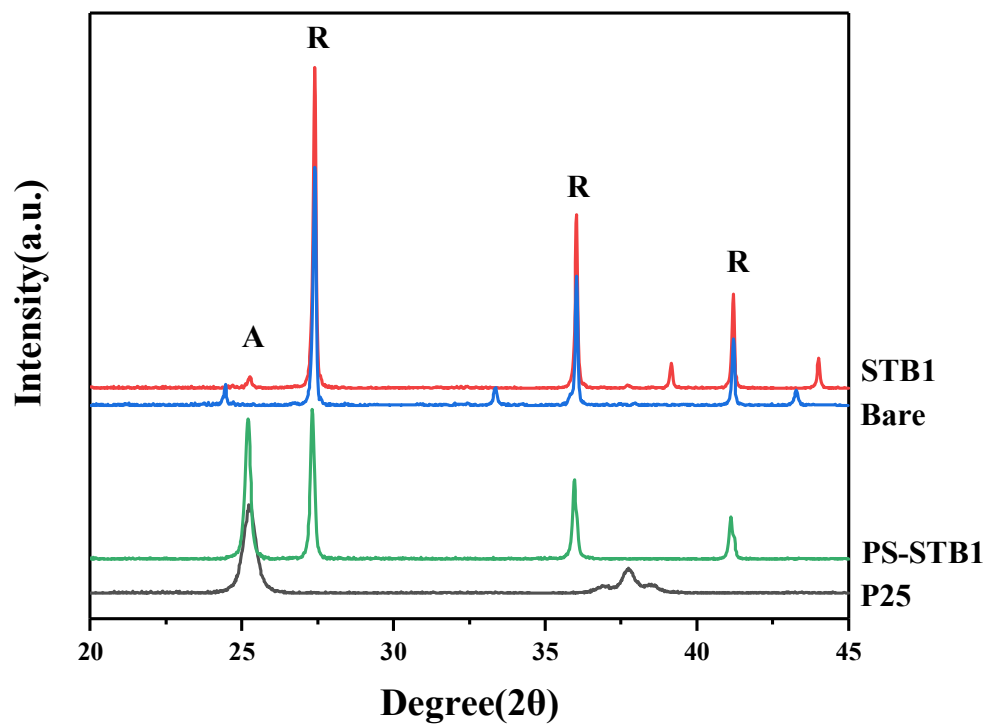


Figure 5-3 XRD spectra of commercial P25 TiO₂, and bare, STB1-, and PS-STB1-TiO₂ after calcination at 800°C.

"A" indicates the peaks present in anatase phase, and "R" indicates those of rutile phase.

5.3.3 Photocatalytic activity

To simulate the photocatalytic performance of P25, bare-, STB1-, and PS-STB1-TiO₂, photocatalytic degradation tests of BPA were performed under solar light simulator. The BPA concentrations in the solutions were plotted in Figure 5-4, as well as the adsorption and photocatalytic reaction times, where PS-STB1-TiO₂ exhibits the highest BPA photodegradation efficiency which arrived 86.3% at 120 min. The best BPA degradation efficiency of PS-STB1-TiO₂ is attributed to the formation of the hollow morphology owing to the efficient interaction with peptide, resulting in the facilitation of the charge transfer. As previously discussed, the appropriate ratio of anatase and rutile of the PS-STB1-TiO₂ may also work for the high photodegradation rate.

The apparent reaction rate constants (k_{app}) were obtained by fitting the reaction data to the first-order reaction model described as the following equation:

$$\ln \frac{C_t}{C_0} = -k_{app} t$$

where t is the irradiation time, and C_0 and C_t are the initial and residual concentrations of BPA aqueous solution, respectively. The kinetic curves were fitted as shown in figure 5-5, and The obtained k_{app} values are listed in Table 5-2. PS-STB1-TiO₂ has the highest k_{app} value ($15.4 \times 10^{-3} \text{ min}^{-1}$), indicating that the peptide-binded sphere morphology induces better photocatalytic performance than the aggregated bare and STB1- TiO₂.

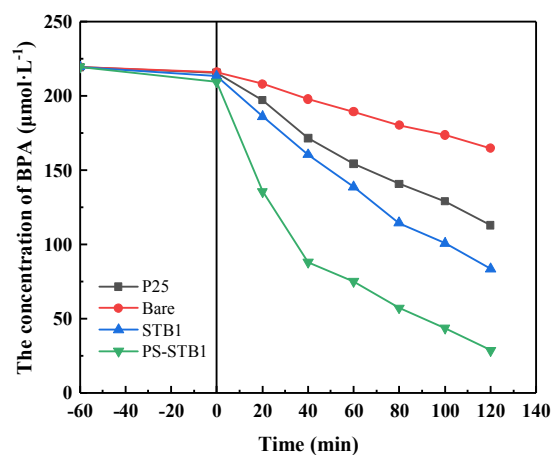


Figure 5-4 Adsorption in the dark and photocatalytic degradation of BPA under the solar light stimulator over the P25, bare-, STB1-, and PS-STB1-TiO₂ photocatalysts at 20 minutes intervals.

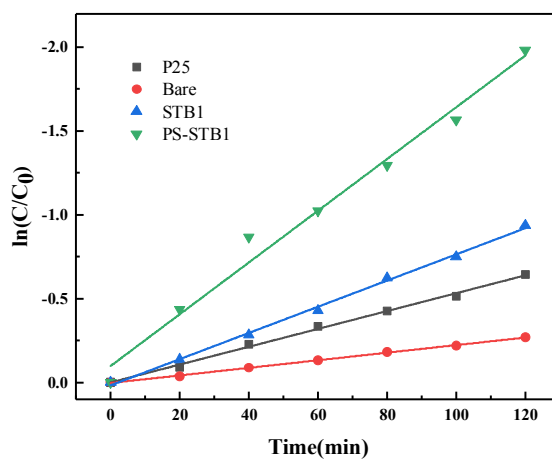


Figure 5-5 kinetic curves for BPA by P25, bare-, STB1-, and PS-STB1-TiO₂ photocatalysts

	Degradation rate	$k_{app} (*10^{-3} \text{ min}^{-1})$
P25	47.5%	5.3
Bare TiO ₂	23.7%	2.3
STB1- TiO ₂	59.8%	7.8

PS-STB1- TiO ₂	86.3%	15.4
---------------------------	-------	------

Table 5-2 Degradation rate and *k*app values for BPA by P25, bare-, STB1-, and PS-STB1-TiO₂

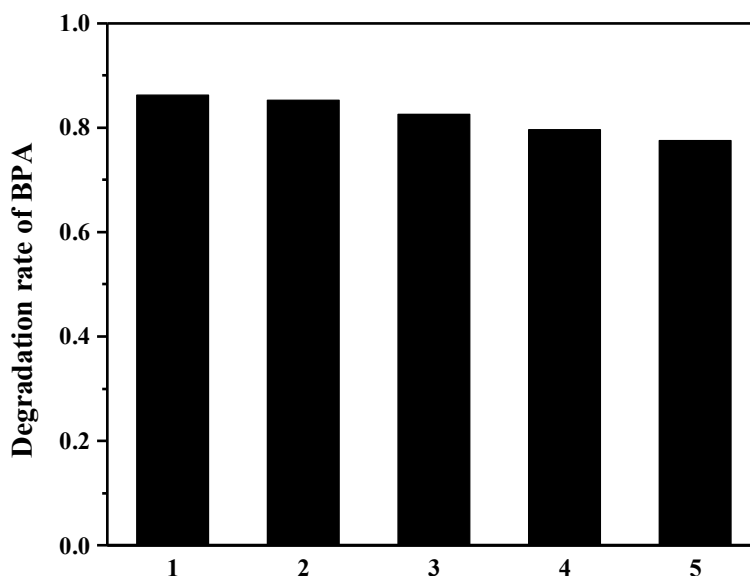


Figure 5-6 Degradation rate of BPA over PS-STB1-TiO₂ for 5 cycles

In order to investigate the potential of reusability of PS-STB1-TiO₂, the same photodegradation experiment was carried out for five round. The final degradation rate was calculated by the remained BPA concentration at 120 min for each round. As shown in figure 5-6, after repeated use for 5 round, the degradation efficiency of the catalyst barely decline about 10%. So, with high photodegradation capacity and good reusability, the biomineralized PS-STB1-TiO₂ has great potential and more investigation need be done in future.

5.4 Conclusions

A TiO₂ specific STB1 peptide was successfully binded to PS bead which construct a new biotemplate to induce TiO₂. The initial concentration of peptide used was investigated to get a prior amount of TiO₂. The biomineralized TiO₂ was characterized

by SEM-EDS and XRD, and the photocatalysis activity was investigated by photodegradation of BPA. The sphere-like morphology indicated that the biomineralized TiO₂ structure closely resembled the morphology of the biotemplate. While the PS-STB1-TiO₂ showed a highest degradation rate of 86.3% compared to commercial P25, bare- and STB1-TiO₂, its favorable fraction of the anatase/rutile mixed crystalline phase is considered to count for it. As traditional TiO₂ catalyst has the problem of hard to be reused, the biomineralized sphere-like TiO₂ can be centrifuged easily and the degradation capacities of BPA after fifth cycle maintained 90% of that for the first degradation, which illustrated that the biomineralized products have the potentiality to be reused.

5.5 Reference

- AHMED, S., RASUL, M. G., MARTENS, W. N., BROWN, R. & HASHIB, M. A. 2010. Advances in Heterogeneous Photocatalytic Degradation of Phenols and Dyes in Wastewater: A Review. *Water, Air, & Soil Pollution*, 215, 3-29.
- ANTONIOU, M. G. & DIONYSIOU, D. D. 2007. Application of immobilized titanium dioxide photocatalysts for the degradation of creatinine and phenol, model organic contaminants found in NASA's spacecrafts wastewater streams. *Catalysis Today*, 124, 215-223.
- BIN YUA, Y. Z., ALKA SHUKLAB, SHYAM S SHUKLAC, KENNETH L DORRISC 2000. The removal of heavy metal from aqueous solutions by sawdust adsorption — removal of copper. *Journal of Hazardous Materials*, 80, 33-42.
- CHEN, G., LI, M., LI, F., SUN, S. & XIA, D. 2010. Protein-mediated synthesis of nanostructured titania with different polymorphs at room temperature. *Adv Mater*, 22, 1258-62.
- CHEN, H., SU, X., NEOH, K. G. & CHOE, W. S. 2006. QCM-D analysis of binding mechanism of phage particles displaying a constrained heptapeptide with specific affinity to SiO₂ and TiO₂. *Anal Chem*, 78, 4872-9.
- CHOI, N., TAN, L., JANG, J. R., UM, Y. M., YOO, P. J. & CHOE, W. S. 2012. The interplay of peptide sequence and local structure in TiO₂ biomineralization. *J Inorg Biochem*, 115, 20-7.

- FAN, T.-X., CHOW, S.-K. & ZHANG, D. 2009. Biomorphing mineralization: From biology to materials. *Progress in Materials Science*, 54, 542-659.
- FATIMA, R., AFRIDI, M. N., KUMAR, V., LEE, J., ALI, I., KIM, K.-H. & KIM, J.-O. 2019. Photocatalytic degradation performance of various types of modified TiO₂ against nitrophenols in aqueous systems. *Journal of Cleaner Production*, 231, 899-912.
- HODAIFA, G., OCHANDO-PULIDO, J. M., RODRIGUEZ-VIVES, S. & MARTINEZ-FEREZ, A. 2013. Optimization of continuous reactor at pilot scale for olive-oil mill wastewater treatment by Fenton-like process. *Chemical Engineering Journal*, 220, 117-124.
- KIM, J. K., JANG, J.-R., SALMAN, M. S., TAN, L., NAM, C.-H., YOO, P. J. & CHOE, W.-S. 2019. Harnessing designer biotemplates for biomineralization of TiO₂ with tunable photocatalytic activity. *Ceramics International*, 45, 6467-6476.
- KIM, J. K., JANG, J. R., CHOI, N., HONG, D., NAM, C. H., YOO, P. J., PARK, J. H. & CHOE, W. S. 2014. Lysozyme-mediated biomineralization of titanium-tungsten oxide hybrid nanoparticles with high photocatalytic activity. *Chem Commun (Camb)*, 50, 12392-5.
- KRIPLANI, U. & KAY, B. K. 2005. Selecting peptides for use in nanoscale materials using phage-displayed combinatorial peptide libraries. *Curr Opin Biotechnol*, 16, 470-5.
- LEE, W. J., LEE, J. M., KOCHUVEEDU, S. T., HAN, T. H., JEONG, H. Y., PARK, M., YUN, J. M., KWON, J., NO, K., KIM, D. H. & KIM, S. O. 2012. Biomineralized N-doped CNT/TiO₂ core/shell nanowires for visible light photocatalysis. *ACS Nano*, 6, 935-43.
- LIU, Z., ZHANG, X., NISHIMOTO, S., JIN, M., TRYK, D. A., MURAKAMI, T. & FUJISHIMA, A. 2007. Anatase TiO₂ nanoparticles on rutile TiO₂ nanorods: a heterogeneous nanostructure via layer-by-layer assembly. *Langmuir*, 23, 10916-9.
- MATSUMURA, S., HORIGUCHI, Y., NISHIMURA, T., SAKAI, H. & KATO, T. 2016. Biomineralization-Inspired Preparation of Zinc Hydroxide Carbonate/Polymer Hybrids and Their Conversion into Zinc Oxide Thin-Film Photocatalysts. *Chemistry – A European Journal*, 22, 7094-7101.
- REDDY, P. V. L., KIM, K. H., KAVITHA, B., KUMAR, V., RAZA, N. & KALAGARA, S. 2018. Photocatalytic degradation of bisphenol A in aqueous media: A review. *J Environ Manage*, 213, 189-205.

- RUTLEDGE, R. D. & WRIGHT, D. W. 2009. Biomineralization: Peptide-Mediated Synthesis of Materials. *Encyclopedia of Inorganic Chemistry*.
- SALAEH, S., KOVACIC, M., KOSIR, D., KUSIC, H., LAVRENCIC STANGAR, U., DIONYSIOU, D. D. & LONCARIC BOZIC, A. 2017. Reuse of TiO₂-based catalyst for solar driven water treatment; thermal and chemical reactivation. *Journal of Photochemistry and Photobiology A: Chemistry*, 333, 117-129.
- SEWELL, S. L. & WRIGHT, D. W. 2006. Biomimetic synthesis of titanium dioxide utilizing the R5 peptide derived from *Cylindrotheca fusiformis*. *Chemistry of Materials*, 18, 3108-3113.
- SPOERKE, E. D. & VOIGT, J. A. 2007. Influence of Engineered Peptides Cadmium Sulfide Nanocrystals. *Advanced Functional Materials*, 17, 2031-2037.
- TSUKAMOTO, D., SHIRAISHI, Y., SUGANO, Y., ICHIKAWA, S., TANAKA, S. & HIRAI, T. 2012. Gold nanoparticles located at the interface of anatase/rutile TiO₂ particles as active plasmonic photocatalysts for aerobic oxidation. *J Am Chem Soc*, 134, 6309-15.
- WANG, N., ZHENG, T., ZHANG, G. & WANG, P. 2016. A review on Fenton-like processes for organic wastewater treatment. *Journal of Environmental Chemical Engineering*, 4, 762-787.
- WANG, S., ZHU, Z., HE, J., YUE, X., PAN, J. & WANG, Z. 2018. Steroidal and phenolic endocrine disrupting chemicals (EDCs) in surface water of Bahe River, China: Distribution, bioaccumulation, risk assessment and estrogenic effect on *Hemiculter leucisculus*. *Environ Pollut*, 243, 103-114.
- WEE, S. Y. & ARIS, A. Z. 2017. Endocrine disrupting compounds in drinking water supply system and human health risk implication. *Environ Int*, 106, 207-233.
- WU, Q., LAM, J. C. W., KWOK, K. Y., TSUI, M. M. P. & LAM, P. K. S. 2017. Occurrence and fate of endogenous steroid hormones, alkylphenol ethoxylates, bisphenol A and phthalates in municipal sewage treatment systems. *J Environ Sci (China)*, 61, 49-58.
- ZHU, S. & WANG, D. 2017. Photocatalysis: Basic Principles, Diverse Forms of Implementations and Emerging Scientific Opportunities. *Advanced Energy Materials*, 7.

Chapter 6

Conclusion

The discharge of pollutants into the environment from petrochemical, agriculture and mechanical industries keep increasing because of the increase in the industrial growth. Especially the contamination of drinking water with heavy metal and bisphenol-A are the major concern of WHO and EPA considering their high toxicity. Considering their harmful effects towards both environment safety and human health, an efficient and cost-effective system is under necessity. Bio-based material has attracted much attention because of its low cost, non-toxicity, simple equipment and operation required and so on. In this study, we constructed several materials for use of environmental micro-pollutants removal, including:

1. Enzymatic synthesis of *m*-phenylenediamine (poly(*m*-PDA)) which require no toxic oxidants for the polymerizations and do not produce harmful byproducts. The polymer of *m*-phenylenediamine (poly(*m*-PDA)), synthesized by mild laccase-catalysis in an aqueous buffer (10 mM citrate-phosphate, pH 3), was investigated for the adsorption of several heavy metal ions including Pb^{2+} , Cu^{2+} , Co^{2+} , and Cr^{3+} . Changes in the chemical structures of the poly(*m*-PDA) due to the adsorption of heavy metal ions were investigated by FT-IR spectroscopy. The structural properties related to the adsorption capacity of the enzymatically synthesized poly(*m*-PDA) were assessed by measuring the Brunauer–Emmett–Teller (BET) specific surface area and pore size distribution of the polymer. The adsorption isotherms of the four heavy metal ions on poly(*m*-PDA) were well described by Langmuir equation. The enzymatically synthesized poly(*m*-PDA) shows high maximum adsorption capacities (q_{max}) for Cu^{2+} , Pb^{2+} , and Cr^{3+} with the values of 556, 526, and 476 $\mu\text{mol g}^{-1}$, respectively, demonstrating that the

adsorption capacities of the enzymatically synthesized poly(*m*-PDA) for heavy metal ions are comparable to the common adsorbents such as activated carbons, carbon nanotubes, biomasses, and etc. Our study suggests that the synthesis of polymeric adsorbents to remove heavy metal ions from waste water can be accomplished through simple and benign enzymatic methods.

2. A 7-mer lead-binding peptide (TNTLSNN) which showed selectivity toward lead ion was covalently bonded onto the surface of magnetic bead to construct a reusable biosorbent to remove Pb^{2+} from water. In order to reduce the influence of adsorption on bare bead, four different kinds of bare bead were investigated and AccuBeadTM COOH magnetic beads which showed a lower lead adsorption capacity and much higher magnetic responsiveness was used. The peptide was conjugated to the activated carboxyl functionalized bead surface through amine group by EDC/NHS. Considering the peptide binding efficiency on bead, which was calculated through the difference between initial concentration and the supernatant concentration after reaction, the sequence TNTLSNN (319 lead molecule per peptide molecule or NNSLTNT (326 lead molecule per peptide molecule) did not significantly influence on whole adsorption capacity of lead. The peptide-linked adsorbent showed 9 times higher removal capacity of lead ($246.05 \mu\text{mol}\cdot\text{g}^{-1}$) to the bare bead without the linked peptides ($29.82 \mu\text{mol}\cdot\text{g}^{-1}$). The adsorption isotherm followed Langmuir fitting well with the maximum adsorption loading (q_{max}) of $308.86 \mu\text{mol}\cdot\text{g}^{-1}$ adsorbent. A selective adsorption of lead in the presence of interfering other metals is verified with individual or combinatory use of four metal ions such as Pb^{2+} , Ni^{2+} , Co^{2+} and Cu^{2+} , even the adsorption capacity in artificial waste water shows 6 times

higher toward Cu^{2+} and 13 times higher toward Ni^{2+} and Co^{2+} . The reusability of bead was verified through desorbing the adsorbed lead from the bead by using EDTA and then the recovered bead was repeatedly used several times (6 cycles tested) without significant loss of adsorption capacity. The newly-constructed biosorbent can be used as a material to selectively separate lead ions from other metals for possible recovery in water treatment.

3. A heptapeptide with specific affinity to BPA, LysSerLeuGluAsnSerTyr (KSLENSY), was binded to magnetic bead to construct a new bio-based adsorbent for selective adsorption of BPA from aqueous solution. While the initial peptide concentration is $500 \text{ mg}\cdot\text{L}^{-1}$, the peptide binding efficiency arrived the maximum binding efficiency of $2.61 \text{ }\mu\text{mol}\cdot\text{g}^{-1}$ which is consistent to the theoretic maximum peptide binding efficiency, $2.75 \text{ }\mu\text{mol}\cdot\text{g}^{-1}$. While the peptide binding efficiency arrived the maximum, the increasing concentration of peptide do not benefit BPA adsorption anymore. Around neutral pH, the adsorption capacity was maximum since the neutral form of BPA was favourable for the adsorption onto peptide. The Langmuir isotherm model is fitted well with a maximum adsorption capacity of $48.61 \text{ }\mu\text{mol}\cdot\text{g}^{-1}$. A selective adsorption of BPA was examined with individual or combinatory use of structural analogs of BPA such as bisphenol F and bisphenol S, the BPA-binding peptide showed 3 times higher selectivity toward BPA than BPF or BPS. Single, double, and triple peptide sequence binded to bead were investigated which resulted 4.34, 8.22, 12.42 BPA molecules per peptide molecule, respectively. In reusability studies, nearly 100% regeneration efficiency for the adsorbent was achieved by the methanol/acetic acid mixture, and the adsorption capacities of BPA after sixth cycle maintained

more than 87% of that for the first adsorption. The newly-constructed peptide-binded bead can be used as a material to selectively separate BPA from waste water and the assembled BPA would be beneficial for further dealing process.

4. The degradation of BPA investigated by using peptide-mineralized photocatalytic TiO₂ particle. Environmentally benign mineralization of TiO₂ particle was induced by using the polystyrene (PS) bead fused with mineralization-inducing peptide (CHKKPSKSC) which has specific affinity to TiO₂. The initial concentration of peptide used was investigated to get a prior amount of TiO₂. The biomineralized TiO₂ was characterized by SEM-EDS, TGA and XRD. The synthesized TiO₂ showed a BPA degradation rate of 86.3% and kinetic curve is fitted well, and its favorable fraction of the anatase/rutile mixed crystalline phase caused by N-doping is considered to count for it. The biomineralized sphere-like TiO₂ can be reused easily and the degradation capacities of BPA after fifth cycle maintained 90%.

With the development of science and technology, green chemistry which is also known as environmentally friendly chemistry and clean chemistry is getting more attention. The three criteria for the green chemistry are the selection of solvent systems, reducing agents, and non-toxic stabilizers that do not pollute the environment. The reaction using biomolecules meets the above criteria. Biomolecules, as the most basic component of life, have special structure and assembly characteristics. Currently, large-scale peptide-induced reaction is hindered by the high peptide cost. However, it is anticipated that cost-effective and environmentally benign alternative processes could be realized through further understanding of designer biomolecules.